THE ANNIHILATION OF POSITRONS

by

SÜREYYA MERİÇ.

Thesis for the Degree of Ph.D.

of

Glasgow University.

THE ANNIHILATION OF POSITRONS.

TABLE OF CONTENTS.

INTRODUCTION

This thesis deals with the investigation of different processes of the annihilation of positrons , mainly two-quanta annihilation in motion and one-quantum annihilation . Before describing the experiments performed it is necessary to review the previous experimental and theoretical work which has been done on annihilation of positrons in general in order to account for the choice of problem and for the experimental technique employed . A brief description of the experiments on pair production will also be included in order to make the historical review more complete .

Our main experimental work consists of the full analysis of the absorption of the annihilation radiation from Cu^{64} produced in different annihilators . In all observations two thin-walled rectangular counters with absorbers between them were used for the measurement of the energy and intensity of the γ-rays by the coincidence counting method . These experiments provide for the first time a definite proof of the existence of the hard radiations resulting from the annihilation of positrons in motion. The experimental value obtained for the ratio of the cross sections for one-quantum annihilation in motion to two-quanta annihilation in motion is in agreement with the predicted theoretical value.

Two additional experiments of considerable importance were also performed: Firstly the angular distribution of two-quanta annihilation radiation was investigated by means of a new type of γ-ray counter possessing high efficiency and high directional resolution. Secondly a study of the correlation between Beta and Gamma radiations from Cu^{64} was made by means of a coincidence method.

A number of experiments which were planned but not carried out because of the limitations of time and equipment during the period of this research will be mentioned at the end of the thesis as possible future investigations.

- o O o -

CHAPTER I

PREVIOUS WORK ON POSITRONS

Section A:- Dirac Hole Theory

The positron was discovered by C.D. Anderson[1] in 1932 in the course of Cosmic-ray investigations. The existence of this new particle had been regarded as a theoretical possibility two years previously by Dirac. In the Dirac relativistic wave equation[2] for a free electron the energy of the electron is given by a square root which could be either positive or negative for a given value of the momentum. Negative solutions correspond to negative energy states.

The connection between these theoretical negative energy states and observed positive electrons is given by the " Dirac hole theory ". According to this theory a positron is regarded as a hole in the negative energy states. It is assumed* firstly that all negative energy states ranging from $-mc^2$ to $-\infty$, in the absence of an external field are normally occupied so that an electron which is in positive energy states can not jump into one of these occupied states. Secondly the electrons filling up the negative

---

* P.A.M. Dirac, "Quantum Mechanics" (1935), Ch. 7 (Hereafter referred to as Q.M)

energy states do not produce an external field and do not contribute to the energy and momentum of the system for which the charge density is infinite. The zero point measurement of the charge, energy and the momentum is represented by that electron distribution in which all negative energy states and no positive energy states are occupied.

Inspite of the fact that the electrons occupying negative energy states can not produce an external field it is assumed that an external field can act on these electrons. A rapidly varying electromagnetic field(high energy γ -rays, or the collision of two fast particles) can cause a transition from one state to another. At the moment of transition from the negative energy states E^- to a positive energy state E^+ , when a negative charge is removed from the negative energy states, an electron pair is created because a hole with a positive charge is produced at the same time as the electron. This process can occur only if the interacting quantum or particle has sufficient energy to remove the electron from negative energy state. The reverse process i.e.transition from the region of positive energy to that of negative energy means the annihilation of this pair, giving rise to the emission of electromagnetic radiation, called " annihilation radiation ". This can happen at any energy of the positron, but has by far the greatest probability of occurrence when the positron possesses no kinetic energy. For this case the energy contained in the annihilation radiation is equivalent to the rest mass of the two electrons.

Section B:- Creation of Positrons

Before Anderson's discovery an indirect evidence of the existence of positrons was obtained by several workers (3, 4) during the course their experiment on the anomalous absorption of high energy γ-rays in heavy material. As a result of the determination of the total absorption coefficient of 2.6 Mev γ-rays from ThC", in lead, the discrepancy between the observed and the calculated values was attributed to a nuclear interaction caused by these γ-rays.(4) In fact, immediately after the positrons were observed as a pair of electron tracks of opposite curvature in a cloud chamber immersed in the magnetic field,(5) Chadwick Blackett and Occhialini (6) showed that these positive electrons can be produced by bombarding lead with radiations from a Polonium - Beryllium source. Curie and Joliot(7) established that in this reaction the positrons were produced by the γ-rays resulting from the transmutation of Beryllium by α-rays and they suggest that electron pairs were created by the interaction of photons with nuclei.

The laws of the conservation of energy and momentum show that this phenomenon of materialisation of photons can take place only in the presence of a third body and only if the photon has an energy greater than a minimum threshold energy for which the value depends on the nature of the third body. If this third body is a nucleus, the minimum photon energy necessary to produce pairs is $2mc^2$, but if it is an electron the photon energy must be greater than $4mc^2$. Other possibilities of pair production exist and these will be indicated later.

(a) Pair Production by Photons in the Field of a Nucleus.

Creation of pairs by the interaction of a photon and a nucleus is the most common process observed, and theorists have calculated the cross-section for this process in terms of Z, the atomic number of the interacting nucleus, and $h\nu$, the energy of the photon. Oppenheimer, Plesset[8] and later Heitler and others[9](10), obtained an expression for the cross-section which was proportional to Z^2 and increasing rapidly with $h\nu$. This is in contrast with Compton scattering cross-section which decreases with increasing photon energy.

Later, the angular distribution of these pairs was investigated[11]* by means of a cloud chamber filled with krypton and it was found that positrons usually make smaller angles with the direction of the incoming photon than the electron does. This fact was attributed to the greater

*This is in good agreement with the theoretical distribution curve given by (10).

kinetic energy of positrons at the point of creation because of the repulsive force between positron and nucleus. This interpretation led to a consideration of the relative values of E_+ and E_- where E_+ is the energy of positron, E_- the energy of electron. The difference $E_+ - E_-$ was calculated (12) and measured experimentally (13) in a Wilson chamber and was found to be proportional to Z , the order of magnitude being 0.12 - 0.28 Mev.

A distribution curve of the total energy of positron-electron pairs produced by γ-rays of 2.62 MeV from ThC" showed (13) that the average value for $E_+ + E_-$ was 1.6 Mev as is expected from theory. The distribution of positron energy also was given theoretically by Heitler*. (His result was checked experimentally in a cloud chamber by observing pairs produced by Na^{24} γ-rays.(14) Better results can still be obtained.)

(b) Pair production by Photon in the field of an Electron. This process was concidered first by Perrin (15) and verified experimentally by Marque Da Silva (16). It was also shown by the latter that the cross-section for this "triplet" process (pair plus rejected electron) was Z times smaller than for the photon-nuclear interaction i.e. the ratio of triplet production to pair production is proportional to 1/Z , which was in quite good agreement with other experimen-

* W. Heitler, *Quantum Theory of Radiation*, (1947), p. 199. (Hereafter referred to as QTR.)

tal results[14]. More detailed calculation of this cross-section was carried out later by several authors[17-20,a] and the results of ~~the~~ relativistic calculations were compared with the earlier work by Perrin and corresponding calculations for nuclear interaction, and it was found that for the very large photon energies the variation of cross-section is the same as that for pair production in the nuclear field.

(c) Pair production by fast Electron.

Oppenheimer and Plesset[8] considered, for the first time, the possibility of materialisation by pair production of the kinetic energy of a charged particle e.g. a fast electron. The cross-section as a function β-ray energy was calculated first by Furry and Carlson[21] and then by Heitler and Nordheim.[22]* The experimental evidence of this process was based upon stereoscopic photograph technique in a Wilson chamber using β-rays from ThC" source[23]. Further accurate investigations gave results which did not agree with the theoretical prediction[24]. The experimental value of the cross-section for pair production by fast β-rays of RaC was of the order of 10^{-22} cm^2, which is about 100 times greater than the cross-section for materialisation by photons of the same energy. Some of the later experiments gave also the same magnitude for ϕ within a factor of about two[25 - 27]. The cross-section measured in these cases was found to be

* See also (22a) – (22d)

proportional to Z, the atomic number of the bombarded element but not to Z^2 as the theory predicts. S. Benedetti[28], using the trochoidal method, confirmed the proportionality of emission of the positrons due to the materialisation of kinetic energy of β-rays from Th(B+C) with Z^2 as is expected theoretically. But some of the experiments show no indication of pair production by such a process[29 - 32]. This indicates a threshold cross-section of the order of 10^{-24} or 10^{-25} cm^2. Although these figures contradict most of the previous experimental results, they give good agreement with theoretical calculation.

The possibility of pair creation by electrons in the neighbourhood of two other electrons was shown by F. Perrin[33] provided that the incident electron has an energy greater than 6 mc^2. (Heitler* requires this amount to exceed 7 mc^2).

The evidence of positron emission from radioactive sources attributed to internal conversion of γ-rays was also indicated by the authors[32],[34]. Halpern and Crane[35] observed a similar effect in the bombardment of F^{19} with protons and found the coefficient of internal conversion to be 1 per 100 γ-rays of 5.8 MeV from this reaction, a value greater than theory would predict. The latter value was calculated by several authors[36-38] and found to be of the order of 10^{-4}, 10^{-3} per γ quantum of energy 5 mc^2.

---

* Heitler, Q.T.R. p. 204

Section C:- Annihilation of positrons.

§. I. General Remarks:

There are several theoretically possible processes of annihilation which are listed below. The energies quoted correspond to the case of zero kinetic energy of the incident positron ($m = m_0$ and assumed to be the same* for electrons and positrons.

(1) The positron combines with a free or loosely bound electron. The mass energy is radiated as two γ-ray quanta in opposite directions, each having an energy of $mc^2 \approx 510$ Kev.

(2) The positron combines with an electron strongly bound to a nucleus. The nucleus takes up the recoil momentum the whole mass energy being confined to one γ-ray quantum of energy $2mc^2 = 1020$ Kev..

(3) The positron combines with an electron in the neighbourhood of another electron and a γ-ray quantum of energy $4/3\ mc^2 = 680$ KeV is emitted.

(4) The positron combines with an electron in the neighbourhood of two other electrons. Two electrons, each having a kinetic energy of mc^2, are ejected in opposite directions.

~~(5) The positron combines with an electron in the neighbourhood of two other electrons (as in (4)) but only one electron is ejected with a kinetic energy of $2mc^2$.~~

(5) The positron combines with an electron in the neighbour-

* A recent experiment has shown the equality of the ratio e/m for the two particles to an accuracy of 2%.

hood of a bound electron . Again only one electron is ejected with a kinetic energy of $2\ mc^2$

(b) The positron combines with a k-electron without emission of radiation.

If positron possesses a kinetic energy E_k at the moment of annihilation in any of the above cases then the total energy of the resulting radiation is $2mc^2 + E_k$. (We must ~~already~~ mention that the probability of some of these annihilation processes for ~~the~~ zero kinetic energy of the positron is zero e.g. i.e. annihilation can take place only while positron is in motion, such as one-quantum annihilation(case(2))]

The cross-section for the two-quanta annihilation (case (1)), the most probable annihilation process, was calculated by Dirac(2a) and found to be

$$\phi_2 = \pi r_0^2 \frac{1}{\gamma+1}\left[\frac{\gamma^2+4\gamma+1}{\gamma^2-1}\log(\gamma+\sqrt{\gamma^2-1}) - \frac{\gamma+3}{\sqrt{\gamma^2-1}}\right]$$

per electron, where $\gamma = E/\mu$, $\mu = mc^2$ and $r_0 = e^2/\mu$.
This cross-section increases as E is diminished. (This is in marked contrast with the cross-section for pair production which increases with the photon energy.) Thus annihilation occurs with the greatest frequency as the positron approaches the end of its ionising track. Experiments on the energy distribution of the γ-rays show that annihilation radiation has a strong component of 0.51 MeV. agreeing with the above deduction that two-quanta annihilation at rest has a very

high probability. The above expression for ϕ_2 tends to an infinite value as the kinetic energy of the positron tends to zero but this does not mean that the probability of annihilation becomes infinite. Since the life-time of the positron is finite the rate of destruction (R) is limited and the cross-section is finite even for small v . The value of R in this case is given by

$$R = \phi N Z v = NZ\pi r_0^2 c$$

where N is the number of atoms per cm^3 and Z is the atomic number of the annihilating substance. For v very small $R = NZ\pi r_0^2 c$ is constant for a given Z.

For E very large the cross section may be taken as

$$\phi = \pi r_0^2 \mu/E \left(\log \frac{2E}{\mu} - 1 \right)$$

in this case the energy is not shared equally between the two quanta and they are not emitted in exactly opposite directions except in extremely relativistic cases where $v \to c$. The quantum emitted in a forward direction acquires nearly all the kinetic energy of the incident positrons and the second quantum has an energy of the order of $\frac{1}{2}mc^2$, The precise values of the two energies can be obtained theoretically. This will be discussed in Chapter II.

The possible types of annihilation and creation of pairs are listed together in a table in order to ilustrate the similarity of these two processes. This is given in Appendix.I.

§.2. Experimental Work on Annihilation.

In the course of absorption measurements of the high energy Gamma-rays, the presence of an unexplained secondary gamma radiation of 0.55 Mev given off during the absorption process was first shown by Chao[(40)(41)] and its existence was confirmed by Gray and Tarrant[(42,43)]. These experiments also pointed out that the energy of this secondary radiation is independent of the absorber material used for the absorption of the primary γ- rays and also does not depend upon the energy of these incident radiations. It was also shown that the existence of the soft (secondary) radiation was possible if the incident photon possessed a minimum energy. By rather indirect methods this minimum was placed approximately as 1.5 Mev .

A connection between these unexplained secondary γ-rays and the annihilation of positrons was first suggested by Blackett and Occhialini[(44)] in 1932.

I: (a)- In 1933 J. Thibaud[(45)] observed the secondary radiation due to pair annihilation, using the trochoidal* method for collecting the positrons, and a film as γ-ray detector. The positron source was a Radon tube surrounded with different materials (Al, Cu, Pb, Bi) which gave rise to positron emission under the influence of γ-rays. Photographic measurements

---

* The full description of this method will be given in Chapter VI, Section A.

were made of the intensity of the γ-rays produced by absorption of the positrons(0.8 Mev mean energy) in platinium placed at the focus of the magnetic separator. From the curve of logarithmic intensity against the superficial mass of γ-ray absorber he obtained a mass absorption coefficient of $\mu/\rho = 0.2\ cm^2/gm$(for 0.8-1.45 gm/cm^2 thickness of Pt) corresponding to $\mu = 2.2\ cm^{-1}$ in lead. By the more direct method of counting the number of photons in a Geiger-Müller counter, he found a smaller value for μ which corresponds approximately to an energy of 0.5 Mev.

(b)- In 1934 F. Joliot (46), using positrons emmited form Al bombarded by the α-rays from 80 millicuries of Polonium , and focussing them on to a 1 mm Pb or 5 mm Al absorber by the trocoidal method again, investigated the absorption of the γ-rays produced in the first absorber(called "radiator") in a second lead absorber of thickness varying from 1.5 to 6 mm (1.71-6.84 gm/cm^2). From a graph of log.intensity of radiation counted in a G-M.counter against the superficial mass absorber he obtained a mass absorption coefficient $\mu/\rho = 0.24$ corresponding to a quantum energy of 485 Kev using Jaeger's relation $\mu_{Pb} = 4240\lambda^2$. The experiment showed that, if a hard component of 1Mev radiation existed its intensity was certainly less than 30% of that of the soft component.

Owing to the small intensity of the source employed by Joliot(5000 positrons per minute on the focus) the number of annihilation γ-rays counted was very small. His complete results are shown below. It will be seen that his statistical error is very large.

Abs. thickness gm/cm^2	no. of γ/min
1.71	2.46 - 0.2
4.56	1.24 - 0.2
6.84	0.65 - 0.25

(c) In the same year, O. Klemperer[47], using a Boron source, and a single counter, enclosed in a lead cylinder, obtained $\mu = 1.34$ cm^{-1} By comparison with a standard RaC γ-ray a correction of about 26% was found to be necessary and the corrected result was $\mu = 1.69$ cm^{-1} in lead which is, within the limit of error, the same as the calculated value of $\mu = \sigma_{scatt.} + \sigma_{Comp.} + \sigma_{Photo} =$ 1.67 for 510 Kev. With a different experimental arrangement of source and counters in coincidence, and with sufficient absorber between the counters to prevent passage of recoil electrons of energy less than about 1 Mev, it has been shown that the annihilation radiation consists only of soft quanta which is homogeneous with a hardness corresponding to 0.5 Mev.

Again in this experiment the statistics are very poor since only about 3 total coincidences per minute (out of which 1.5/min. was cosmic ray coincidences) were observed.

(d) Crane and Lauritsen[48] using Carbon activated with 10 microamps of 0.9 Mev deuterons (N^{13}) obtained $\mu = 1.58$ cm^{-1}.

The intensity of ionisation due to the annihilation radiation was measured in an ionisation chamber. To determine the absorption coefficient of the γ-rays a sheet of lead 7.1 mm thick was interposed between the two chambers(The first chamber was used in order to measure the positron intensity) The readings were taken every 4 minutes with lead and one min. without lead alternately.From a graph of logarithmic intensity of both processes against time measuring the difference between the position of these two curves they have calculated the linear absorption coefficient of above value.

A few months later McMillan(49) found $\mu = 1.71\ cm^{-1}$ using the same source and experimental technique.

In all the above experiments the number of γ-rays emitted per positron was estimated and found to be very roughly equal to 2.

II:(a)More precise values of the quantum energy of annhilation radiation have been obtained from cloud chamber investigations of the γ-rays accompanying the positron emmision from certain artificial radio-elements. In such experiments a screen of mica or carbon is usually situated within the cloud chamber and irradiated by the γ-rays. The curvatures in a magnetic field of the tracks of the Compton electrons emitted from this screen are measured statistically and the quantum energies of the incident γ-rays can be deduced by making appropriate corrections for the energy of the scattered quanta.

in such investigations evidence has often been obtained of the existence of a strong γ-ray line with quantum energy approximating closely to the value 0.51 MeV to be expected from the two-quanta process of annihilation of positrons.

Experimental results obtained by Richardson and Kurie[50] indicates the presence of radiations corresponding to the annihilation at rest from the positrons of N^{13}.(The source was obtained by bombardment of C^{12} with 4mev deuterons) The maximum momentum available from the main line was 2280 $H\rho$. (H=250 gauss, cloud chamber diameter =7"). The author suggest that occasional electrons exhibiting a momentum greater than that to be ascribed to this main line may be due to either contamination of the source,or the radiation emitted when a positron is annihilated while in motion(hard component of the two-quanta in motion and one-quantum annihilation).

In a later paper Richardson[51] investigated the γ-rays emitted from N^{13}, V^{48},Cu^{64} with a carbon radiator of the same thickness as mica(because of the low energy of the expected γ-radiation the radiator was only 40 mg/cm^2) in a cloud chamber of 12" diameter filled with hydrogen to a pressure of about 100cm. Under the improved experimental conditions the result obtained from N^{13} is practically the same as the previous one. In the case of V^{48}(prepared by the bombardment of Ti with 5.5 MeV deuteron), in contrast with the N^{13} distribution curve a strong 1.05 MeV line appears in addition to the main group(upper limit 2400 $H\rho$ = 0.53 MeV) in the ratio of 1.9 to 1. This was at first thought to be due to one quantum annihilation, in view of the agreement between the energy of the γ-ray of 1.05 Mev with the energy 1.02 MeV to be expected from the annihilation of a positron in the field of a nucleus; but intensity considerations made it clear that it was the radiation accompanying K-electron capture. The tail although present is probably obscured by the large amount of this high energy radiation. The radiations from Cu^{64} was also complicated because of the more pronounced tail with high upper limits. However the major part of the radiation consists again of the ordinary two-quanta radiation and the tail is a very small fraction of the intensity of the main line. Hence the statistics are not good enough in any case to make a numerical estimate of the hard radiations.

In a paper published a few months later than this an account is given of a more accurate experiment by the same author(52) which showed a quite different momentum distribution curve for N^{13}, containing two distinct lines of energies 0.34 MeV, 0.42 MeV corresponding to the compton and photoelectrons due to the 0.51 Mev radiation. The main difference in the experimental arrangement was merely the use of a very fine lead radiator of thickness 0.0017 cm which is much more sensitive in the low energy region. Cu^{61} obtained by bombarding Nickel with deuterons also was investigated in this experiment and a similar result was obtained.

(b) A very accurate study of the annihilation radiation spectrum has been made by Martin Deutsch (53) using a " Magnetic Lens Spectrometer ". The source used was Cu^{64}. The result of the distribution of compton and photoelectrons converted in a relatively thick radiator (50 mg/cm^2) showed a distinct 0.5 MeV line and this was followed by a tail ending with a single line at 1.35 MeV which was ascribed to the nuclear γ-ray. The intensity of this line indicated a production of 1 per 40 positrons when compared with the Na^{22} nuclear γ-ray of 1.28 MeV which is known to emit 1 γ per positron. This is the almost only publication which claims that the 1.35 line is due to a nuclear γ-ray . The possibility of ascribing this γ-ray to the result of one-quantum annihilation of Cu^{64} positrons(0.3 MeV mean energy) will be discussed in Chap.VII.

C.S. Cook and Langer (54) have investigated the same source* with a high resolution magnetic spectrometer.(The radius of curvature was 40 cm, $\Delta H\rho/H$ = 0.5% and the transmission angle was 0.1% of the total solid angle). They used a Pb radiator of 0.0263 gm/cm^2 and a very thin window 2.42 mg/cm^2 which is 35 Kev thick. (Later 2 Kev "Zapon" window counter was used.) The result was that no hard radiation beyond 0.5

* Annihilation radiations from Radio-Nitrogen was also investigated by these authors using the same method. See reference 79.

MeV could be seen on their graph showing the distribution of the recoil electrons. This perhaps was on account of the limitation of the geometry of the apparatus . For 0.51 MeV the groups of the Compton and the photo-electrons are very distinct; even the K, L, M lines are very clearly visible. Moreover they found no evidence of a nuclear γ-ray of 0.38 or 0.19 MeV with an intensity of more than 2% * of the positron emission and they also state that the 1.35 MeV nuclear γ-ray was correlated with K-capture . There is no mention of any experimental verification of this statement.

A very precise value of the wave length of the annihilation radiation from a Cu^{64} source was determined by Dumond, Lind and Watson (55) with a two-metre focus crystal spectrometer. The experiment originated from the idea of the calibration of the spectrometer and an exact experimental value of the Compton distribution from a homogeneous γ-ray source such as "pure annihilation" radiation. Therefore all attention was concentrated on the radiations due to the annilation at rest. No evidence of hard radiations would be expected from such arrangement.

---

* This fact rejects the possibility of ascribing the excess of particles at low energy to the spectra being complex. It was found previously that the Cu^{64} (β^-, β^+) do not follow the Fermi distribution. (56 - 59, 60) The deviation at low energy was such that 9% of the β^+ and 6% of the β^- transitions would be expected to be forbidden ones. (54)

III:- Angular Distribution of Annihilation Radiation.

(a) It was Otto Klemperer(47) who established first the simultaneous emission of two γ-ray quanta in opposite directions in the annihilation process with the help of two G-M counters of nearly 2π solid angle in coincidence. The counters had a semi-cylindrical crosssection of diameter 2 cm, (8cm long). The counters were placed with their flat sides, which were covered with windows 0.02 gr/cm^2 thick, facing each other spaced 5 mm apart. When the source (activated carbon by bombardment of 600 kev protons) was placed between the two counters after being wrapped in sufficient material to stop all the positrons, 300 single counts only were obtainable in each counter and roughly 3 coincidences per minute were recorded under this geometry; when the whole system was covered with lead (6 cm thick) this number was reduced to 1.5/min. the latter being the natural background coincidences.

(b) Better angular resolution was obtained by Alikhanian, Alichanow and Arzimowich (61), in whose experiments the solid angle subtended by one counter was about 0.7 steradian. They have used two pairs of coincidence counters one pair on each side of the source. The source was radio-phosphorus obtained by bombarding Al with α-rays from 500 mC Rn. But the intensity obtained was only about 10^5 which gave rise to 150 single counts (on the average) in each counter and the maximum number of coincidences per minute were only 1-2 for various distances of source from the counter. In order to show how large the statistical error was, their complete results are given below.

	Background 3 min.	with P^{30}_{15} 3 min.	Observed coincidences 3 minutes	Cosmicray + ord. background c.
RunI d=3.5 cm	510	935	4.7 ± 0.47	1.3 ± 0.2
	490	890	2.8 ± 0.6	2.7 ± 0.35
RunII d=2.5 cm	516	1095	7.6 ± 1.0	1.1 ± 0.3
	510	890	2.6 ± 1.0	3.6 ± 0.6

(c) Beringer and Montgomery (62) used two small counters (1.05 cm to 3 cm long) subtending a solid angle of 0.015 steradian at the source. One of these counters ~~counters~~ could rotate round the source in order to measure the ratio of coincidences to the single counts for various angular deviations of one counter from the line through the other counter and the source. The annihilation radiation source was a Cu^{64} foil activated by bombardment by 3.7 MeV deuterons. From 10 such sources a total of 800 coincidences was recorded with a circuit of 3 μsec resolving time. The angular distribution curve obtained was much superior to any other previous work on this matter. But the authors seems rather optimistic in estimating a colinearity of 15' of the two quanta from their result. However some factors such as the efficiency of the counter and the resolving time of the circuit could still be improved in order to obtain better statistics. These points will be revived again in Chapter III in connection of with one of our experiments.

IV:- Angular Correlation Effect with Annihilation Radiation.

A different type of investigation of the annihilation radiation could be mentioned here in order to complete the list of experiments on the positron annihilation. It has been pointed out by Wheeler [63] that according to pair theory, the planes of polarisation of the two quanta resulting from the annihilation of a positron should be at right angles. The correlation between the states of polarisation of the two quanta, which is the equivalent of the angular momentum conservation in the process of annihilation at rest, has been experimentally verified by Snyder et al.[64] and others [65]. The azimuthal variation of intensity of the simultaneous Compton scattering of the two quanta has been calculated by several authors [64,66, 67]. The experimental results are in very good agreement with the theory.

The arrangement used [64] to determine the angular correlation was as follows: Cu^{64} prepared by deuteron irradiation was used as the annhilation source. The two opposite γ-ray beams collimated in a lead channel were scattered by two cylindrical Al scatterers and the scattered radiations were detected by two bell-shaped counters (with lead cathode) placed above the scatterers. Coincidences were measured as a function of the azimuthal angle between the axis of the two counters for $\varphi = 0^{\circ}$, 90°, 180°. In all cases $C_{90^{\circ}}$ was greater than $C_{180^{\circ}}$. The ratio of $C_{90^{\circ}}/C_{180^{\circ}}$ was found equal to 1.9 which is close to the value 1.7 predicted by the theory. Because of the absorption in the scatterers, the maximum number of coincidences were obtained for φ less than 90°, close to the theoretical maximum of anisotropy (82°).

Summary of Experimental Work on Annihilation:

I- The early experiments(1933-1934), were confined to the measurement of the energy of the annihilation radiation by the absorption method which depend upon measuring the absorption coefficient μ and the calculation of the energy from a relation between μ and λ, the wave length of the radiation. The detectors used to determine the intensity of radiation in these experiments were photographic film, G-M. counters,and, ionisation chamber.

Generally the results obtained by this method were not very accurate even in the case of two-quanta annihilation of positrons at rest; experiments of this kind can give the order of the energy of the radiation and the approximate number of quanta emitted per positron.

II- In the next stage (1936 - 1938) attempts were made to obtain the more precise value of the quantum energy of the annihilation radiation in order to confirm the theory.

The energy measurements were based upon the determination of $H\rho$ for the compton recoil electrons or photoelectrons produced by the annihilation radiation. In this method, the recording apparatus consisted of (a)- Wilson chamber in a magnetic field,(b)- The counters combined with a magnetic separator placed in a magnetic field, (c)- Crystal spectrometer.

The results obtained from the cloud chamber recoil electron measurements generally show agreement with the 0.51 MeV radiation as predicted from the theory, but do not seem to exhibit adequate proof of the existence of radiation due to the annihilation of positrons in motion. It must be noted that the data upon quanta of energy greater than mc^2 is inadequate in amount and accuracy in this method.

Study of the compton recoils and photoelectrons by means of magnetic spectrometer technique (1945-1948) with the improvement achieved on the resolution of these spectrometers, determines the energy of radiation with a great accuracy, but the attention is mostly paid to the commun type of annihilation process which give rise to the radiation of 0.51 MeV, hence the existence of the hard component of the two-quanta annihilation radiation and the one-quantum annihilation radiation which is harder than the former could not be brought to light during the course of these experiments.

Moreover, even after the very recent(1949)study of the energy of the annihilation radiation by a"crystal" spectrometer , the evidence of these rare types of annihilation radiations of energy higher than 0.5 MeV still remains obscure.

III- Several experimental attempts have been made to study the directional properties of the emitted radiation. The earliest experiments were bound to show that the two quanta produced in annihilation at rest are emitted in opposite directions(1934-1936). As the geometry of the experimental arrangements and the counters were improved, better results were obtained illustrating the angular distribution of the annihilation radiation (1942). The method used in these series of experiments was coincidence counting between the two G-M counters placed to receive radiation in opposite directions: the first measurements were taken only for $\theta = 180^{\circ}$. In the later experiments the variation of the number of coincidences with θ was investigated. The results obtained confirm only the existence of the annihilation at rest. The possibility of investigating the two-quanta annihilation in motion by this method is noted in Chapter.VII.

IV- A different type of experiment to show that the two quanta are emitted at 180° as a result of annihilation at rest, was to investigate the two scattered quanta which have been polarised in two different planes making 90° with each other. The experimental technique was again the coincidence counting between the ~~the~~ two scattered quanta as a function of the azimuthal angle between the two counters. The applicability of this method to the annihilation in motion requires theoretical investigation.

CHAPTER II

THE CROSS-SECTIONS FOR ANNIHILATION PROCESSES

In this chapter we shall consider two-quanta annihilation and one-quantum annihilation from the theoretical point of view. The probability of annihilation in motion and at rest and the cross-section as a function of positron energy will be discussed for the two processes. Finally the ratio of the two cross-sections will be given for different velocities and annihilating media.

Section A:- The probability of two-quanta annihilation as a function of positron energy .

§.1. Range:-The average range, R , of an electron of initial energy E_0 may be calculated from the formula *

$$R\,(E) = \int_0^{E_0} \frac{dE}{(-dE/dx)} \qquad (1)$$

where, -dE/dx is the energy loss per cm. of path in the m medium concerned. For lead -dE/dx as a function of energy E is shown graphically in Fig.(1). The full curve indicates the total energy loss and the dotted curves show the contribution to the energy loss by collision and radiation. From

---

* W. Heitler, Q.T.R. p.223

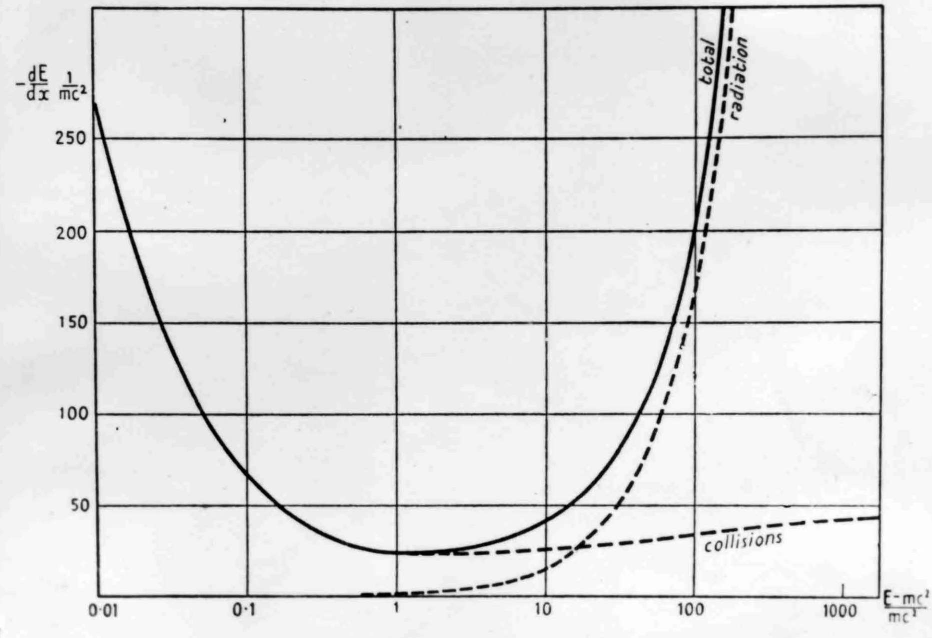

$-\frac{dE}{dx}\ \frac{1}{mc^2}$
250
200
150
100
50
0·01
0·1
1
10
100
1000
$\frac{E-mc^2}{mc^2}$
total
radiation
collisions

FIG. 1

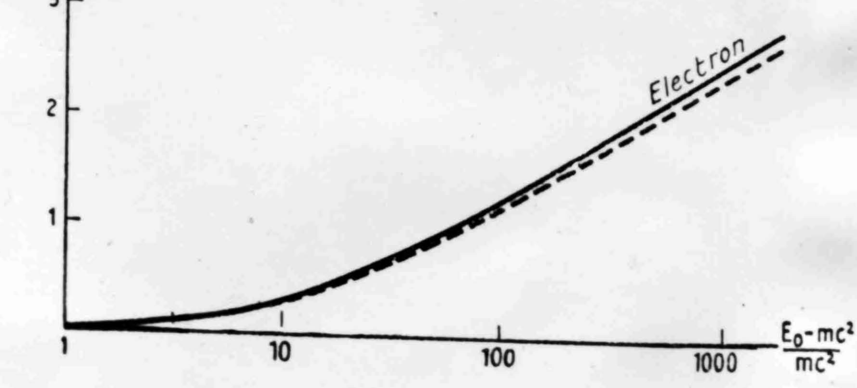

R (cm)
4
3
2
1
1
10
100
1000
$\frac{E_0-mc^2}{mc^2}$
Electron

FIG. 2

this curve we can derive by means of the formula (1) the curve giving the average range of an electron as a function of the primary energy. This curve is the full curve of Fig(2). The average range of a positron of a prescribed initial energy is less than that of an electron of the same energy because of the possibility of the annihilation of positron while in motion.

If we denote by $w(E')dE'$ the probability that the positron is annihilated while its energy is between E' and $E' - dE'$ then the function $w(E')$ can be calculated theoretically. Considering two-quanta annihilation only the form of variation $w(E')$ with E' is found to be that shown in Fig(3). This probability of annihilation while in motion diminishes the average range of the positron by R, where

$$R = \int_0^{E_0} R(E')w(E')dE'$$

From the curves for R, w we can compute R as a function of E_0 and so obtain a curve for the range of a positron as a function of its initial energy. This is shown as the dotted curve in Fig.(2). A few numerical values of the measured ranges $\underline{r}$ are given below for the different substences and various energy of positrons:

E_k (MeV)	r (cm)	
3	0.06	in lead
2	0.07	" ; 0.9 in water
0.8	0.28	in air
0.3	0.04	in aluminium

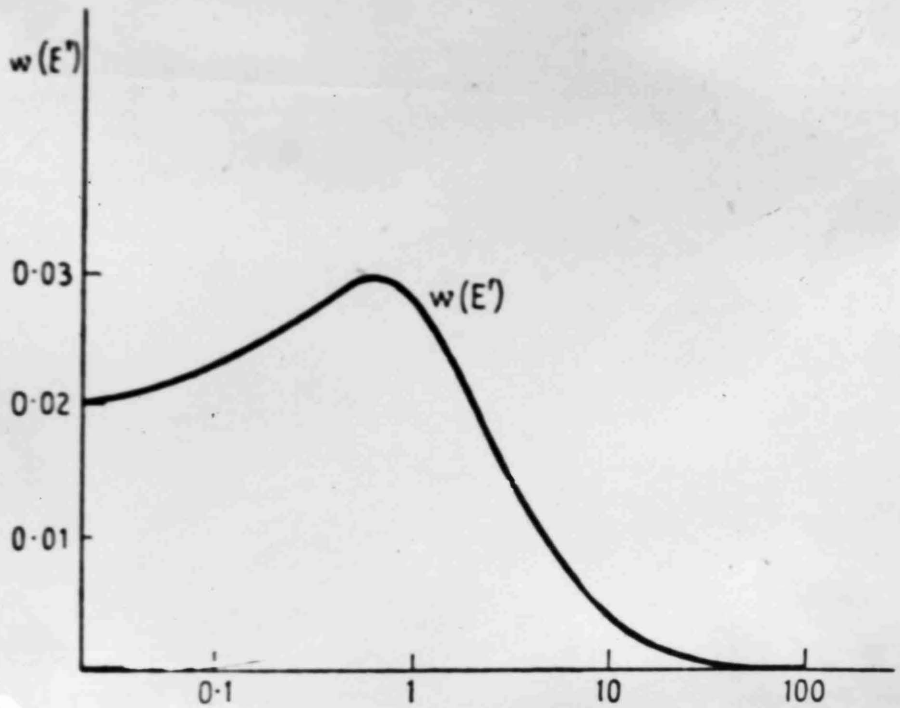

FIG.3

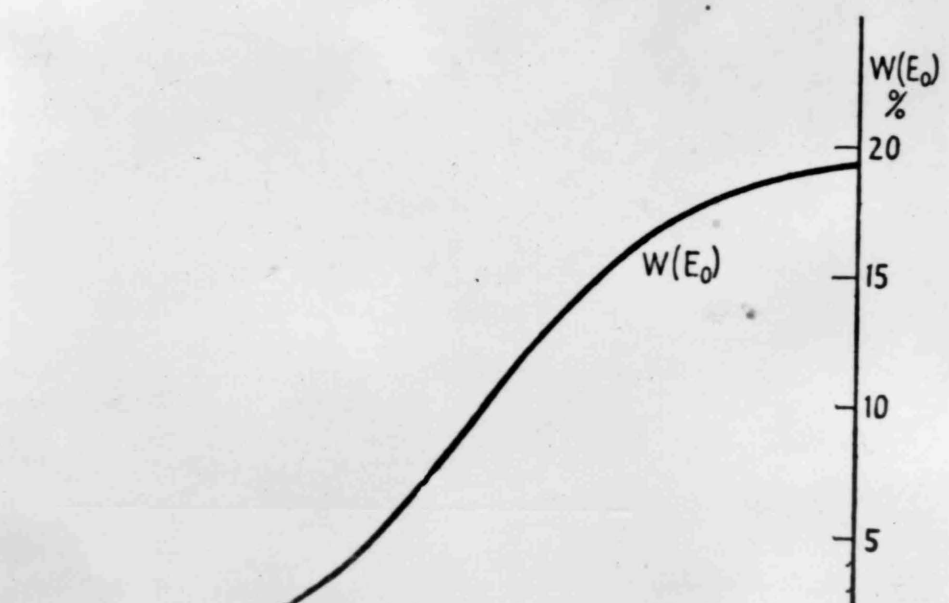

§.2. The total probability of annihilation in motion.

If we denote by $W(E_0)$ the total probability of annihilation of a positron of initial energy E_0 before it comes to the end of the range R, (while in motion) then

$$W(E_0) = \int_0^{E_0} w(E')dE' \qquad (2)$$

This probability increases with E_0, and in lead it rises to a maximum of about 18 %. See Fig(4). Namely this fraction of a beam of very fast positrons are annihilated while in motion and the remaining ones come to the end of their range when they are annihilated at a rate of $\phi n Z v$.

As a further clarification we proceed to interpret Fig(4). In this figure the difference between the two ordinates corresponding to two different energies (E_0 , E say) represents the total probability of annihilation of a positron of initial energy E_0 during its slowing down to an energy E. Let N_0 be the number of positrons with this initial energy E_0 and suppose that N(E) is the number of positrons with energy E which survive annihilation. Then, since the probability of annihilation within the interval dE is w(E)dE, the number of positrons annihilated in this interval dE is

$$dN(E) = N(E)w(E)dE$$

therefore
$$dN(E)/N(E) = w(E)dE \qquad (3)$$

(That is to say in Fig(3) the ordinate showing the probability of annihilation represents the ratio of the number of positrons annihlated in the range dE to the number of surviving positrons with energy E).

If we integrate (3) from E_0 to E we obtain the number of surviving positrons at energy E, when the initial number was known :

$$N(E) = N_0 e^{-W(E_0) - W(E)} \qquad (4)$$

$N_0 - N$, should give us the number of positrons annihilated between the energy limits E_0 and E , ($E_0 > E$). We proceed to determine the ratio $(N_0 - N)/N_0$ from equation (4). Let the difference

$$W(E_0) - W(E) = W_0(E)$$

Substituting this value in (4) we obtain

$$N(E) = N_0 e^{-W_0(E)}$$

Expanding the exponential term in a series and satisfying only with the first two terms, from last equation we derive

$$\frac{N_0 - N}{N_0} = W_0(E) \qquad (5)$$

The left hand side of equation (5) gives us the number of positrons annihilated while in motion in an energy interval $E_0 - E$ as a fraction of the initial number N_0 of positrons with energy E_0. The right side is the difference of two total probabilities of annihilation corresponding to that energy interval. Thus the difference between the 2 ordinates in Fig(4) gives us a value of the number of annihilated particles with a very slight difference from the actual value .

Let us take an example. Suppose that the initial kinetic energy of our positron is $E_0 = 100\ mc^2$. If we start with 100 positrons having this initial energy, 18 of them will be annihilated while in motion according to Fig(4). If we start from $E_\delta = 10\ mc^2$, the total probability of annihilation should decrease to 12 % again according to the same figure. Hence the number of positrons annihilated between 100 mc^2 and 10 mc^2 is 6 % = (18 % - 12 %). But the real number is a little less than that because of the term $\varepsilon = (1 - e^{-W_0}) - W_0$. In the above case E_δ corresponds to E . In this manner we can construct the following table:

TABLE 1

$E_{\cancel{\delta}}$ (mc^2)	$W_0(E) = W(E_0) - W(E)$	$\frac{N_0 - N(E)}{N_0} = 1 - e^{-W_0(E)}$	F %
10	0.06 = 18% - 12%	0.0582	94.18
5	0.09 = 18% - 9 %	0.0861	91.39
2	0.12 = 18% - 6%	0.1131	88.69
1	0.14 = 18% - 4%	0.1307	86.93
0.5	0.16 = 18% - 2%	0.1479	85.21
0.1	0.18% = 18% - f (<0.5%)	0.1467	83.53

The fourth column represents the percentage of ~~the initially high energy~~ a group of positrons initially of energy 100 mc^2 which survive at energy E. (Col.I)

The graph illustrating the surviving percentage as a function of the kinetic energy of positron is given in Fig(5)

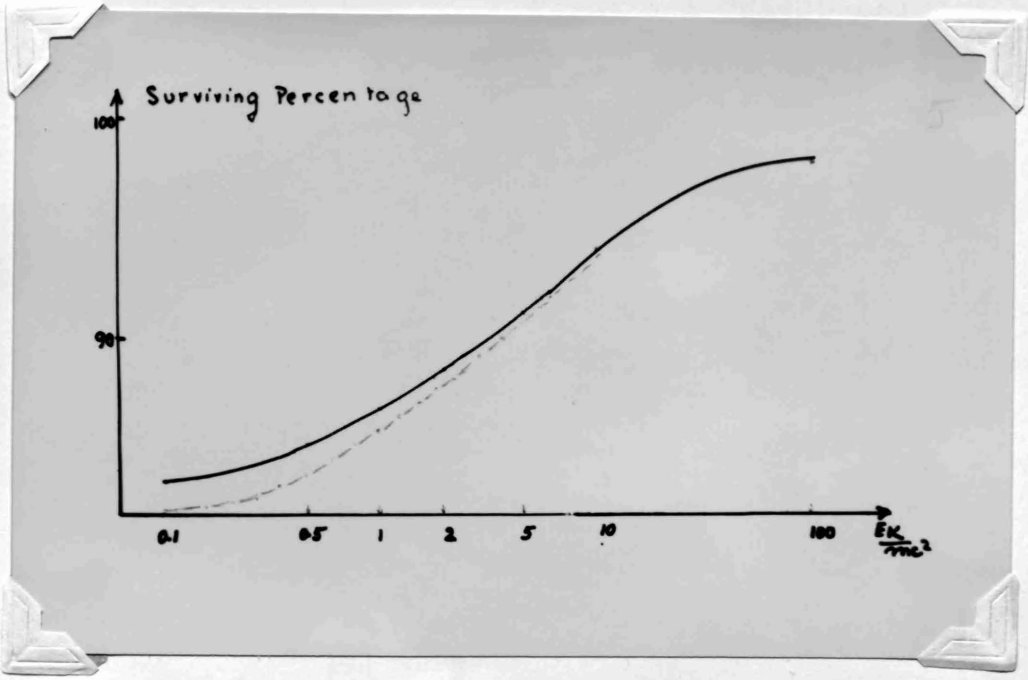

Fig(5)

a- Full curve shows the variation of surviving percentages with the energy, ordinates being calculated from Column.3 .Table (1).

b- Dotted curve shows the approximate value of this curve i.e. ordinates are taken from column.2.of the same table .

§.3. <u>Two-quanta annihilation of slow positron and positron " life-time "</u> :- The rate of destruction of very low velocity positrons by the two-quanta process is found to be given by

$$R = N\pi e^4 / m^2 c^3 = 7.10^{-15} N$$

where N is electron density (Fermi and Uhlenbeck)[68] .
The nuclear repulsion prevents the positron from reaching the inner part of the atom. Therefore not all electrons are effective, so that N will lie between n and nZ , n being the number of atoms per unit volume. For lead

$$R = 2.5\ 10^8 f\ \mathrm{sec.}^{-1} \quad (1 < f < Z) \ (68)$$

For $f = Z$ we have $R = 2.\ 10^{10}\ \mathrm{sec.}^{-1}$ (Heitler)[*]
The total cross-section for this type of annihilation was calculated by Dirac[2a] and found equal to

$$\phi = \pi r_o^2 \frac{1}{\gamma+1} \left[\frac{\gamma^2+4\gamma+1}{\gamma^2-1} \log \left\{ \gamma + \sqrt{\gamma^2-1} \right\} - \frac{\gamma+3}{\sqrt{\gamma^2-1}} \right] \quad (6)$$

where $\gamma = E/\mu$, E = total energy of positron in the system where electron is at rest; $\mu = mc^2$ and $r_o = e^2/\mu$
From this formulae F. Joliot[46] calculated the free path λ, of a positron in matter for which the number of electrons per cm^3 is N , to be

$$\lambda = 1/N\phi$$

For a positron of 2Mev , ϕ from Dirac's formula = $0.115\ 10^{-24}$ cm^2. Whence = 3.1 cm. in lead and 26 cm. in water, whereas the ionosing ranges of an electron of this energy is 0.07 cm. in lead and 0.9 cm. in water. In this way one can construct a table of corresponding calculated values of λ and experimental values of the ranges r for electrons of different

* W. Heitler Q.T.R. p.208.

kinetic energies lying between 3 MeV and 10 KeV. The probability of annihilation P of the positron while its kinetic energy decreases from W_1 and W_2 because of the retardation (ralentissement) in the material is given by

$$\log \left[1 - r(W_1, W_2) \right] = \int_{W_1}^{W_2} dr/\lambda \qquad (7)$$

knowing the above mentioned tabular relation between r and λ we can integrate the right hand side of equation (7). The calculation of this probability in unit time shows that the ratio $P(W_1, W_2)/\Delta t$ increases as the kinetic energy of the positron decreases and reaches a constant value of about 2.9 sec^{-1} in water beyond W_1 equal to 100 KeV . Blackett and Occhialini(69) pointed out that the constancy of this ratio at low energies means that positron annihilation follows a law identical with that which applies to the disintegration of radioactive substance as function of time. Thus the constant of dematerialisation is defined by the relation

$$(dN/N)\ 1/dt = -\Lambda = -2.9\ 10^9\ sec.^{-1}$$

N being the number of positron at time t, dN = the number of positrons which disappear between t and t+dt . The "mean life-time" of positrons in water is, therefore, equal to $1/\Lambda = 3.5\ 10^{-10}$ sec and $3.8\ 10^{-11}$ in lead.

The actual life-time of a positron can be determined in cases where abrupt termination of ionising track can be seen to occur before the velocity has fallen below the appropriate ionisation limit e.g. from cloud track photographs in a magnetic field where there is an absence of low energy scattering . Determination of individual life-time and a statistical check upon the above " radioactive " description might be possible by measurement in the region 0 - 100 KeV.[46] Measurement of completed ranges of positron tracks will yield only minimum values of positron life-time. For example for positrons of different energy " duration of the measurable track " = t_{min} is given below:

E_k (MeV)	t (sec.)	
3	$0.7\ 10^{-11}$	in lead (Joliot)[46]
1	$0.3\ 10^{-11}$	" (Fermi-Uhlenbeck)[68]
0.8	$1.2\ 10^{-8}$	in air (Thibaud)[45]

Section B:- The Equation of the Conservation of Energy and Momentum for the Positron Annihilation by Two-Quanta.

§.1. Energy distribution of the annihilation in motion in the observation system. (Electron is always assumed to be at rest in this system).

For simplicity let us express the energy and the momenta in units of mc^2 and mc respectively; assuming $c = 1$, $m = 1$, the equations of the conservation of energy and momentum become as follows:

$$E + 1 = k_1 + k_2 \tag{8}$$

$$\vec{p} = \vec{k_1} + \vec{k_2} \tag{9}$$

where k_1 is the energy and momentum of the forward quantum, k_2 is the energy and momentum of the backward quantum, and E, p are the total energy, and, the momentum of the positron. On the other hand, according to the solution of Dirac's relativistic equation for a free particle the total energy is given by

$$E = \mp\sqrt{p^2 + \mu^2}$$

where p is equal to $mvc/\sqrt{1-\beta^2}$ and $\mu = mc^2$; hence we can write

$$p = \sqrt{E^2 - 1} \qquad (10)$$

Inserting this value of p in the equations (8) and (9), it can be shown that

$$1 - \cos\theta = (k_1 + k_2)/k_1 k_2 \qquad (11)$$

where θ is the angle between the two quanta. If we denote by θ_1 the angle which k_1 makes with the direction of incoming positron and by θ_2 the one corresponding to k_2, $\theta = \theta_1 + \theta_2$.

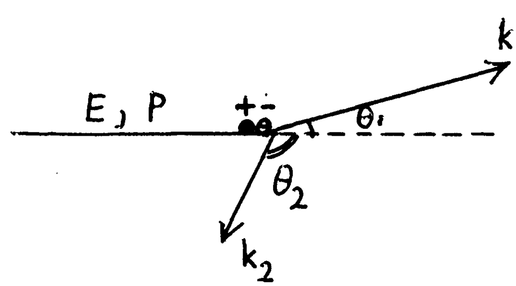

Fig(6)

(a)- For $\theta = \pi$ and $E_k \neq 0$, the left hand side of the equation is a maximum, hence k_1 and k_2 are bound to have a maximum and a minimum value respectively. The maximum and the minimum energy of the two quanta can be expressed in the following way: Since the two quanta are emitted in opposit directions, (9) becomes

$$p = k_1 - k_2 \qquad (12)$$

From (8) and (12) we obtain

$$k_1 = \tfrac{1}{2}(E + 1 + \sqrt{E^2 - 1}) \qquad (13)$$

$$k_2 = \tfrac{1}{2}(E + 1 - \sqrt{E^2 - 1}) \qquad (14)$$

Innthe extremely relativistic case, $v \to c$, (13) and (14) become

$$k_1 \to E - \tfrac{1}{2} \qquad (15)$$

$$k_2 \to \tfrac{1}{2} \qquad (16) .$$

It must be noted that the asymptotic value of the energy of the forward quantum is still less than the value of one-quantum annihilation radiation by $\frac{1}{2}$ $mc^2 = \frac{1}{4}$ MeV , assuming that the energy of single quantum for one-quantum annihilation radiation is $E + mc^2$. See Fig(7).

For $v = 0$ from (13) and (14) we obtain

$$k_1 = k_2 \equiv k_0 = 1$$

which corresponds to two-quanta annihilation at rest, and , each quantum in this case has an energy of $mc^2 = \frac{1}{2}$ MeV.

(b)- For $\theta \not< \pi$, the right hand side of (11) is a minimum when

$$k_1 = k_2 = (k_1 + k_2)/2$$

Then

$$(1 - \cos\theta)_{min} = 4/(E+1) \qquad (17)$$

This corresponds to the minimum value of the possible angle between these two equal quanta(each > than k_0), which is given by

$$\theta_{min} = \mathrm{Arc}\cos\left[1 - 4/(E+1)\right] \qquad (18)$$

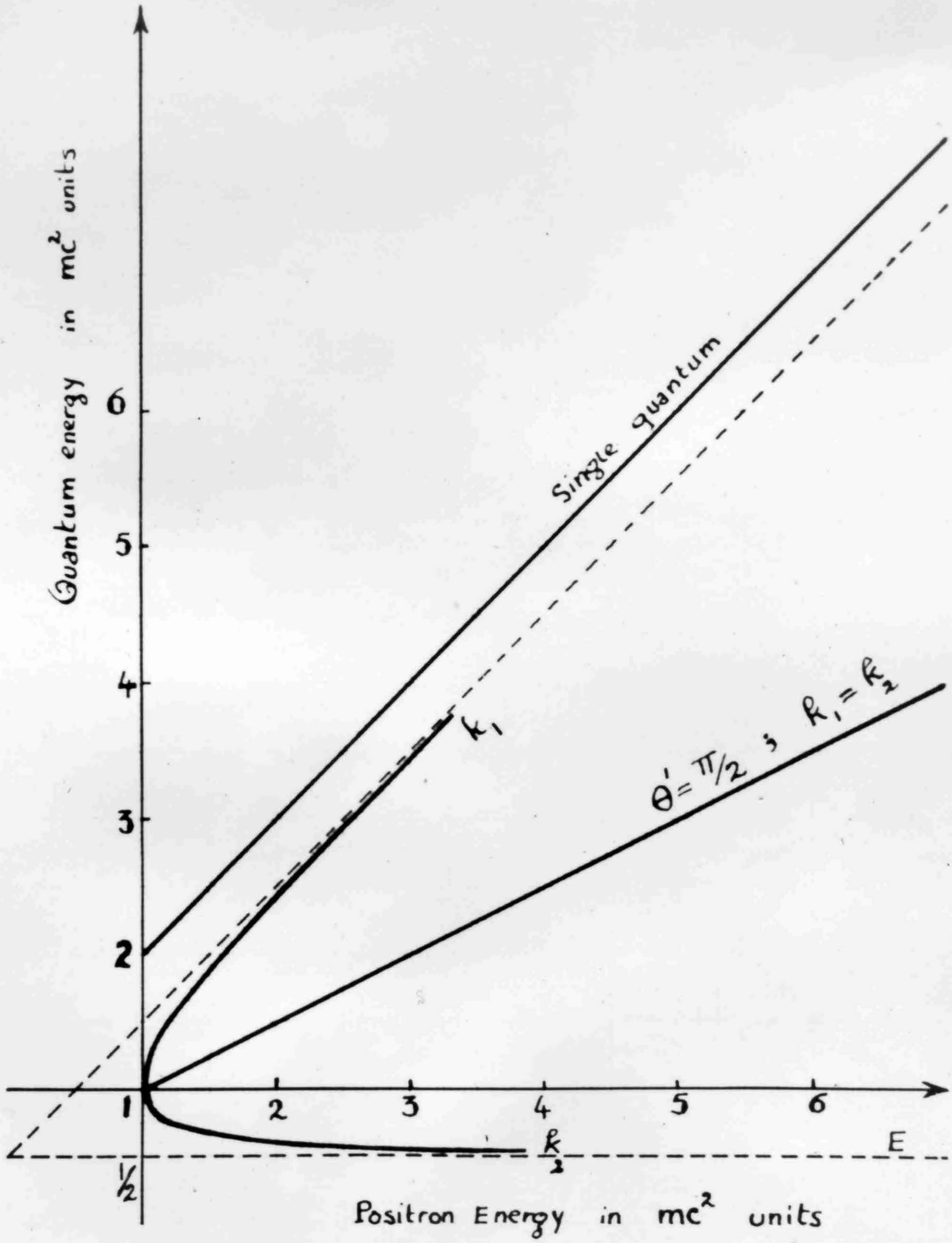
Quantum energy in mc^2 units
6
5
4
3
2
1
1/2
2
3
4
5
6
E
Single quantum
k_1
$\theta' = \pi/2$; $k_1 = k_2$
k_2
Positron Energy in mc^2 units

FIG. 7.

Or, substituting $\theta_0 = \theta/2$, where $\theta_0 = \theta_1 = \theta_2$, we can write

$$\theta_0 = \text{Arc tg}\left(2/(E-1) \right)^{1/2} \qquad (19)$$

Table.2 . gives the numerical values of θ_0 for different E.

TABLE 2

$E(mc^2)$	E_k(MeV)	$tg\theta_0$	θ_0	$k_1 = k_2$ (mc^2)
3/2	0.25	2	$63^0\ 34'$	5/4
2	0.5	1.414	$54^0\ 54'$	3/2
5/2	0.75	1.333	$49^0\ 54'$	7/4
3	1	1	45^0	2
9	4		26^0	5

However, in the process of annihilation in motion the probability of obtaining two quanta of equal energy is much smaller than that of two quanta emitted with minimum and maximum energy. Therefore in nearly all cases when a fast positron is annihilated before it comes to rest one of the annihilation quanta acquires practically all the energy and the other quantum is very soft having only an energy of about $\frac{1}{4}$ MeV. The variation of the quantum energy as a function of energy of the incoming positron is shown graphically in Fig(7). A frequency distribution curve[70] is given in Fig(8) for positrons of $4mc^2$ total energy.

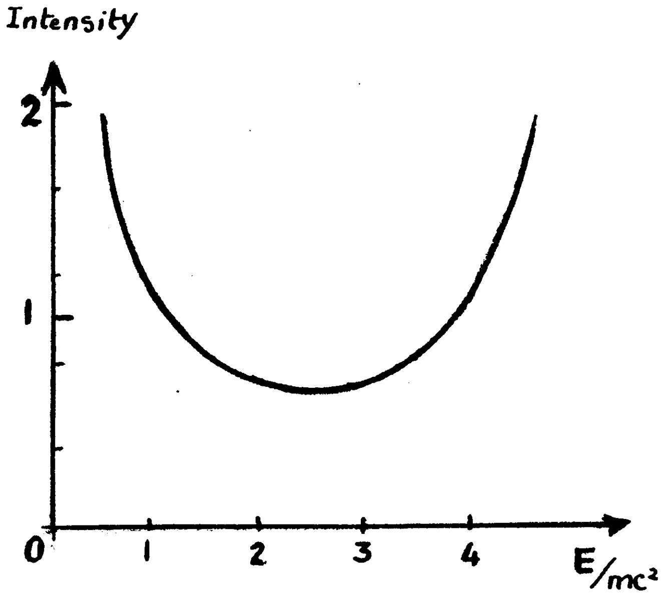

FIG. 8.

a- abscissa show the energy of quantum in mc^2 units.

b- ordinate shows the intensity of that particular quantum in average intensity units.

g.2. The angular distribution of the annihilation radiation in the observation system.

The angular distribution of the two-quanta process in the centre of gravity system is isotropic. The positron and the electron both are in motion in this system with a velocity of v/2 in opposite directions, and , the centre of gravity moves relative to the observation system with a velocity determined by the energy of the positron in that system.

(a)- Let us consider first a special case where the two quanta are emitted at right angle to the direction of motion of the positron and the electron in the centre of gravity system. If the velocity of the centre of gravity system is V, then the relation between the direction of the positron and the emitted quantum θ' in that system and θ in the observation system is given by

$$tg\theta = \frac{\sqrt{1 - V^2}\, c\sin\theta'}{V - c\cos\theta'} \qquad (20)$$

For the special case

$$\theta' = 90^\circ$$

maximum correspondance to $\pm 90^o$ of the C.G system in the observation system is

$$tg\theta = \frac{\sqrt{1 - V^2}}{V} \qquad (21)$$

(V is expressed in terms of c units.)

If $V = 0$ we find $\theta = \pi/2$ in the observer system . This

corresponds to the annihilation at rest for which the angular distribution is spherical in both system.
For $V \neq 0$, θ is a function of V and therefore is a function of E also. The relationship between E and V can be obtained as follows : Let the momentum of the positron, coming with a total energy E, be p_1 and the momentum of electron which is at rest(energy = mc^2) be p_2 in the observer system, and p_1' , p_2' in the C.G system respectively. Hence

$$\left.\begin{aligned} p_1 &= p \\ p_2 &= 0 \\ p_1' &\equiv - p_2' \end{aligned}\right\} \qquad (22)$$

The Lorentz transformation for the momenta follows the same rule as that of space coordinates. Therefore

$$p_1' = \frac{p_1 - VE_1}{\sqrt{1 - V^2}} = \frac{p - VE}{\sqrt{1 - V^2}} \qquad (23)$$

$$p_2' = \frac{p_2 - VE_2}{\sqrt{1 - V^2}} = \frac{- V}{\sqrt{1 - V^2}} \qquad (24)$$

From (22) and (23),(24)

$$p - VE = V$$

and hence $$p = V(E+1)$$

Substituting the value of p from (10) we obtain

$$V = \sqrt{\frac{E - 1}{E + 1}} \qquad (25)$$

Inserting this value in (20) we obtain a relation between θ , θ' and E but it is not practical in general.(A satisfactory graphical method relating E to θ (θ_1, θ_2)directly soon will be described). For the special case,θ' = $90^\circ$and $k_1 = k_2$ (in motion) from (21) and (25) θ becomes

$$tg\theta = \sqrt{2/(E-1)} \tag{19}$$

which is identical with the previously described value of θ_0 for this case.

(b)- For the general case $k_1 \neq k_2$ the value of the angle between the two quanta can be obtained in the following way: We know that the distribution of quanta in the observation is such that $k_1 + k_2 = p$ for a given momentum. Hence in Fig9) the point Q must be lie on an ellipse.

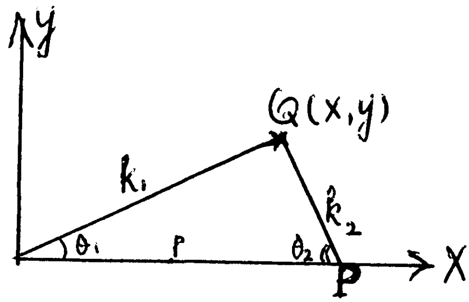

Fig9.

Let $\quad = 1+E = k_1 + k_2$

We have
$$k_1^2 = x^2 + y^2,$$
$$k_2^2 = (p-x)^2 + y^2 ,$$

hence the locus of Q is

$$x^2 + \frac{\varepsilon^2}{\varepsilon^2 - p^2} y^2 - px - \frac{\varepsilon^2 - p^2}{4} = 0$$

or

$$\frac{4}{\varepsilon^2}(x - p/2)^2 + \frac{4}{\varepsilon^2 - p^2} y^2 = 1$$

The semi-axis of the ellipse are $a = \varepsilon/2$, $b = \frac{\sqrt{\varepsilon^2 - p^2}}{2}$,

and the eccentricity $e = p/\mathcal{E}$. The eccentricity is thus a function of the positron energy. For $v \rightarrow 0$ the locus of Q becomes a circle and for $v \rightarrow c$ the locus becomes a parabola whose equation is given by $b = \sqrt{a}$.
For all energies of the positron the angular and the energy distribution of the two quanta can be shown in one diagram.
To be able to draw the different ellipses lying between these two above limit cases corresponding to various energy values of E, for simplicity , it is necessary first to draw the parabola $y^2 = x$, and after having placed the major axis of the ellipse given by E+1 on x , the minor axis can be determined from the intersection point of the line $x = a$ with the parabola . The ~~rayon~~ radius vectors of these ellipses originating from the focus will determine the energy of the forward and the backward quanta,and,the angle which they make with the direction x of incoming positron. An illustration of this method is given in Fig(10) . As seen the possible minimum and maximum value of the two quanta is limited by $a \pm x_0$ where $x_0 = p/2$ (the abscissa of the center of the ellipse. in Fig 9)
Hence the energy of the backward quantum for different energies of positron, corresponding to this minimum limit will vary ~~between~~ from one to half mc^2 as the total energy increases. In the case of two equal quanta different from ko = 1 the angle θ_0 is b/x_0 and the measured values check the previously calculated values of θ_0 (Cf. Table. 2.)

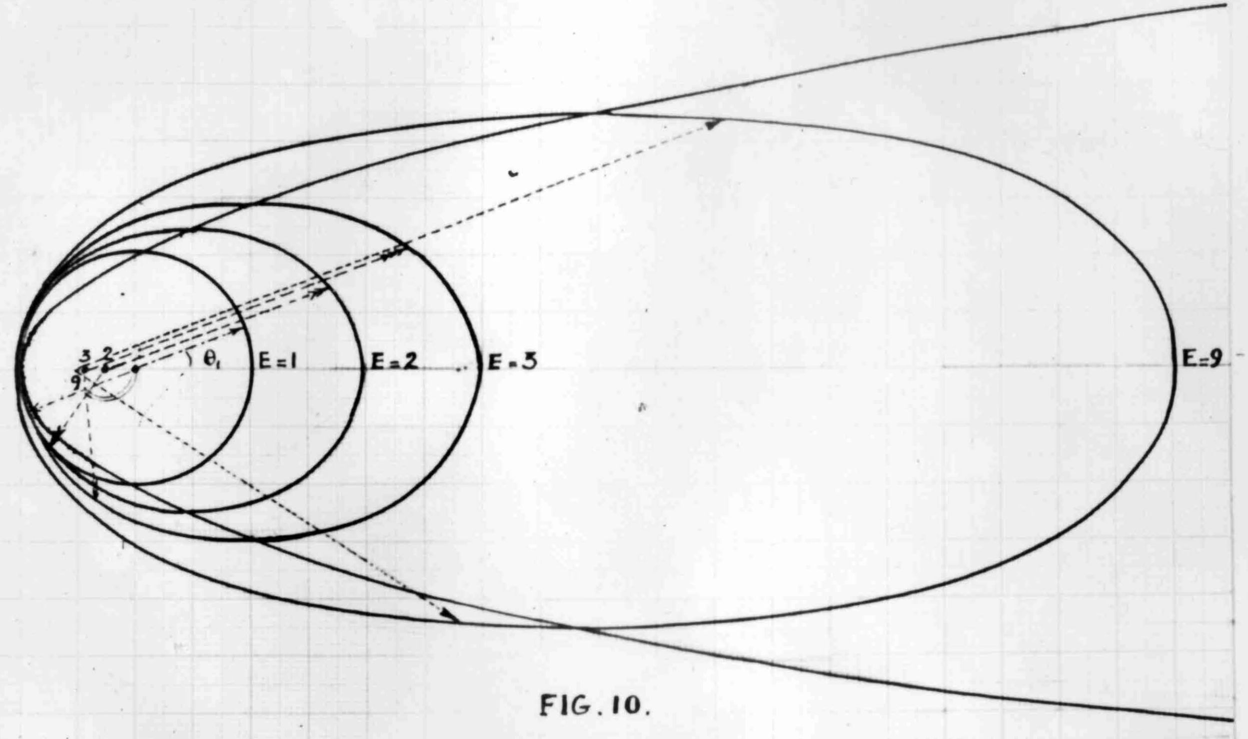

FIG. 10.

This figure illustrates the distribution of energy and direction of the two quanta resulting from the annihilation of a positron in motion for different energies E of the positron. The dotted lines indicate the magnitude and direction of the second quantum associated with a first quantum of given direction θ_1, for the various values of E.

Section C:- The Cross-section for One-quantum Annihilation as a Function of Energy.

The probability of one -quantum annhilation was first calculated by Fermi and Uhlenbeck[68] and found to be rather smaller than that of two-quanta annihilation for a particle of the same energy. The cross-section for this process is given approximately by*

$$\sigma_1 \equiv 2\Phi = \frac{4\pi}{3}\, r_0^2 \frac{Z^5}{137^4} \frac{p}{\mu} \qquad (N.R) \tag{26}$$

and for relativistic energies the exact formula is

$$\sigma_1 \equiv 2\Phi_{1k} = 4\pi r_0^2 \frac{Z^5}{137^4} \frac{1}{(\gamma+1)^2(\gamma-1)^{\frac{1}{2}}} \left\{\gamma^2 + \frac{2}{3}\gamma + \frac{4}{5} - \frac{\gamma+2}{\gamma^2-1} \log\left[\gamma + (\gamma^2-1)^{\frac{1}{2}}\right]\right\} \tag{27}$$

For a positron of 0.1 MeV the cross-section in lead is $25r_0^2$ i.e. = 1/16 of that for two-quanta annihilation in motion. In two-quanta annihilation the cross-section increases as energy decreases; but in one-quantum annihilation the cross-section increases with increase in positron energy up to a certain point and exhibits a rather flat maximum round about mc^2. The probability of one-quantum annihilation is extremely small for slow positrons because of the fact that they would never get near the K-shell owing to the repulsion of the nucleus. A curve illusrating the cross-section as a function of the total energy of positron is deduced theoretically by Jaeger and Hulme[71]. This is given in Fig(11).

* Heitler, Q.T.R. p.211

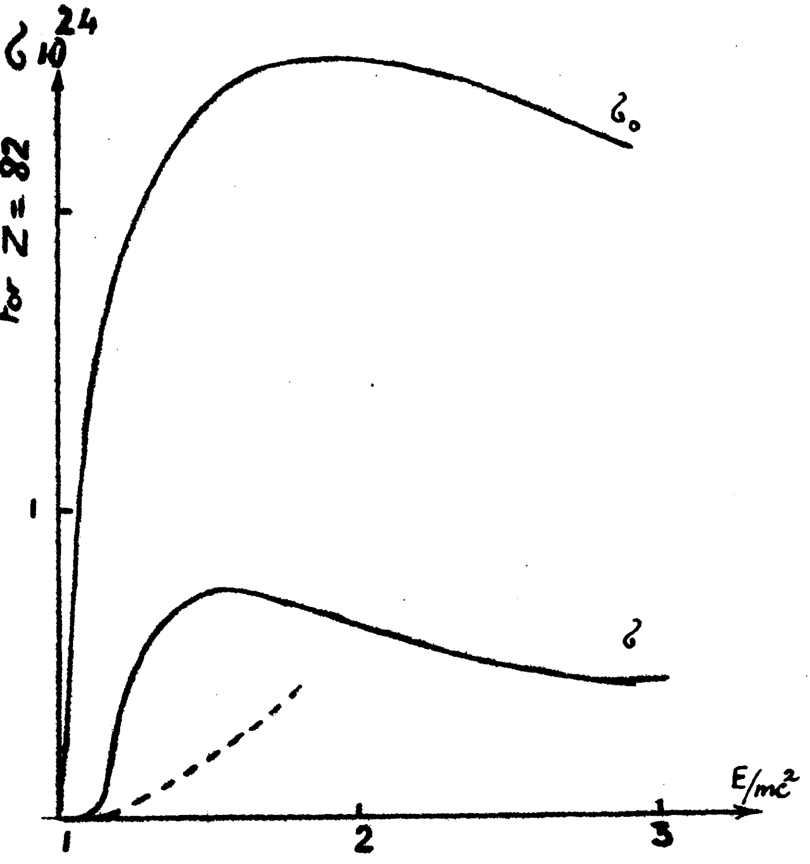

FIG. 11.

In this graph σ_0 represent the cross-section per atom calculated by Born's approximation. The exact criterion for the validity of this approximation is

$$2\pi\xi = 2\pi\alpha/\beta \ll 1$$

where $\alpha = Z/137$ and $\beta = v/c$. This condition holds also in the relativistic case where it is always satisfied except for very heavy elements, even then $Z/137\beta < 1$, for $\beta \rightarrow 1$. However to obtain an accurate value for the annihilation probability it is necessary to use a very accurate wave function in order to calculate the probability of an electron in the K-shell making a transition to a state of negative energy. The cross-section for that is represented by σ. The difference is considerable especially for low energy where the Born approximation is not valid. The correction factor is given by

$$\sigma/\sigma_0 = \frac{1}{\alpha\, 2\pi^2 e^{\alpha(\pi - 2\alpha)}}$$

For slow positron annihilation the correction factor is in fact appreciably different from this.[72] The dotted curve shows the result when a non-relativistic wave function is used.

The rate of annihilation of fast positrons by electrons in the K-shell is theoretically investigated by Bahbha- Hulme[73]. All their calculations are valid for $E \geqq 2\mu$, that is when the kinetic energy E_k is not small compared with $\mu = mc^2$ i.e. $\beta \sim 0.8$ or greater and also $\alpha \ll 1$ that is to say for elements of small atomic number.

With this restriction, the total number of annihilation processes with a beam of positrons of unit intensity falling on the atom i.e. annihilation cross-section due to electrons in the K-shell ,

$$\sigma = \frac{he^2}{m^2c^3}\alpha^5 Z^5 \frac{\beta\gamma^2}{(1+\gamma)^3}\left\{-\frac{4}{3} + \frac{1-2\gamma}{\gamma(1-\gamma)}\left[1 + \frac{\gamma^2}{2\beta}\ \lg \frac{\gamma^2}{1+\beta^2}\right]\right\}$$

In the limit of very large energies $\gamma \to \infty$, and we obtain for the cross-section

$$\sigma = 6.8\ 10^{-23}\ (\alpha Z)^5 \frac{mc^2}{E}$$

which does not differ from the above more exact formula by more than 2% for energies greater than 100 mc^2 and the deviation is less than 15% for energies greater than 10 mc^2. A table of values of σ_1 is given below for two different energies and various elements. A comparison of the cross sections per atom for one-quantum and two-quanta processes is also indicated.

TABLE.3 .

Total energy		Cross-sections			
E		O_8	Al_{13}	Fe_{26}	Pb_{82}
2 mc^2	σ_1	1.08 10^{-29}	1.23 10^{-28}	3.93 10^{-27}	1.23 10^{-24}
	σ_2	1.88 10^{-24}			1.93 10^{-23}
100 mc^2	σ_1	4.59 10^{-31}	5.20 10^{-30}	1.65 10^{-28}	5.21 10^{-26}
	σ_2	0.90 10^{-25}			0.92 10^{-24}

As seen from the above table, one-quantum annhilation is negligible in light materials; even for lead it is still very much smaller than that of two-quanta: For a positron with energies in the range 3 mc^2 - 20 mc^2 the one-quantum annhilation is about 16% of two-quanta process(Jaeger-Hulme) and for $E \sim 2mc^2$ and $100mc^2$ is about 5-6 percent(Bhabha-Hulme) For oxygen the two-quanta process is greater by a factor of the order of 10^5 .

The cross section for one -quantum annihilation for a strongly bound electron i.e K-shell electron, and also L-shell electron, neglecting the screening by the outer electrons, are given by Fermi-Uhlenbeck(68). σ_L can be expressed by

$$\sigma_L = \sigma_K \cdot \frac{1-Z^2/W}{32(4-7Z^2/W)}$$

where W is the energy of positron expressed in Rydbergs. For large energies $W > 10^5$ (about 3 mc^2), σ_L is at least a factor of 10^2 smaller than σ_K .(For positrons of low energy screening can not be neglected.)

The rate of destruction for one quantum process is also given by the above authors. Numerical values of R for lead are given below. They indicate that the positrons which have completely lost their initial velocity can not give rise to a hard component because of the very small rate for this process at very low energies.

W (energy in Rydberg)	R = δ Nv (rate of destruction for one quantum process) (N is electronic density)
1	$2.\ 10^{-5}$
100	10
10000	$5\ .\ 10^{7}$
75000	$10\ .\ 10^{8}$

The rate of destruction for positrons annihilation at the beginning of their path is found to be higher since the probability for destruction is then much higher. But even the maximum rate of 10^{9} suggests a very small total probability of destruction by one quantum process. To obtain an estimate, for a positron of 1 MeV ($r = 0.06$ cm in lead and time required is about $3\ 10^{-12}$) from the rate of 10^{9} we get, as total probability, $3\ 10^{-3}$. As the authors pointed out, this result can be increased appreciably by introducing relativistic correction in the calculation of the cross section. For a positron of energy of 1 MeV the rate value for transition to S-shell is $0.4\ 10^{9}$ non-relativistic and $2.3\ 10^{7}$ relativistic.

Section D:- Ratio of One-quantum to Two-quanta Annihilation.

Since there are two K-electrons in an atom which may give rise to one-quantum annihilation and Z electrons altogether which are capable of two-quanta annihilation, the ratio of the processes is, according to the formulae giving the cross-sections per atom (δ_1 , δ_2) or per electron (φ_1, φ_2), given by ,

$$\sigma_1/\sigma_2 = (2/Z).\Phi_1/\Phi_2 = (\alpha_0 Z)^4 \chi(\gamma)$$

where α_0 is the fine structure constant and $\chi(\gamma)$

$$\chi(\gamma) = 4\left(\frac{\gamma-1}{\gamma+1}\right)^{\frac{1}{2}} \frac{\gamma^2-2/3\gamma-4/3-(\gamma+2)(\gamma-1)^{-\frac{1}{2}}\lg[\gamma-(\gamma-1)^{\frac{1}{2}}]}{(\gamma^2-4\gamma+1)\lg(\gamma+(\gamma^2-1)^{\frac{1}{2}})-(\gamma-3)(\gamma-1)^{\frac{1}{2}}}$$

As shown on the graph of $\chi(\gamma)$ against E, fig 12 (70), the pronounced maximum value of the curve lies in the range 5–9 mc^2 which corresponds 2–4 Mev kinetic energy, and $\chi(\gamma)$ has got a value of 1.32 for which the ratio of the two processes is 0.185 for lead. For $E = 2\ mc^2$ i.e. $E_k = 0.5$ meV, $\chi(\gamma) = 1$ and the ratio, of one-quantum annihilation to two-quanta annhilation as calculated from $(\alpha_0 Z)^4$ in different materials is given in table. 4 . The results of Bhabha-Hulme are shown for comparison

TABLE. 4.

Z	O_8	Al_{13}	Fe_{26}	Pb_{82}
$(\alpha_0 Z)^4$ Bethe($2\Phi_1/Z\Phi_2$)	$1.163\ 10^{-5}$	$8.107\ 10^{-5}$	$1.29\ 10^{-3}$	$12.83\ 10^{-2}$
B-H ($\Phi_1/Z\Phi_2$) *	$0.574\ 10^{-5}$			$6.37\ 10^{-2}$

* Because of a factor of 2 missing in the calculation of Bhabha-Hulme the result should be $1.148\ 10^{-5}$ for oxygen, and, $12.74\ 10^{-2}$ for lead which is in quite good agreement with Bethe's result.

$\chi(\gamma) \to$ zero for $\gamma \to 1$ which means that for very small energies of the positrons, one-quantum annihilation is very improbable compared with the two-quanta type, This is in agreement with the result of Fermi-Uhlenbeck (loc. cit.). According to their calculation , the cross-section is even smaller than Bethe's at low energies owing to the repulsion of the positron by the atomic field, and the screening effect. These have not been taken into account in Bethe's formula which are based on Born's approximation. (The screening will tend to diminish the probability for the outer shells still further; for Pb the probability of one quantum annihilation by the outer electron is about 16% of that by K-electron[70]).
$\chi(\gamma)$ reaches a very flat maximum value of 1.2 over the region about 3 mc^2 to 20 mc^2. The probability of the one-quantum process over this whole energy range is proportional to that of the two-quanta annihilation e.g., for lead it amounts to 16% of the latter, whereas for air the one quantum annihilation is extremely rare, having about 10^{-5} times the probability of the ordinary two-quanta annihilation[70] which is in good agreement with Bhabha-Hulme[72] result. At very high energies, the "ratio" decreases as $1/\log\gamma$, i.e. the one quantum annihilation becomes less probable as well as the two-quanta one. For comparison, σ_1 and σ_2 are illustrated together in Fig(13), and their ratio as a function of energy

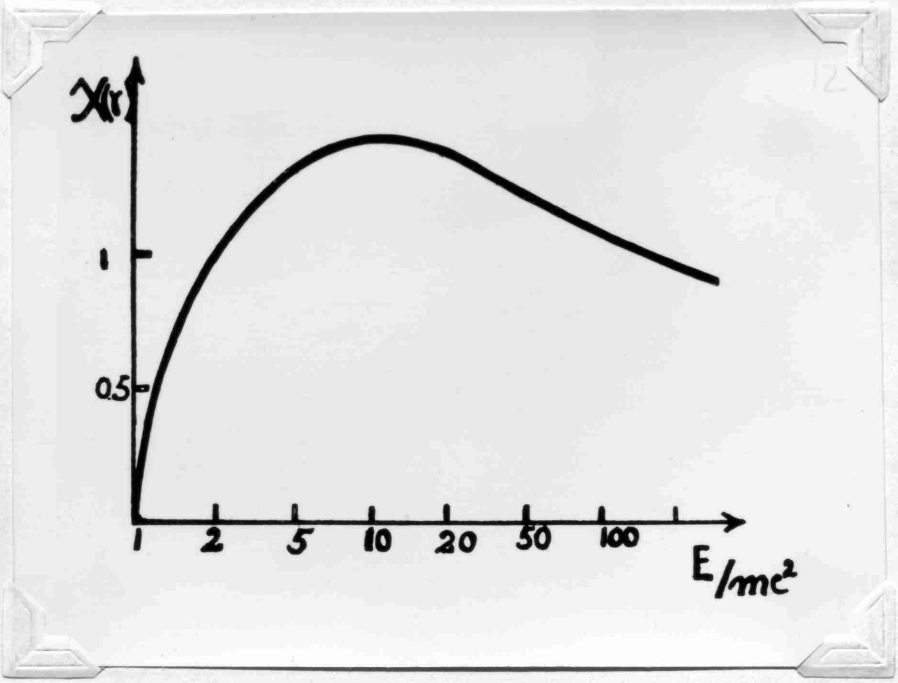

χ(r)
1
0.5
1
2
5
10
20
50
100
E/mc²

FIG. 12.

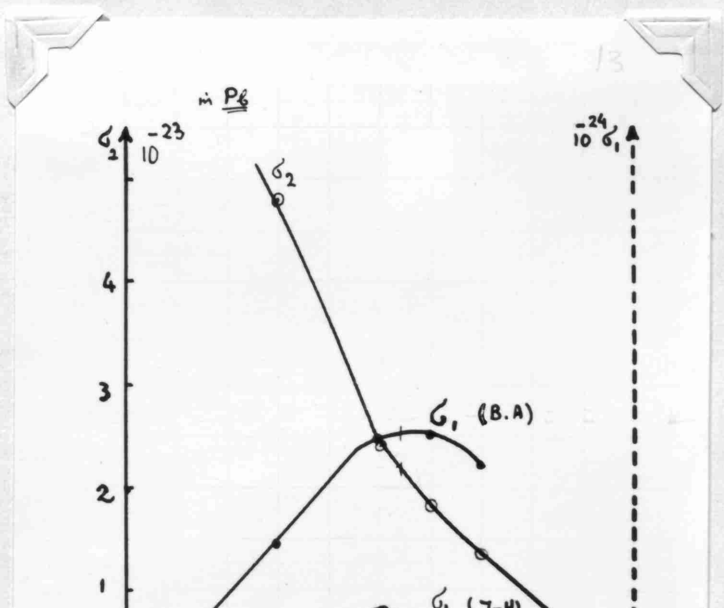

in Pb
σ₂ 10⁻²³
10⁻²⁴ σ₁
σ₂
σ₁ (B.A)
σ₁ (J-H)
4
3
2
1
0.1
0.5
1.0
2.0
10.0
E_K/mc²

FIG. 13.

is given graphically in Fig(14) and Fig(15). The values of σ_1 are deduced from curve in fig(11), and σ_2 is numerically calculated by transfering the curve of differential probability into cross-section. The necessary procedure for that is to divide the ordinate of the Fig(3) by the number of electrons per cm^3 and multiply by the energy loss per cm of path given in Fig(1). The numerical detail of the calculations is shown in table. 5 .

TABLE. 5 .

E_k (mc^2)	E (mc^2)	wdE (10^{-4})	dE/dx (cm^{-1})	Φ_2 $(10^{-25} cm^2)$	Φ_1 cm^2 (10^{-24})	σ_2 cm^2 (10^{-23})	σ_1 $(10^{-24}$ $cm^2)$	σ_1/σ_2
0	1			max.	0	max.	B.A 0 / J-H 0	B.A 0 / J-H 0
0·1	1.1	228	70	5.907	0.725	4.844	1.45 / 0.625	2.99 / 0.05
0.5	1.5	310	25	2.870	1.2	2.354	2.4 / 0.77	10.2 / 3.3
1	2	279	22	2.306	1.25	1.935	2.5 / 0.65	12.92 / 3.36
2	3	195	23	1.661	1.1	1.362	2.2 / 0.45	16.15 / 3.3
10	11	40	42	0.617		0.505		~16 / ~3.3

<u>Remark</u> :- The ratio ofone-quantum annihilation to two-quanta should be expressed by $2/(Z-2).\Phi_1/\Phi_2$ instead of $(2/Z)\Phi_1/\Phi_2$ because the two K-shell elctrons are included in the number Z, and they can only give rise to one-quantum annihilation since they are so near to the nuclei. Hence the two-quanta annihilation is Z-2 times probable and that is maximum. However the difference is small, only a few percent.

—o0o—

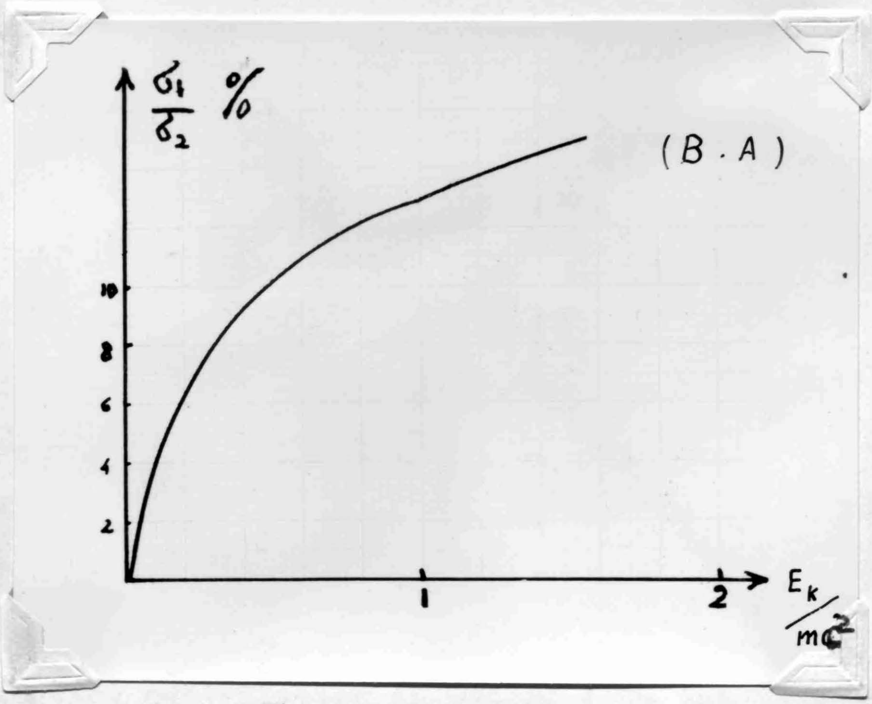
$\frac{\sigma_1}{\sigma_2}$ %
(B . A)
10
8
6
4
2
1
2
E_k/mc^2

FIG. 14.

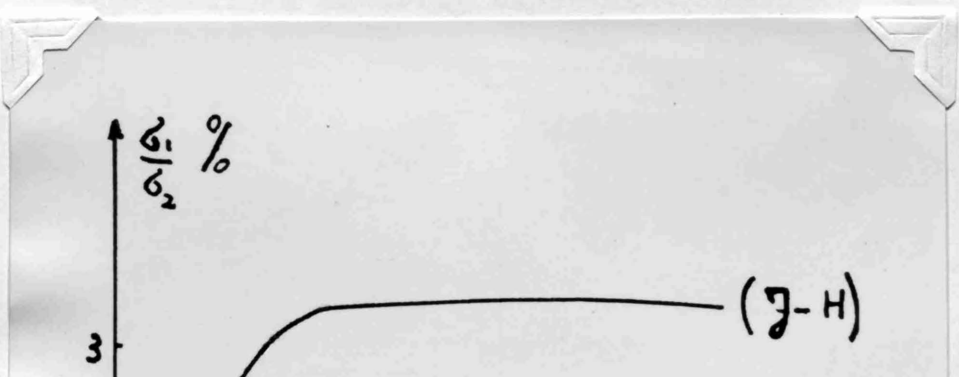
$\frac{\sigma_1}{\sigma_2}$ %
(J- H)
3
2
1
1
2
E_k/mc^2

FIG. 15.

CHAPTER III

THE ANGULAR DISTRIBUTION OF TWO-QUANTA ANNIHILATION RADIATION *

The purpose of this experiment was two-fold:

(a) To make a more detailed investigation of the directions of the two quanta produced by positron annihilation at rest.

(b) To attempt to reach a conclusion on the existence of two-quanta annihilation in motion from the form of the angular distribution curve.

Improvements on early experiments were:

(1) The use of a source of much greater intensity,

(2) the use of a new counter of high γ-ray efficiency and good directional resolution,

(3) the small resolving time of the recording circuits.

The Multiple Parallel Plate Gamma-ray Counter

The low efficiency of the ordinary Geiger-Müller counter for γ-rays, renders difficult and tedious any experiments involving γ-ray coincidences. Methods of

---

*This work was carried out before Beringer's paper came to our attention.

increasing the efficiency by using an assembly of several plates with wires between them have been described previously.(74,75) A new type of parallel plate counter was designed for this experiment.

Fig. 16 illustrates the construction. The counter is in the form of a pyramid of square cross-section. Sixteen copper plates, 1.6 mm. thick, of edge varying from 1" to 3".5 were mounted 1cm. apart in slots cut in two ebonite walls (A,B). The two other walls of the pyramid consisted of copper plates screwed to A,B. To form the anodes a tungsten wire 0".004 in diameter was threaded through holes drilled in A and B so that the wire occupied a central position between successive plates. The whole assembly was enclosed in a brass lining $\frac{1}{8}$" thick, the larger end-plate carrying a small filling tube and anode terminal.

Tests of different mixtures showed that a filling of 7 cm. argon and 1 cm. alcohol gave satisfactory temperature stability. The operating potential was 975 volts with a plateau of about 50 volts. The low value of the latter was probably due to inaccuracies in the centralisation of the wires. A comparison of the efficiency of the counter with that of G-M. counter was made by mounting a small Co^{60} source at the apex of the pyramid and placing the G - M.

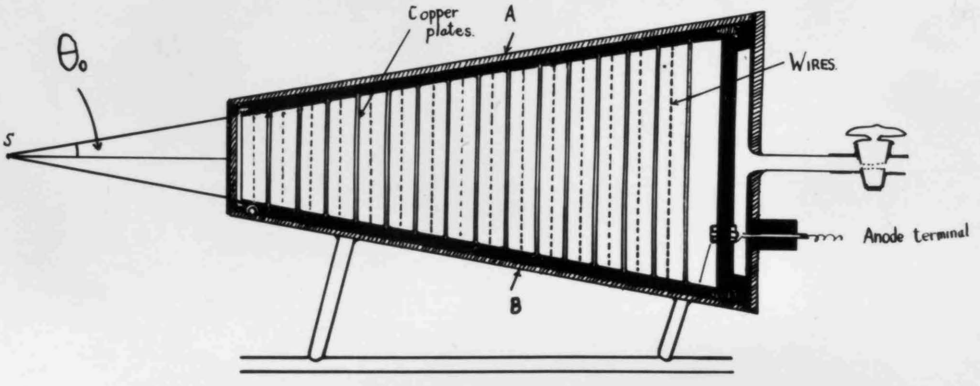

Parallel plate counter

FIG. 16

counter in such a position that it subtended the same solid angle. The gain in efficiency depended on the filling, the factor being 12.5 for 9 cm. total pressure and 10.3 for 8 cm. The reduction from the possible value of about 15 can be attributed to inefficiency of collection of electrons from the outer regions of the larger sections.(This defect can be remedied by inserting two additional wires in these sections)

Experimental arrangement.

Two counters of above construction were used in coincidence; one of them was fixed and the other rotated in a circle with the source as centre. The source was a copper wire (Cu^{64}) of 2.6 mm. in diameter, surrounded by Aluminium 1 mm. thick (sufficient to stop all positrons) placed at the apices of the pyramids. The anode wires of each counter were vertical and in the same plane as the source. Over 5000 coincidence counts were recorded in one series of experiments. (resolving time of the circuit 0.9 μ sec.). The variation of the coincidence counting rate with θ , the angle between the axes of the counters, is shown in Fig. 17 . The ordinate K_r is the number of real coincidences per minute, after corrections for background (cosmic rays and chance coincidences) and decay have been made. The discrepancy from a single line at 180^o is mainly due to the angular width of the counter.

If we assume that two quanta are emitted exacly in opposite

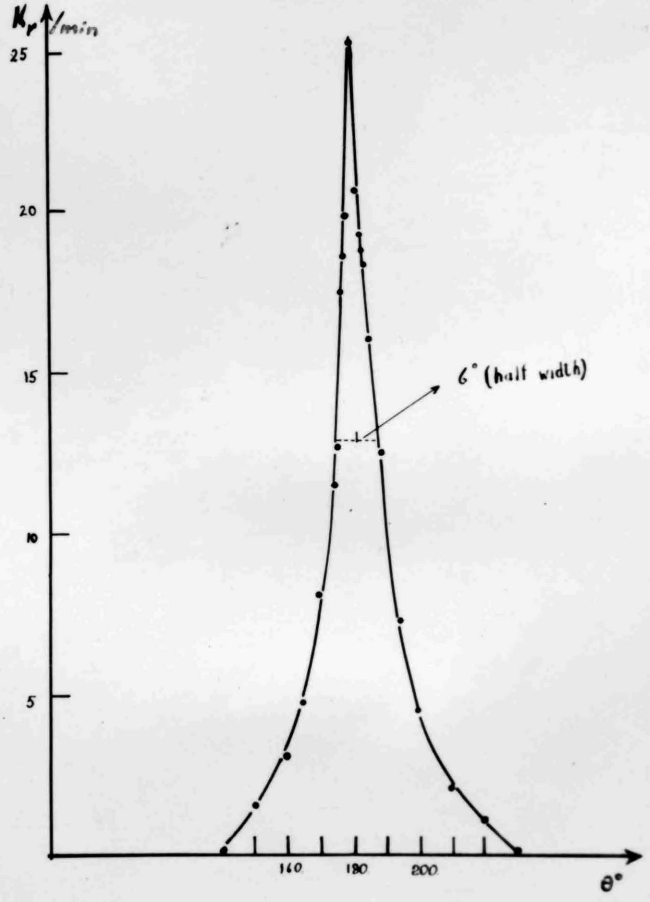

ANGULAR DISTRIBUTION OF ANNIHILATION RADIATION.

FIG. 17

directions, the rate of real coincidences due to the annihilation radiation would be a function of the angle β common to both counters, as one counter deviates by an angle α from $\theta = 180^{\circ}$.

Let θ_0 be the half-angle subtended by counter (which is 10° in our case) then,

$$\beta = 2\theta_0 - 2\alpha$$

If we denote the rate of real coincidences by K_r, then

$$K_r = \chi\varepsilon \frac{\beta}{2\theta_0} = \chi\varepsilon\left(1 - \frac{\alpha}{\theta_0}\right) \qquad (28)$$

where

$$\chi = N_0\,\omega\,\varepsilon$$

is the number of single counts per min. in one counter, ε, the efficiency of that counter (ω, is the effective solid angle subtended by the counter). The relation (28) gives us two straight lines which intersect at $\alpha = 0$ where $K_r = \chi\varepsilon$ and meet the θ axis at $\theta = \pm\alpha$. If θ_0 is not small, equation (28) takes the form of

$$K_r = \chi\varepsilon \frac{tg^2(\theta_0 - \alpha)}{tg^2\theta_0} \qquad (29)$$

which gives two slightly curved lines. See Fig(17a).

The positive value of K_r outside the region $180^{\circ} \pm 10^{\circ}$, can be attributed to the effect of scattered quanta from the counter walls or the source itself.

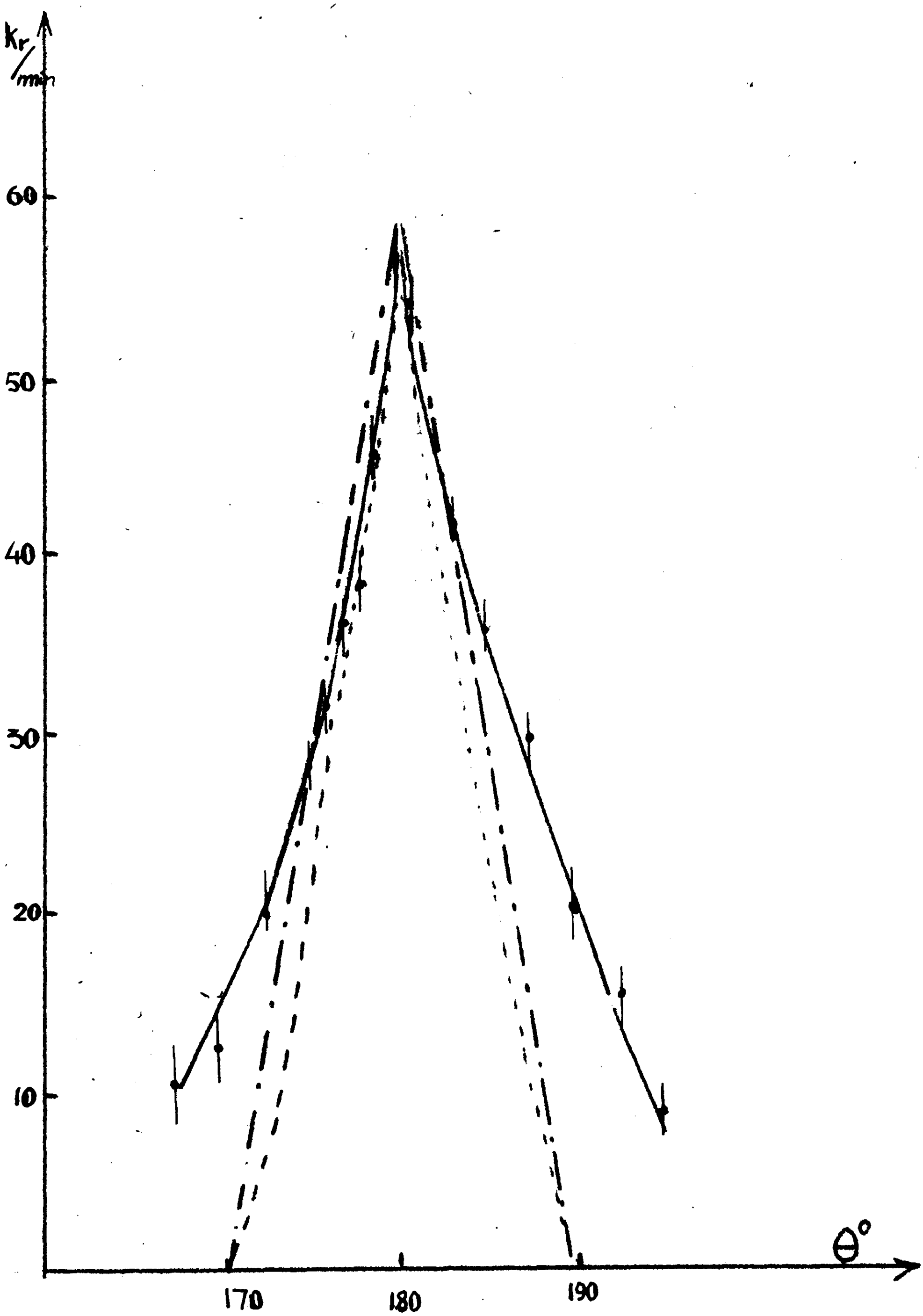

FIG 17 a

Angular distribution curve obtained by using a more intense source. Dotted lines illustrate the 180° emission of the two-quanta.

K_r , can be calculated in the following way from the observed total number of coincidences K_t . The latter was assumed to be the sum of the following components:

$$K_t = K_r + K_s + K_c + K_{sc} + K_0$$

where;

K_s is the number of the chance coincidences due to the presence of the source, which is given by

$$2n_1 n_2 \tau$$

where n_1 , n_2 are the numbers of single counts in the first and second counter and τ is the resolving time of the circuit*

K_c is the number of chance coincidences due to the presence of the high background which is equal to $2a_1 a_2 \tau$ where a_1 , a_2 are the number of cosmic ray counts per minute in each counter (about 2000 /min.) ‡

K_{sc} is the number of chance coincidences between the source and cosmic rays which is equal to $2\tau(n_1 a_2 + n_2 a_1)$

K_0 is the number of genuine cosmic ray coincidences.

Inserting these values in the above equation we obtain

$$K_t = K_r + K_0 + 2\tau(n_1 + a_1)(n_2 + a_2)$$

The quantities we measure in the presence of the source are $N_1 = n_1 + a_1$, $N = n_2 + a_2$ and K_t, and in the absence of the source we measure $K = K_0 + K_c$, a_1, a_2. Therefore the convenient form of the correction formula would be

$$K_r = K_t - K - 2\tau(N_1 N_2 - a_1 a_2)$$

*. Strictly $K_s = 2\tau(n_1 - K_r)(n_2 - K_r)$ but K_r is of order 0.1% of n_1 and n_2

‡ With similar approximation to above.

The results of the experiment are shown on the next page.

The experimental value of the peak is slightly less than the estimated value $K_r = X\mathcal{E}$. This difference might be du due to the Cu^{64} nuclear γ - ray[53,76] which produces single counts but not coincidences.

If we denote the number of nuclear γ - rays by N_1 and annihilation radiation quanta by N_2 emitted in to 4π and the efficiency of the counter for both γ - rays $\mathcal{E}_1$, $\mathcal{E}_2$ respectively, the number of single counts X detected in each counter will be

$$X = X_1 + X_2$$

where

$$X_1 = N_1 \mathcal{E}_1 \omega$$

$$X_2 = N_2 \mathcal{E}_2 \omega$$

As we know[53] there is one γ - quantum of 1.35 MeV per 40 positrons, and 2 γ - quanta of 0.51 MeV per positron;

Therefore:

$$N_1 = \frac{2.5}{100 \times 2} N_2 .$$

It was found, by comparison of the relative efficiency of the pyramid counter with different sources of different energy, that for 0.5 MeV radiation only a factor of 5.6 was obtained in favour of the pyramid counter against G -M counter.

Hence $\mathcal{E}_1 \geqq 2\mathcal{E}_2$

$$\frac{X_1}{X_2} = \frac{N_1}{N_2}\frac{\mathcal{E}_1}{\mathcal{E}_2} \simeq 3\%$$

Absolute time in minute TT	$e^{\lambda t}$ decay cor. factor	θ^0	K_t' total count per minute	K_t corrected for decay	K_r corrected for chance+backgr.
0	1	180	32.1	32.1±146	24.78
13.5	1.010	181	28.3	28.58±1.53	20.36
25	1022	179	27.1	27.79±1.65	19.57
35.5	1.031	182	26.4	27.21±1.52	19.00
46.5	1.041	178	25.4	26.55±1.45	18.33
50	1051	183	25.5	26.80±1.60	18.58
62	1.061	177	23.9	25.42±1.51	17.20
73	1.071	184	24.6	26.35±1.52	18.13
84	1.081	176	19.5	20.60±1.50	12.38
95	1.090	185	22.0	23.98±1.51	15.76
105	1.100	175	17.7	19.47±1.35	11.25
145	1.140	190	18.8	20.52±1.42	12.30
~~155~~	1.144	170	14.0	16.02±152	7.80
190	1.183	160	9.3	11.00±0.60	2.78
235	1.234	200	10.1	12.46±0.51	4.24
250	1.252	195	13.6	15.30±1.20	7.08
260	1.263	165	10.0	12.63±1.0	4.41
270	1.273	210	8.9	10.03±1.0	1.81
280	1.286	150	7.4	9.50±0.9	1.28

Hence the presence of the nuclear γ- rays will reduce the value of the peak by 3%.

The experiment gives no definite indication of radiations from the annihilation of positrons in motion for the following reasons ;

a- Small probability (cross section) of annihilation in motion at small energies , compared with the annihilation at rest.

b- The large compton scattering effect from the source and the surrounding for which the cross section varies with Z as in the case of two quanta annihilation.

c- The low coincidence rate at the base line of the distribution curve (beyond $180^{0} \pm \theta_{0}$) which entails large statistical errors. This is where the annihilation in motion (mostly) would be observable.

For further investigation of this phenomenon a counter of even higher efficiency would be desirable. This could be achieved by increasing the number of sections and using lead[77] plates of suitable thickness.

— --o 0 o-- —

CHAPTER IV

THE STUDY OF ONE-QUANTUM ANNIHILATION. PART.I.

In Chapter II we have seen that the cross section for one quantum annihilation varies with Z^5 while the cross section for two - quanta annihilation varies as Z. This factor of Z^4 in the ratio of the cross sections means that one- quantum annihilation would be negligible in aluminium as compared with that in lead. Thus if absorption curves are taken with these two substances as annihilators one would expect a difference between the two curves which would be due to the greater number of hard γ - rays produced by one-quantum annihilation in lead.

The experimental technique used for this experiment consisted of coincidence measurements in two counters between which an Al absorber of varying thickness could be inserted. The γ - ray energies were measured in terms of the range of the converted electrons in aluminium. The ratio of the number of real coincidences to the number obtained with no absorber was plotted against the energy of the γ - rays.

Apparatus: Two thin walled ~~rectangular~~ counters were made from a rectangular copper wave guide of dimensions 2½" x 1" x 1½"

The windows were formed by soldering Cu foils 0.001" thick, on to both sides of this cathode frame (1.6 mm. thick). The anode was a 0.008" tungsten wire of $1\frac{1}{4}$" effective length. The counters were filled with a mixture of alcohol and argon up to a total pressure of 7.5 cm. in the ratio of $1\frac{1}{2}$ to 6 cm. respectively. Under these circumstances a plateau of 200 volts minimum was obtainable at an operating voltage of 1100- 1300 V.

Experimental Arrangement:

Two of the above counters were placed 4 mm. apart and the first counter window was covered with 0.4 mm. of lead sheet. This absorbed any incident β- rays and also increased the efficiency of the counter by a factor of more than two. This factor was determined by measuring the efficiency of the counter with and without the lead covering, using a standard Radium source of strength 0.6 mc. The absolute value of the efficiency (with lead on) was found by comparison with a G - M counter of known efficiency. The values obtained for 0.5 MeV and 1 MeV (approx.), were 0.2 and 0.45 percent.

The source consisted of an activated Cu^{64} -foil 0.001" thick placed $\frac{3}{4}$" from the first counter. When it was covered on both sides with Al foil 1.6 mm. thick or Pb foil 0.4 mm. thick alternately (each thick enough to stop all the positrons) about 30,000 to 40,000 counts per min. were recorded in the first counter.

A quick run within the life of one Cu^{64} source gave a satisfactory result. Using the Pb and Al annihilator alternately two absorption curves were obtained, the curve for Pb being above the Al curve. (see Fig.18).

We should expect the Pb curve to be above the Al curve for the following reason: Let f be the factor for the abundance of one-quantum annihilation compared to the two-quantum so that $f \ll 1$. Let us indicate the efficiency of the counter for one-quantum annihilation by ε_1 and for the two-quantum process by ε_2. We should expect, for n positrons, nf of one-quantum annihilation and 2n(1-f) of the two-quanta type. Then the number of γ's which we would detect in the same counter at 4π solid angle is

$$2n(1-f)\varepsilon_2 + nf\varepsilon_1 = n\left[2\varepsilon_2 + f(\varepsilon_1 - 2\varepsilon_2)\right] \quad ---(30).$$

From measurements of ε_1 and ε_2 as functions of the quantum energy we know that $\varepsilon_1 - 2\varepsilon_2$ is positive. Further, if f is positive (i.e. if the one-quantum process occurs), the additional term $f(\varepsilon_1 - 2\varepsilon_2)$ is positive in (30). Thus the larger f is, the greater is n_c^*, and hence the curve for Pb is expected to be slightly above the curve for Al.

To make certain that this difference was real the experiment was repeated with very long readings. In order to reduce the statistical error to a satisfactory value, especially at the greater absorber thicknesses where the number of coincidences per minute is very low, 10-15 hours continuous counting

(n_c = no of coincidences in the two counters) was required for each point. Since the half-life of the Cu^{64} is only 12.8 hours it was necessary to use different sources of slightly different size and distance for various points of the absorption curve.

To be sure of the consistency of the apparatus during long counting periods, single counts in both counters were taken for one minute and the efficiency of the counters was checked by means of the standard radium source after each run.

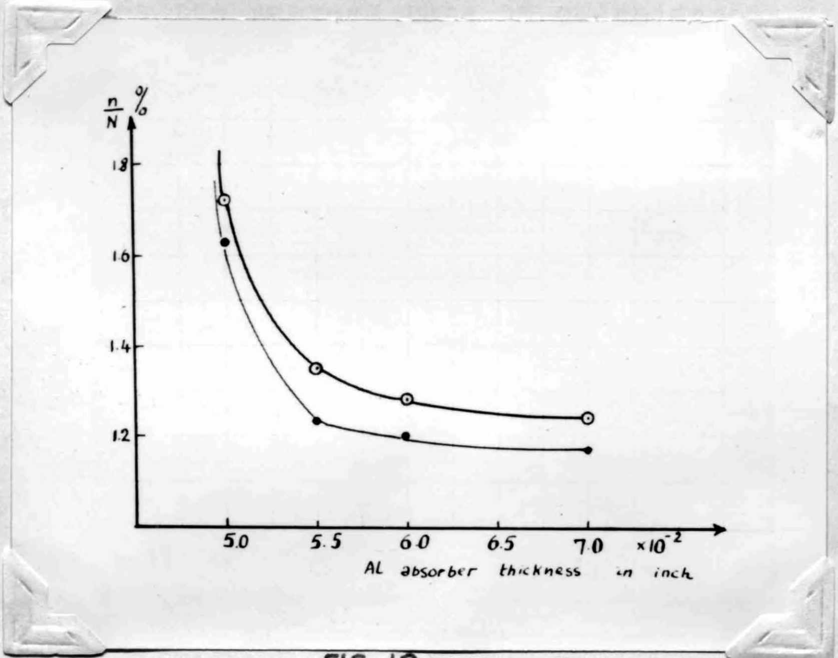

FIG. 18

At the time of performing this experiment only one scaler was available and therefore single counts and coincidence counts could not be made simultaneously. The procedure for taking readings for each point was as follows:

(1) Single counts in both counters without absorber.

(2) Number of coincidences with no absorber.

(3) Number of coincidences with a given absorber thickness.

(4) Single counts in both counters with absorber.

(5) Check of efficiency of counters.

This procedure was repeated for each annihilator. The total number of coincidences divided by the time of observation was taken as the average rate of coincidences at the middle of this interval, and the decay correction factor $e^{\lambda t}$ was applied, t being the period, from the middle of one interval to the middle of the next interval. It can be shown that the error involved in this assumption is smaller than 3% even for $t = 19$ hours.

The chance coincidences from the source were calculated from the relation $2n_1n_2\tau$, where, τ is the resolving time of the recording circuit. This was measured and found to be 1.65 μsec. The same kind of decay correction was also applied to the chance coincidence counts; in this case the correction factor was $e^{2\lambda t}$. (The chance coincidences between cosmic rays and source were neglegted since the cosmic ray count is extremely small; a maximum of 70-75 per min, in each counter.) The true cosmic ray coincidences were measured as a function of the absorber thickness.

The real number of coincidences n_c from the

╪ See opposite.

The justification for normalisation to the no. of coincidences for zero absorber thickness (N_c) lies in the fact that both theoretically and from these measurements one quantum (1 Mev) radiation is < 1% of the two quantum radiation from the annihilator. Normalisation should therefore result in differences of ordinate of < 1% at values of t > range of 0.5 Mev electrons. Further justification that the observed differences of ordinate at such t values is not accountable to the normalisation process may be derived from

(a) the fact that the observed N_c values for ~~Al~~ Pb & Al were < 1%

(b) the coincidence of the ~~γ~~ absorption curves (with Pb & Al in the position of annihilator) for ^{60}Co - γ - rays - Fig. 20.

(c) the coincidence of the absorption curves for ^{198}Au (γ - rays of 0.41 Mev) with Pb & Al in the annihilator position. (Fig. 45). This figure is plotted at reduced scale ~~#~~ but the observed coincidence of ordinate values for large t was as accurate as in Fig 20.

source was obtained by subtracting the sum of the calculated chance coincidences and measured cosmic ray coincidences from the total number of coincidences observed at a given absorber thickness. The same procedure was applied to the calculation of the initial number of coincidences N_c at zero absorber thickness. Each n_c was normalised to the corresponding N_c. (N_c was measured separately for each n_c).

The ratio of n_c / N_c was plotted against the absorber thickness the statistical accuracy being 1% (See Fig 13). The difference between the ordinates of the two absorption curves for Z=82 and Z=13 lies between 6% - 11% which is much greater than the probable error.

To ensure that this real difference is not accidental but due to positron annihilation, the experiment was repeated with a different source, not a positron emitter, exactly under the same conditions. A Co^{60} source was found suitable for comparison because of its long life time(5 years) It emits two γ - rays of 1.155 and 1.317 MeV and β ~~-rays~~. (78)(a,b,c)* When a source of a few square mm. in size was wrapped with Al and Pb alternately as in the case of the Cu^{64} source, the same number of single counts was obtained in the first counter at the same distance. The number of coincidences corrected for background was plotted against absorber thickness after being normalised to the initial number of coincidences.

* The more recent values are 1.1711 , 1.3318 See ref. 78 (d,e,f)

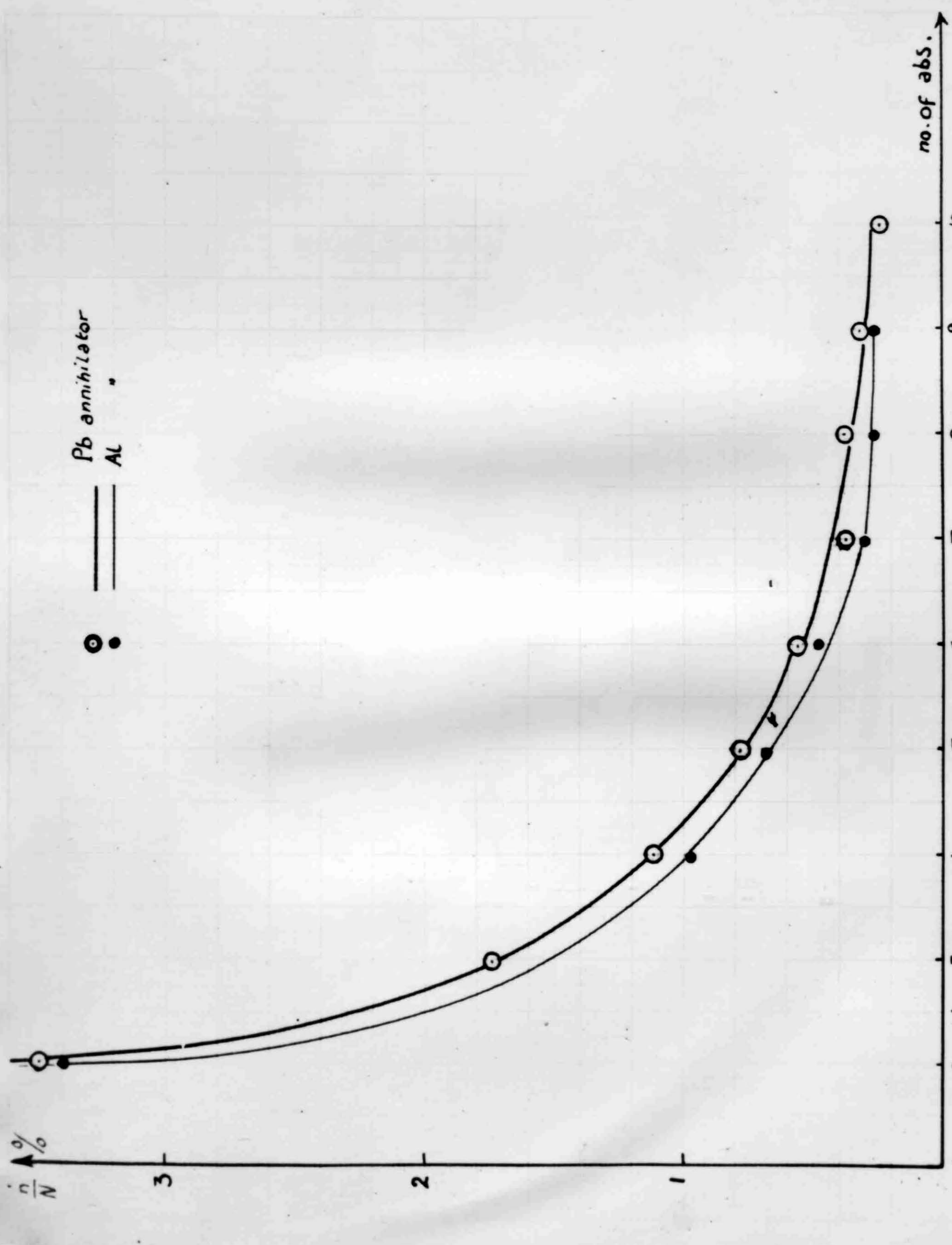

Fig (19)

The results are given in Fig. 20 . The two absorption curves are identical in nature , they are parallel to each other, the Al curve being slightly above the Pb one. This discrepancy could be attributed to the difference in the superficial mass of the two annihilators.(1.6 mm. Al 0.432 gm/cm^2 ; 0.4 mm. Pb 0.448 gm/cm^2).

On the abscissae of the above graphs is indicated the energy of the electrons of range corresponding to the absorber thickness. These figures were obtained from the range-energy curve for homogenous β- rays as given in " The Science and Engineering of Nuclear Power " p.52 Fig. 1-24.

To show that these figures are direcly applicable to our apparatus an absorption curve of β - rays of RaE was obtained . This curve had an end point 543 mg/cm^2 Al which according to the table corresponds to an energy of 1.32 MeV , in agreement with the known energy of these β-rays. (In deriving the above figure, allowance was made for the three copper windows, involved in the coincidences, each of which was 0.001" thick. The stopping power of the copper relative to that of aluminium was obtained by direct comparison of end-point measurements and half-value layers. Mean value of this factor was 4) .

The experiment proves conclusively the existence of one-quantum annihilation which appears to have an end

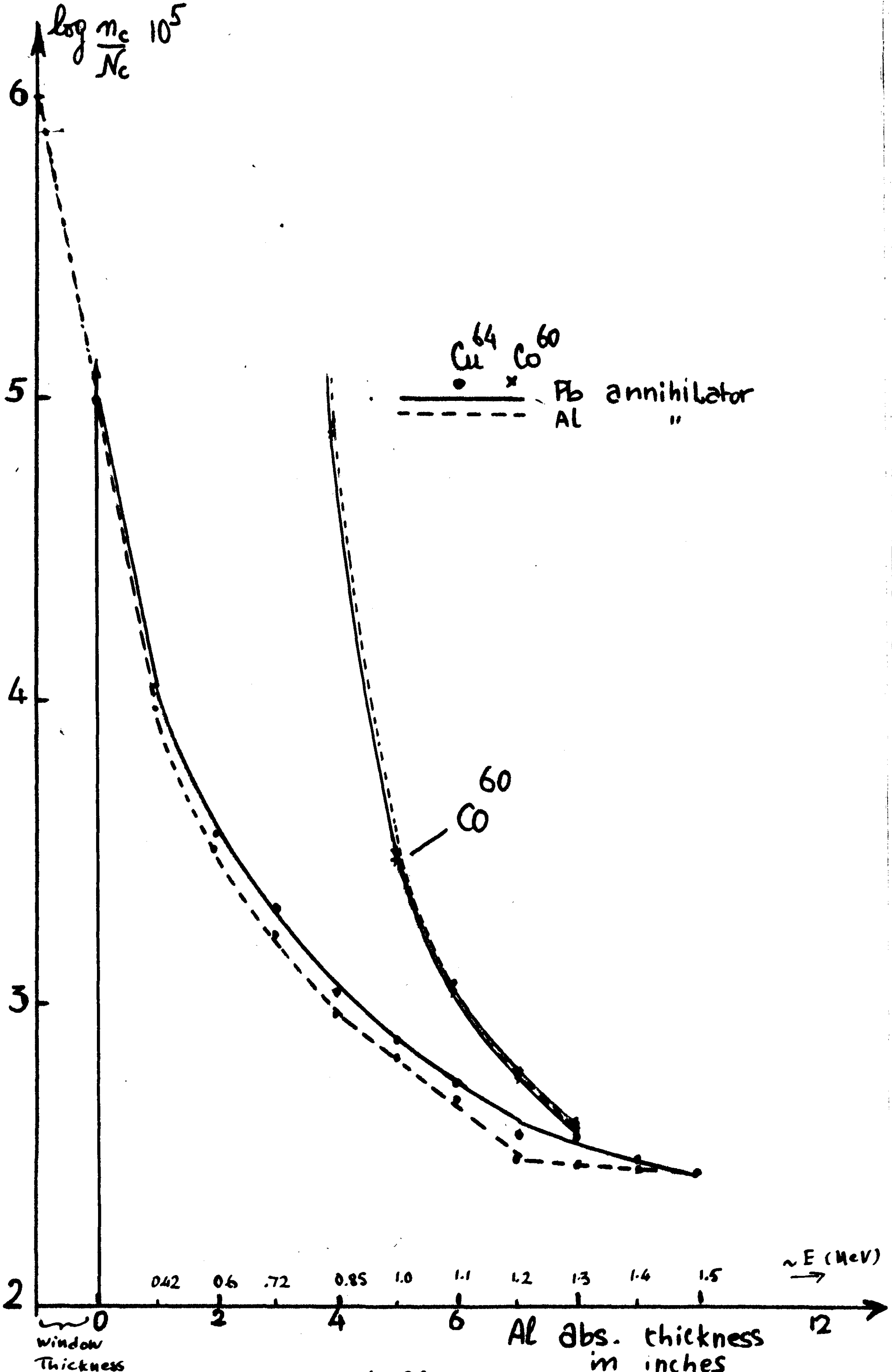

log $\frac{n_c}{N_c}$ 10^5
6
5
4
3
2
Cu^{64} Co^{60}
Pb annihilator
Al "
Co^{60}
0.42
0.6
.72
0.85
1.0
1.1
1.2
1.3
1.4
1.5
~ E (MeV)
0
2
4
6
12
Window Thickness
Al abs. thickness in inches

FIG. 20.

FIG. 20

point(mainly due to the compton elctrons) in the neighbourhood of 1.3 MeV. It is not possible,however ,to make any quantitative analysis of the result or to compare it with theory, because it is very difficult to assess the effect of the nuclear γ - ray which is now known to have an energy of 1.35 MeV.

There are other features of this experiment which render very difficult any attempt to predict the shape of the absorption curve. The γ - rays which are incident on the wall of the first counter are heteregeneous and consist theoretically of the following components:

(a) X-rays* (K-radiation accompanying one-quantum annihilation and K-electron capture)

(b) $< \frac{1}{2}$ MeV (Backwards component of two-quanta annihilation in motion)

(c) $\frac{1}{2}$ MeV (Two-quanta annihilation at rest)

(d) $> \frac{1}{2}$ MeV (Forward component of two-quanta annihilation in motion)

(e) > 1 MeV (One-quantum annihilation in motion)

The $\frac{1}{2}$ MeV radiation will form the larger part of these γ - rays but even assuming that the incident beam were homogeneous the effect of the wall of the first counter

---

* These most probably will be stopped by the counter's window .

will be to produce a wide variation of energy ofthe conversion electrons. The total thickness of the lead foil and copper window is of the order of the range of a 1 MeV electron. Photoelectrons produced inside the wall will lose energy before reaching the inside of the first counter. For $\frac{1}{2}$ MeV γ-rays in lead Compton electrons and photoelectrons are produced in approximately equal amounts. Therefore, in any case, fifty percent of the recoil electrons will have energies varying from zero up to 340 KeV. (These will also be affected by energy losses in the wall). Thus the beam of electrons entering the first counter will have an arbitary energy distribution which will bear little resemblance to the energy distribution of the original γ-radiation. In addition to these considerations we have in this experiment large solid angles subtended by the counters and also a variation of counting efficiency with energy. The complexity of the problem is such that it is not possible to make any reliable estimate of the cross-section for the two-quanta annihilation process by introducing very many approximations in deriving the shape of the absorption curve.

The difficulties due to the presence of the nuclear γ-rays can, however, be eliminated by two methods;

(1) The use of a positron source which has no nuclear γ-rays (at least no γ-rays of energy>1 MeV) such as N^{13}.[52,79] Since

N^{13} has a short life-time (11 min.) the experiment would have to be performed with a continuous supply produced by nuclear transformation e. g. in conjunction with a high voltage generator. (The department H.T. generator was not in operation at that time).

(2) The separation of the positron beams from the nuclear γ -radiation with the aid of a magnetic field.

This method was adopted and the experiment is described in Chapter VI .

— o O o —

CHAPTER.V.

CORRELATION BETWEEN THE BETA- AND GAMMA-RADIATIONS FROM Cu^{64}.

One reason for selecting Cu^{64} as the positron source was that it was thought ~~to be~~ that the γ-radiation was that of a pure annihilation ~~radiation~~ source. In every paper relating to Cu^{64} published before 1946 there is a positive assertion of the absence of ~~the~~ nuclear γ- rays.[57,58,80-3] In a preliminary experiment we have done as a test of the source the absorption of γ - radiation from Cu^{64} by a coincidence method showed a prolonged tail up to 1.3 MeV which was ascribed to the existence of the nuclear γ - ray (Fig. 21) (The study of the end-point is given on a larger scale; it indicates the precise value of the maximum energy of the recoil Compton electrons which is equal to 1.105 - 0.015 MeV. The intensity of the tail first appears to be too large to regard it as due to the hard component of the annihilation radiation.)

In this Chapter an additional experiment attempting to relate this γ - ray to the energy scheme of Cu^{64} will be described.

The apparatus used in this experiment consisted of two square counters as previously described , a small magnet

FIG. 21

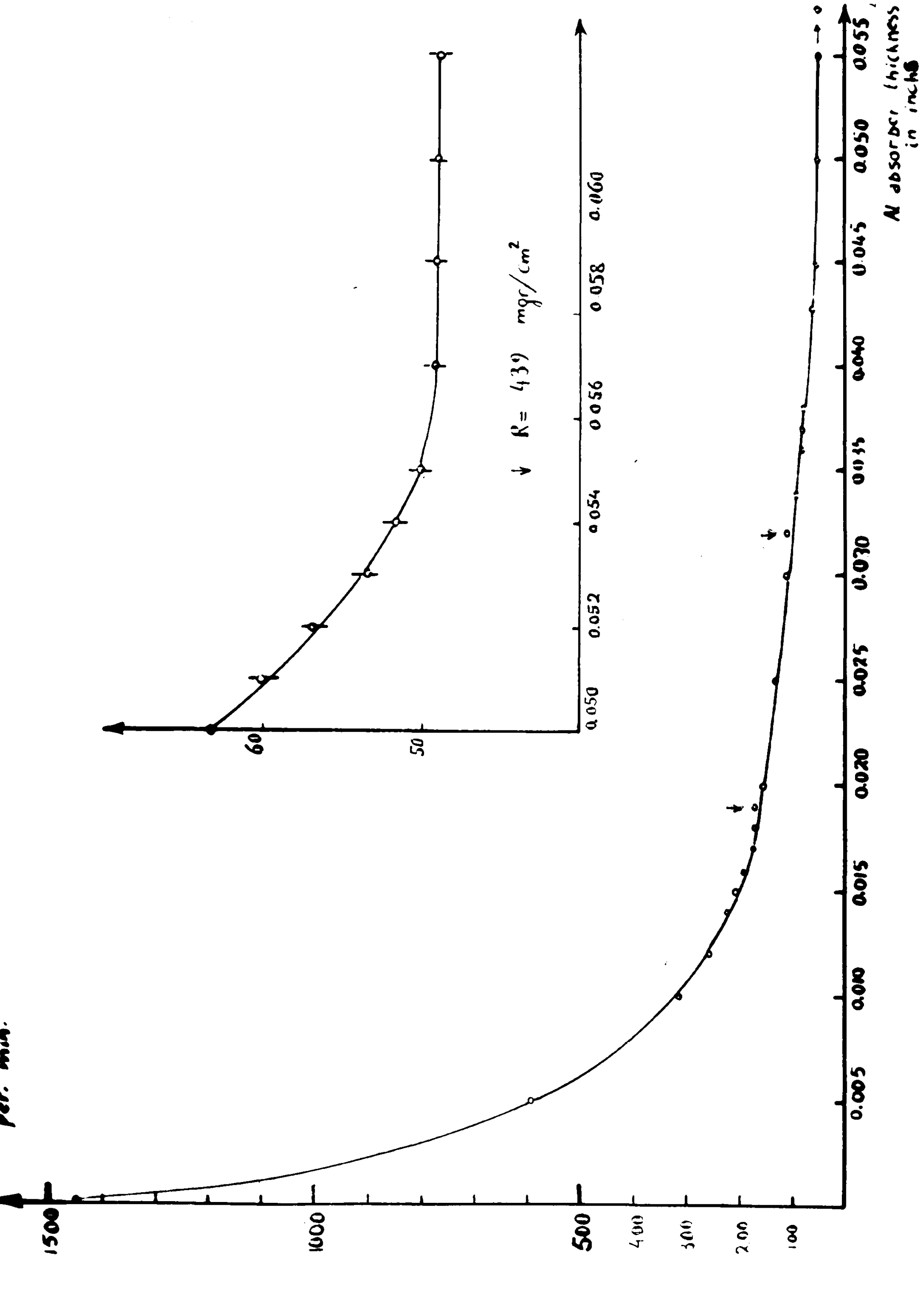
No. of coincidences per. min.
Al absorber thickness in inchs
R = 439 mgr/cm^2
1500
1000
500
400
300
200
100
0.005
0.010
0.015
0.020
0.025
0.030
0.035
0.040
0.045
0.050
0.055
60
50
0.050
0.052
0.054
0.056
0.058
0.060

having pole pieces of 2" in diameter (which provides 3000 Gauss at 1 amp. 3.5 cm. pole gap) and the same recording devices.

Experimental Arrangement*; The two counters were placed in the magnetic field. One was used for counting β - rays and was placed in the pole gap with the window horizontal; the other was placed at right angles to the first counter and separated from it by a few mm. This was used as a γ - ray counter with 0.4 mm lead covering on the window. The source, a thick Cu^{64} foil of area 2x10 mm was mounted in the space between the two counters. (See Fig. 22). The position of the source and the counters was adjusted so as to collect the maximum number of positrons (or electrons) and γ- rays in the β and γ ray counters respectively. The number of real(β,γ)coincidences was investigated for positrons and for electrons as a function of the energy of the β particles. This was achieved by varying the field in direction and magnitude.

The real number of (β,γ)coincidences was obtained from the following observations :

(1)- Number of single γ-ray counts in the γ- ray counter.

(2)- Number of single ($\beta+\gamma$) counts in the β - ray counter.

(3)- Number of γ- ray counts in the β - ray counter. (The last was obtained by covering the thin window of the counter

* As a check on the correct operation of the apparatus ThC source was analysed before commencing the experiment with Cu^{64}. The results, a typical example of which is shown in Appendix IV, indicate that the experimental arrangement is satisfactory.

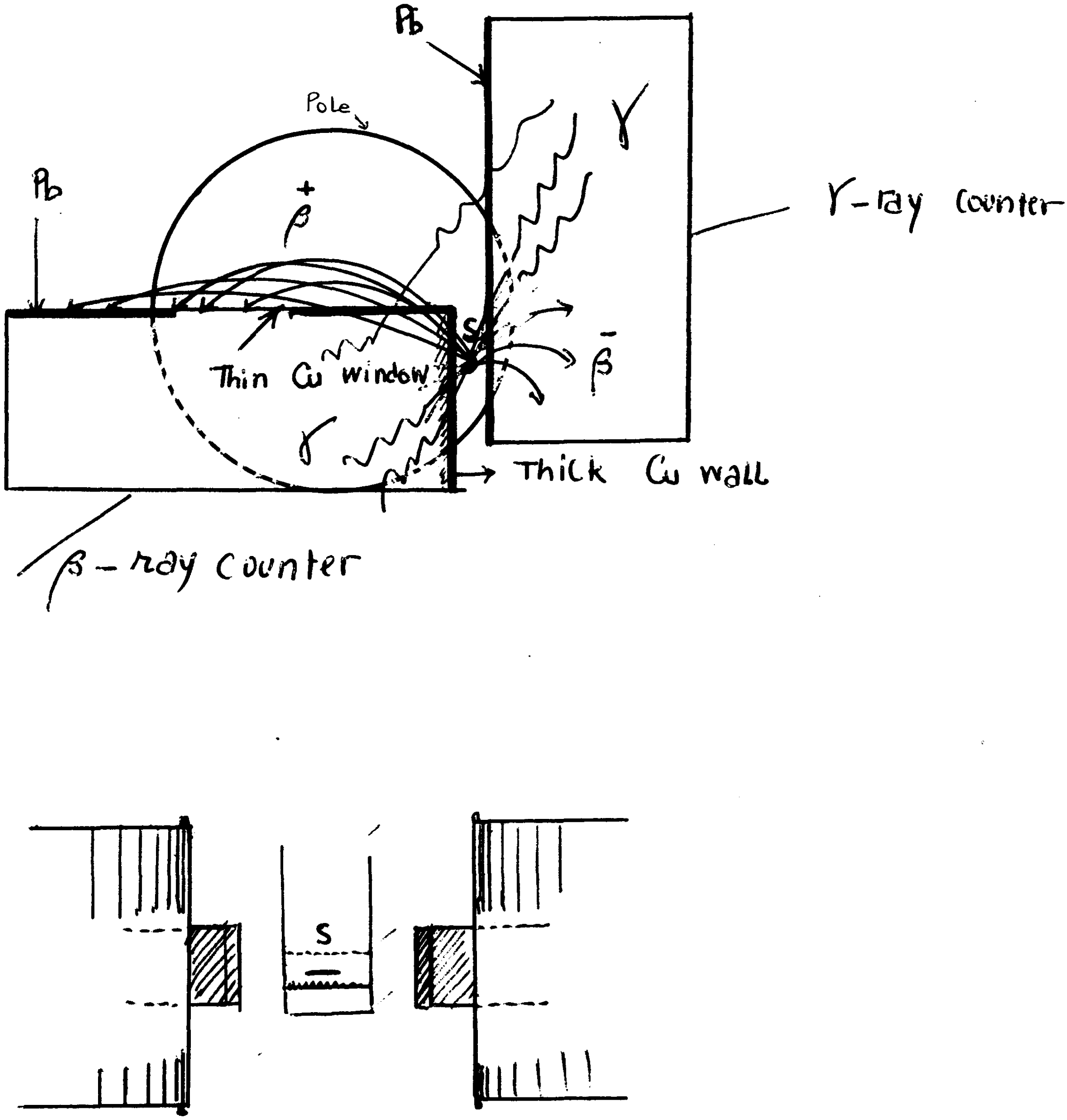

Pb
Pole
Pb
$\overset{+}{\beta}$
γ
γ-ray counter
S
Thin Cu window
$\bar{\beta}$
γ
Thick Cu wall
β – ray counter
S

FIG. 22.

FIG. 22.

with a lead sheet thick enough to stop all the β - rays. In this case the change in the efficiency of the counter for γ - rays is negligible because they enter the counter mostly through the same thick copper end-wall as in case (2).

(4)- Total number of coincidences between γ and $(\beta+\gamma)$

(5)- Number of $(\gamma-\gamma)$ coincidences.

(4) and (5) include cosmic ray coincidences. Therefore the difference between (4) and (5) would give the sum of

a- Number of real (β,γ) coincidences

b- Number of chance coincidences from these β and γ.

(b) was calculated by means of the formula $2n_1n_2\tau$, where n_1 is the single γ count measured in (1), n_2 is the single β count which can be obtained by subtracting (3) from (2), and τ is the resolving time of the circuit which was measured and found to be 1.65 μsec. (Under these conditions, from a maximum of 25000 total single counts per minute the maximum total number of coincidences obtained was of the order of 25 and 10 per minute for β^+ and β^- respectively). All readings were taken for positrons and electrons alternately for each point corresponding to ~~the different~~ a given field intensity (The duration of observation was 1 min. for single counts and 10 min. for coincidence counts). The variation of the real number of (β,γ) coincidences with the energy of the positrons and electrons is shown in Fig. 23 .

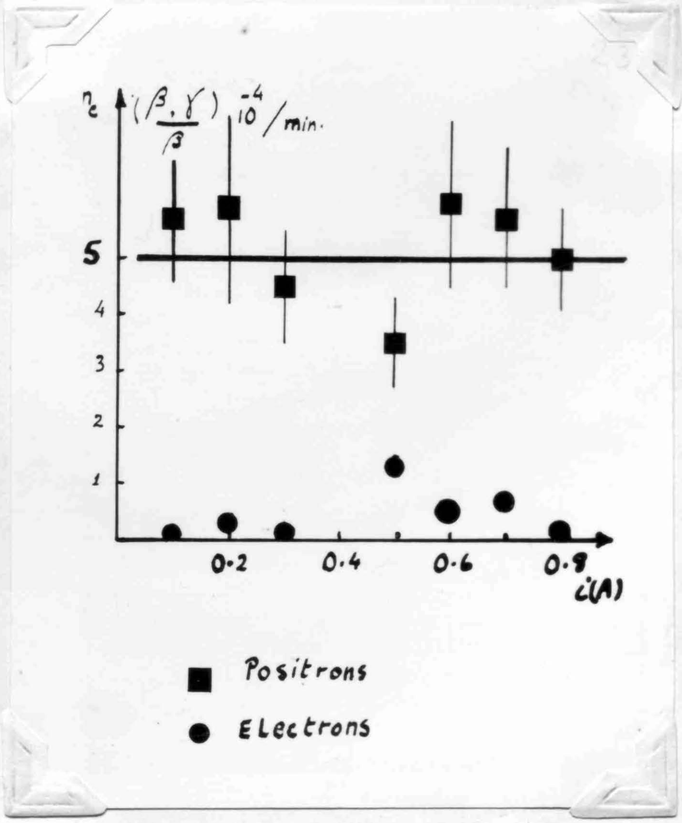

FIG. 23

i (A)	no β^+/min	Total no of coincidences	(γ,γ) coinci. per min.	Chance coin. per min.	Real number of (β,γ) coincidences.	$\left(\frac{\beta,\gamma}{\beta}\right) \cdot 10^4$
0.1	343	5.18 ∓ 0.75	5.6 ∓ 0.75	—	2.18	5.30
0.2	6358	13.4 ∓ 1.5	8.0 ∓ 1.5	1.95	3.45	5.42_7
0.3	10 376	9.8 ∓ 1.0	3.9 ∓ 0.62	1.13	4.77	4.59_7
0.5	21 398	23.8 ∓ 1.5	11.9 ∓ 1.2	2.30	7.60	3.55
0.6	14 447	17.4 ∓ 2.0	6.1 ∓ 1.0	2.25	9.15	6.3
0.7	16 467	15.7 ∓ 1.25	3.5 ∓ 0.57	2.49	9.71	5.88_8
0.8	7358	14.6 ∓ 1.1	8.6 ∓ 1.2	2.3	3.70	5.02
	β^-/min					
0.1	407	5.1 ∓ 0.75	5.1 ∓ 0.7	—	0	0
0.2	16440	15.4 ∓ 0.3	10.4 ∓ 0.4	4.586	0.42	0.25_4
0.3	11837	7.3 ∓ 0.84	5.5 ∓ 0.75	1.58	0.22	0.18_6
~~0.4~~						
0.5	17570	17.4 ∓ 0.2	10.0 ∓ 0.38	5.01	2.30	1.31_1
0.6	17617	10.2 ∓ 1.0	6.2 ∓ 0.65	2.94	1.06	0.57_7
0.7	6447	5.0 ∓ 0.7	3.6 ∓ 0.6	0.95	0.45	0.69_8
0.8	4785	4.8 ∓ 0.6	4.0 ∓ 0.5	0.73	0.07	0.14_5

The ordinate indicates the ratio of the number of (β, γ) coincidences to the number of single β counts. The abscissa gives the value of the magnetic field strength.

As we see from the graph there is a correlation between γ- rays and β^+ of the order of 1γ to 5 positrons. This figure is uncertain at least by a factor of two, firstly because of the large statistical errors involved in such a low coincidence counting rate and secondly because of the uncertainty of the energy of this γ- ray which will affect the counter's efficiency.*

An attempt to determine the energy of the coinciding γ- rays was made by using a triple coincidence arrangement: a pair of coincidence counters to measure the γ- ray energy as a function of absorber thickness was set in coincidence with the β ray counter . The experiment failed because of the very low coincidence rate(0.5 per minute) which was recorded at zero absorber thickness.

---

* If there was one to one correspondance between β^+ and γ the coincidence rate $\frac{(\beta, \gamma)}{\beta}$ would be equal to the efficiency of the γ - ray counter. Hence in general

$$\eta = \frac{(\beta, \gamma)}{\beta} = f \cdot \varepsilon$$

where $f \leqq 1$ and $\varepsilon = \varepsilon(E_\gamma)$.

An additional check on the measurement of the (β, γ) coincidences was made, repeating the experiment with slightly improved conditions. The collection of the β particles was localised to a small area of the β - ray counter . This was achieved by covering the thin window with a lead sheet 1 mm. thick which had a square aperture $\frac{1}{2}$" x $\frac{1}{2}$" in the middle , where the efficiency of the counter is uniform. (The variation of the efficiency of the counter along the wire is shown in Fig. 24). The total number of <u>chance</u> coincidences between β and γ, and , γ and γ was <u>measured</u> by means of a new method in which the β radiation from Cu^{64} was replaced by the β radiation emitted by a different source. The procedure was as follows : First of all the total number of $(\beta+\gamma)$ single counts and $(\beta+\gamma)$, γ coincidences from Cu^{64} were measured at a certain field strength; afterwards RaE needles of different intensities wrapped in very thin Al foil were placed right on the top of the β - ray counter underneath a lead screen over the aperture and their strength was adjusted until the same number of total single counts was obtained from the sum of Cu^{64} γ - rays and RaE β - rays . Then the number of coincidences were ~~also~~ measured also for this case. The difference between the two total coincidence rates gives directly the number of the real (β, γ) coincidences, The experiment was performed with a thin Cu^{64} foil, 0.001"

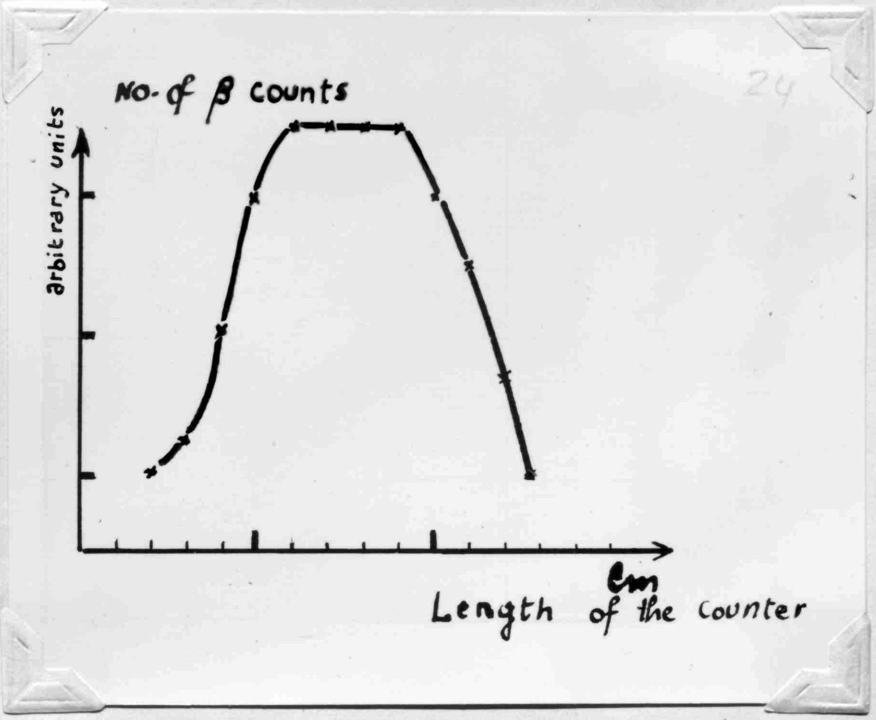

FIG. 24.

FIGS. 25, 26 show the variation of the γ-ray counting rate in the β and γ-ray counters as a function of the field intensity. The curves H(I) correspond to the direction of the field necessary for the collection of positrons in the β-ray counter; the curves H(II) correspond to the direction of the field for the collection of negative electrons in the β-ray counter. (See the next Page).

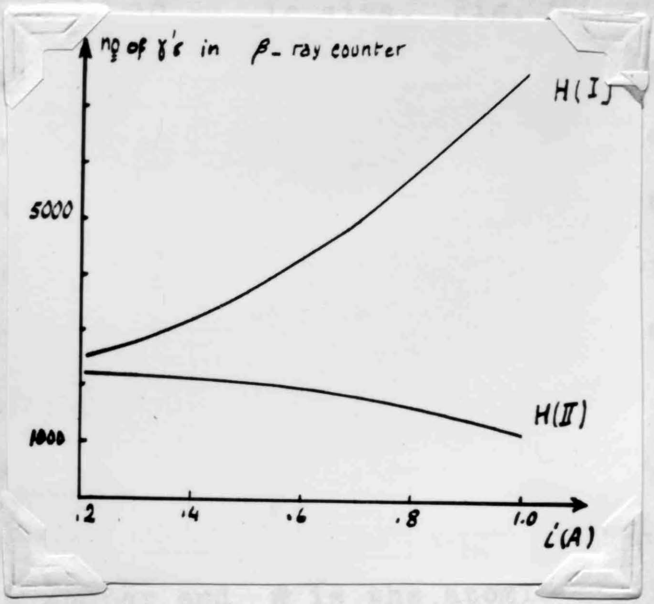
no of γ's in β- ray counter
H(I)
H(II)
5000
1000
.2
.4
.6
.8
1.0
i(A)

FIG. 25

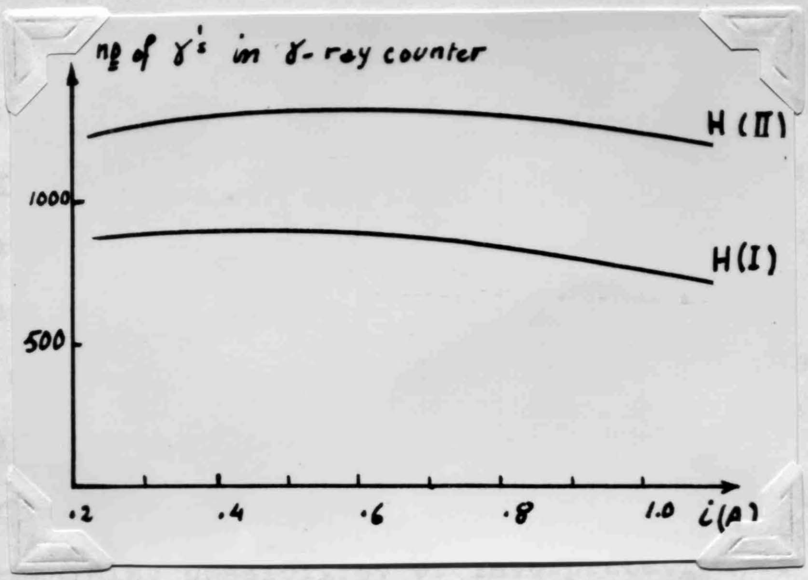
no of γ's in γ- ray counter
H(II)
H(I)
1000
500
.2
.4
.6
.8
1.0
i(A)

FIG. 26.

thick ,4 mm. by 10 mm. in size. Fig. 27 shows the result of this run. It indicates the correlation of γ- rays with positrons in the ratio of 1 to 10 . The apparent independence of the (β, γ) coincidence rate with positron energy suggests that this γ- ray is of nuclear origin . The difficulty of interpreting the result of this experiment arises from the fact that it is impossible to fit a nuclear γ- ray, which is known to have an energy of 1.35 meV, in to the energy scheme of Cu^{64} . The values of M - A , where A is the mass number and M is the atomic weight, for the three isobar of mass 64 (Cu , Zn , Ni) are :-

Cu	-507.4	10^{-4}	mass unit
Zn	-513.6	"	"
Ni	-525.6	"	"

The energy available for the transmutation Cu → Ni, is equal to 18.2 10^{-4}/ 11 10^{-4} = 1.66 MeV . This accounts for the creation of the positron and its known maximum kinetic energy (cf. Cu^{64}). According to the latest investigation of of the Fermi distribution of Cu^{64} positrons the probability of the existence of even a low energy nuclear γ- ray is very small (84). (The positron distribution at low energy differs from the Fermi distribution only by 1 percent ; this discrepancy could be easily due to experimental error .) The remaining possibility of interpretation of the result could be to attribute this γ - ray to some type of annihilation radiation. However the accuracy of the present experiment is not high enough to make a final decision.

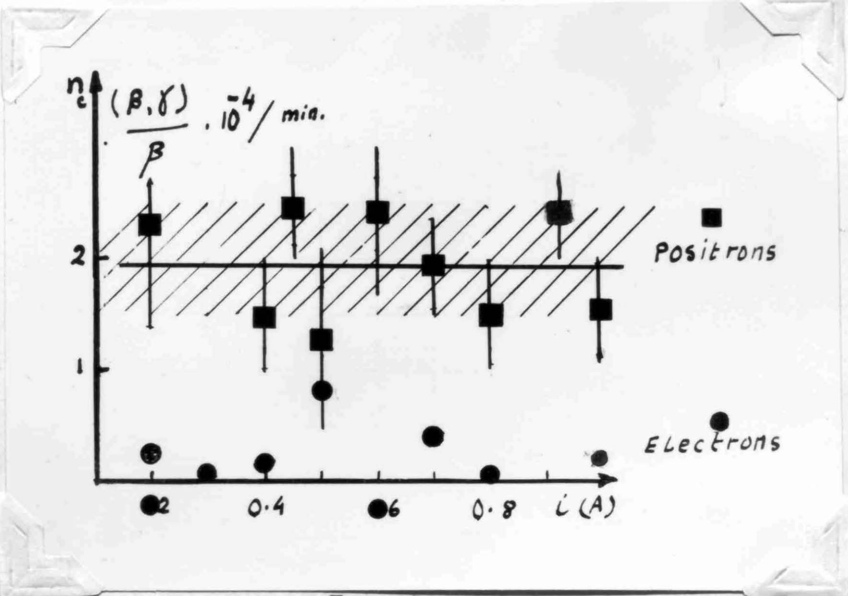

FIG. 27.

i (A)	β^+	Cu^{64} (β,γ) coinci. + other coin	(Cu^{64} + RaE)(β,γ) coin. + other coin	Decay correction	($\beta.\gamma$) coincidence	$\frac{(\beta+\gamma)}{\gamma} 10^{4}$
0.2	6538	2.5 ∓ 0.5	1.0 ∓ 0.3	0.02	1.52	2.33
0.3	22124	5.1 ∓ 0.7	1.7 ∓ 0.4	0.05	3.45	1.56
0.4	16 306	8.1 ∓ 0.9	4.4 ∓ 0.6	0.08	3.78	2.41
0.5	11 878	6.5 ∓ 0.8	5.0 ∓ 0.7	0.06	1.56	1.31
0.6	26781	8.8 ∓ 0.9	2.3 ∓ 0.5	0.09	6.59	2.43
0.7	9981	6.0 ∓ 0.75	4.0 ∓ 0.5	0.06	2.06	2.07
0.8	10797	2.4 ∓ 0.5	0.9 ∓ 0.3	0.02	1.52	1.41
0.9	5511	5.0 ∓ 0.7	3.7 ∓ 0.6	0.05	1.35	2.43
1.0	12 420	2.3 ∓ 0.5	0.5 ∓ 0.2	0.02	1.82	1.465
	β^-					
0.2	28280	4.6 ∓ 0.7	5.1 ∓ 0.7	0.04	−0.54	−0.17
0.2	6815	0.6 ∓ 0.2	0.4 ∓ 0.17	0.006	0.206	0.303
0.3	24967	5.4 ∓ 0.75	5.41 ∓ 0.73	0.05	0.05	0.02
0.4	19959	1.7 ∓ 0.4	1.3 ∓ 0.35	0.017	0.417	0.209
0.5	11 903	4.5 ∓ 0.67	3.5 ∓ 0.6	0.04	1.04	0.87
0.6	12 556	0.7 ∓ 0.26	1.0 ∓ 0.3	0.007	−0.3	−0.24
0.7	18824	6.1 ∓ 0.8	5.1 ∓ 0.7	0.06	1.06	0.52
0.8	4545	1.0 ∓ 0.3	1.0 ∓ 0.17	0.01	0.01	0.02
1.0	6262	0.7 ∓ 0.26	0.5 ∓ 0.2	0.007	0.207	0.315

CHAPTER VI

THE STUDY OF ONE-QUANTUM ANNIHILATION - PART II.

The separation of the positrons from the nuclear γ-rays of Cu^{64} was achieved by the trochoidal method. This method was selected because it offered much greater efficiency of collection than methods employing any orthodox magnetic spectrometer. The latter instrument involves a small solid angle for collection in producing energy resolution and is a factor of 10^{-3} to 10^{-5} down in efficiency of collecting positrons on to a small target. Thus the use of a spectrometer would have involved a source strength of the order of one curie which is impossible to obtain in the thickness and size required for this experiment.

Section A:- The Trochoidal Method.

§.1. This technique of collecting particles by using the fringing field of an electromagnet was first introduced by J. Thibaud(85) specially for the study of positrons. The trajectory of the particles emitted from a source which is placed in such a field, possessing an appreciable radial gradient, will be a trochoid if the initial velocity of the particles is perpendicular to the lines of force and in the median plane. The magnitude of the precession δ , which is caused by the existence of the radial field gradient ΔH, is proportional to the radius r of the elementary circular orbit of the particle (defined by $mv^2/r = Hev$), is given by

$$\delta = \pi r\ (\Delta H)_r/H \qquad (30)$$

where H represents the field strength in the centre of the elementary orbit; $(\Delta H)_r$ the variation of the field along r in the median plane . For a given charge, δ will cause a displacement always in the same direction irrespective of the initial direction of emission and velocity of the particle. Therefore in the case of a point source, all positrons emitted in the median plane will be transported to the other end of the tube. But the finite size of the source will cause a loss which increases in the ratio of the source diameter to the magnitude of δ .

The total path L of the electron from the source to the diametrically opposite point will also be a function of the field intensity and gradient and is given by

$$L = \frac{2\pi R}{(\Delta H)_r/H} \qquad (31)$$

Here R is the radius of the mean circle. See Fig. 28 . (For $R = 30$ cm and $\frac{(\Delta H)_r}{H} = 1.19 \cdot 10^{-3}$ the most energetic positrons from Cu^{64} will travel a distance of approximately 2 Km . These figures are quoted from our experimental arrangement, further explanation will be given in the next paragraph.

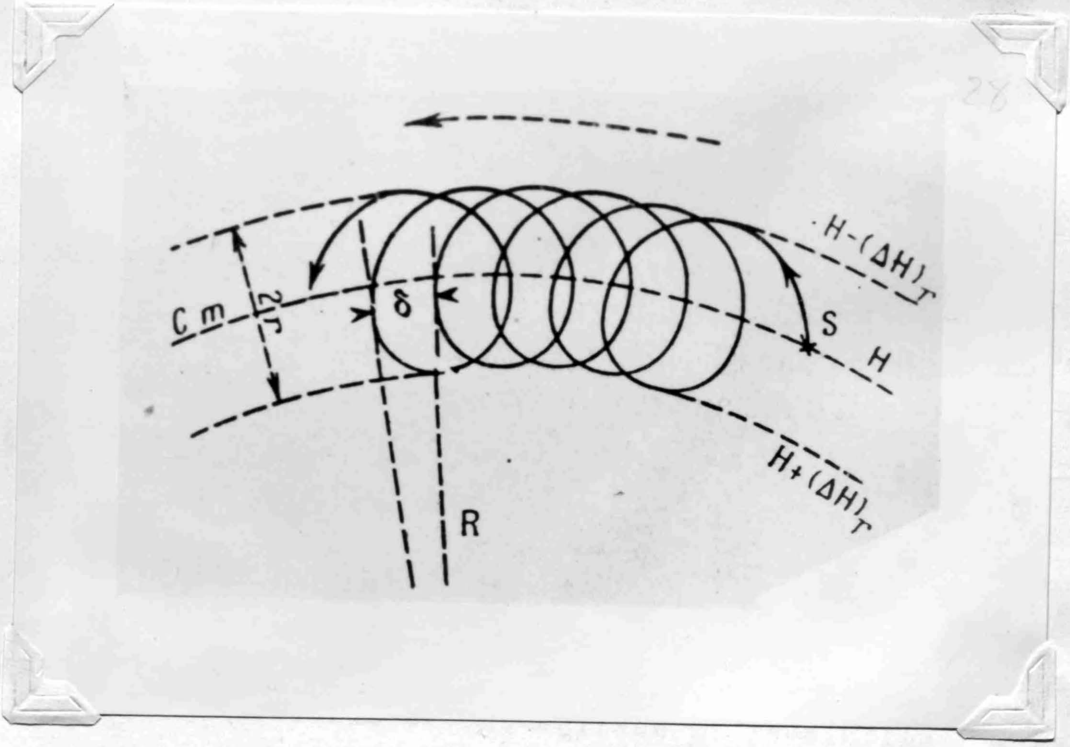

FIG. 28.

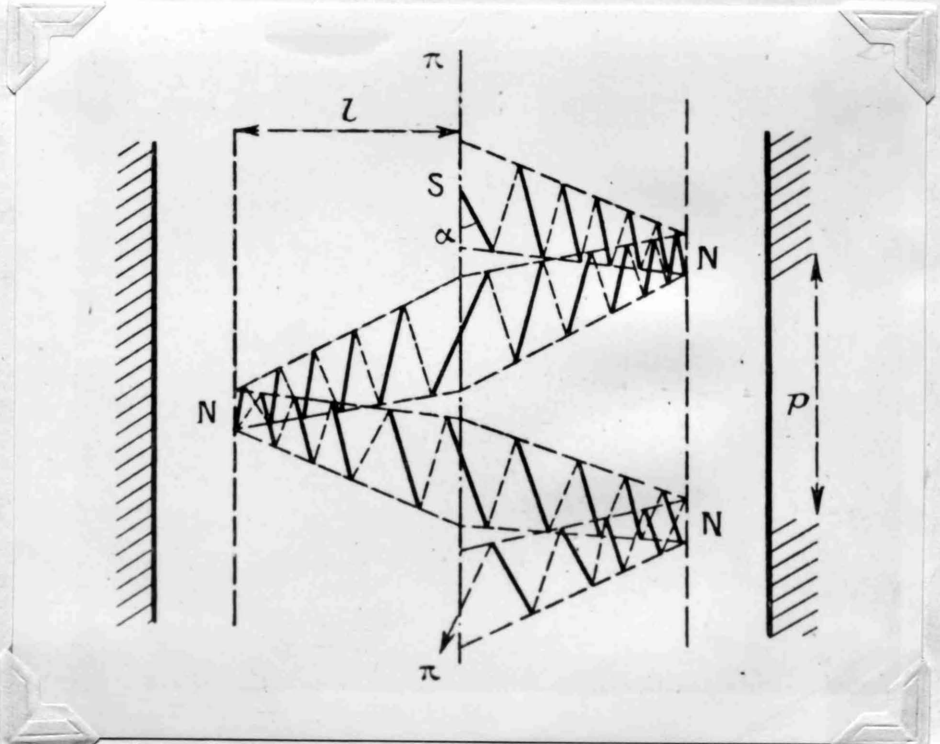

FIG. 29

In the general case where the source emits particles in all directions and the initial velocities are no longer in the median plane, the path will depend upon the field variation in the transverse direction as well as in the radial direction ; and the trajectory of the electron, where the tubes of force are transformed from a cylinder to a cone will be given by the equation

$$r\cos\alpha = \text{constant} \tag{32}$$

This is a geodesic of a surface of revolution and α is the angle which the initial velocity of the β particle makes with the meridian of the surface of revolution , r is the radius of the cone at a point where $\alpha \neq 0$, and, the value of the constant is determined by $r = r_0$ corresponding to $\alpha = 0$.

As seen from Fig. 29-31 the path of the electrons is no longer helicoidal because of the conicity. This expression " conicity " is defined by Thibaud as being the half angle of the cone which is in question and the value of this angle ω is given by

$$tg\omega = r(1-\cos\alpha)/l = (2A\sin^2\tfrac{\alpha}{2})/lH \tag{33}$$

where

$$l = d-d_0 \quad \text{and} \quad A = rH \quad \text{(See fig. 31 .)}$$

If we denote the value of the field at the point S by H and at M by H_0 and the difference of the two by (δH) it is possible to derive another relation for ω in terms of these measurable quantities, and ω is given by

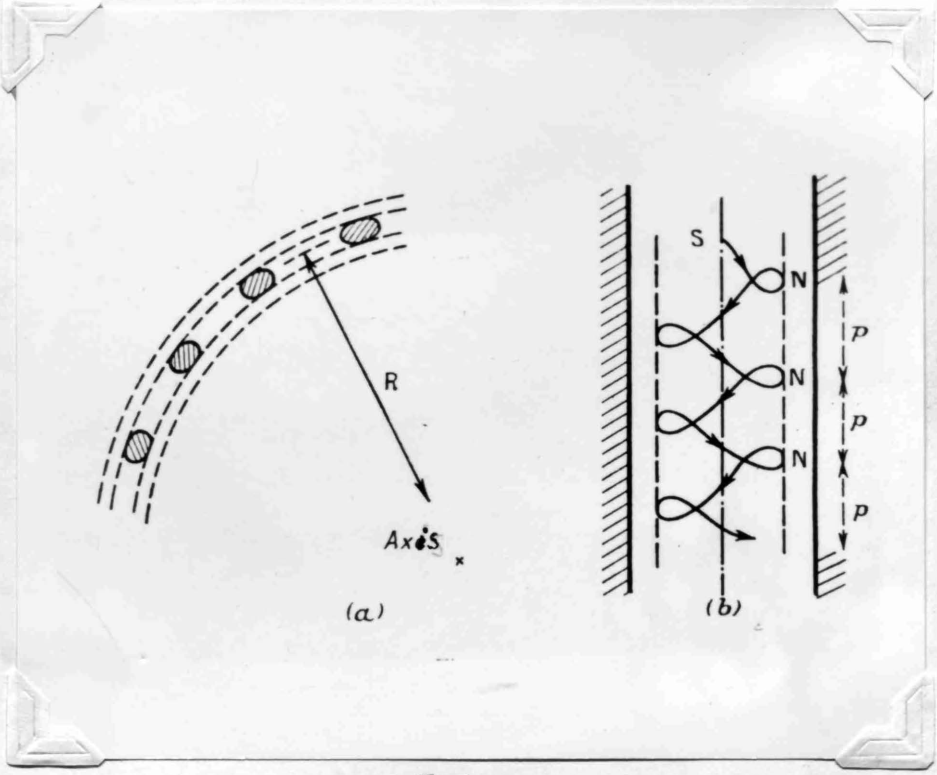

FIG. 30.

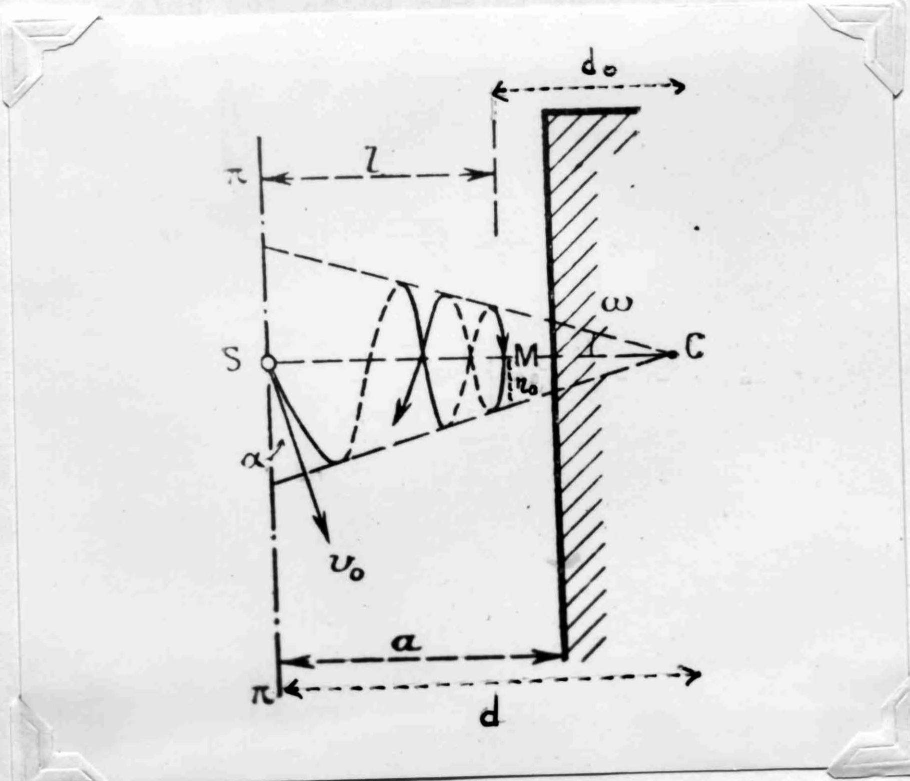

FIG. 31.

$$\omega = A\delta H \,/\, 2\ell H^2 \qquad (34)$$

This relation holds for ω and α small; and as seen, the conicity of the tubes of force is not constant but varies as the pole is approached. Substituting the above value of ω in (33) and concidering the case where $\ell = a$, (a is the width of the gap of the magnet) we obtain a limiting value α_m given by

$$\sin \frac{\alpha_m}{2} = \frac{1}{2}\,(\delta H/H)^{\frac{1}{2}} \qquad 35$$

This limiting angle will restrict the lateral oscillation of the particles, hence it will play a part on their collection. For a point source the efficient region of emission is represented by the complementary volume of the double cone of aperture of $(\pi - 2\alpha_m)$. See Fig. 32. The fraction of particles collected can be expressed as the ratio of this volume V to the sphere. The numerical value of the fractional yield will differ from one system to another. In our experimental arrangement, for $\ell = 1\frac{3}{4}$" and $\delta H/H = 2.84\ 10^{-2}$ α was found equal to 9° 36' and the percentage yield given by $V/4\pi$ corresponding to the above value of α_m was equal to 16.8 %. The experimental results of the measurement of the yield will be given later in detail.

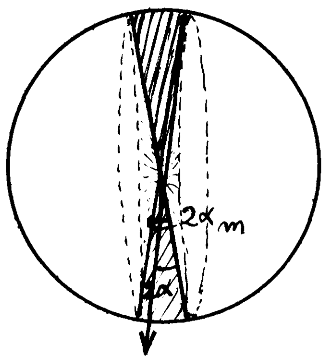

FIG. 32.

§2. Apparatus : (a)- Glasgow university's 15 tons ~~big~~ magnet was used to provide the necessary field. The pole diameter of this electromagnet was 2 feet and the gap between the poles was originally 8" . This was reduced to 4" later by the addition of two extra pole-pieces . The field intensity obtainable in the 4" gap as a function of the current is given in Fig. 33(a). For the maximum value of i = 40 A. used here the magnetic field measured in the centre of the gap was 12000 gauss. The radial distribution of the field in the median plane and in the plane parallel to it each at an inch apart was studied for 8" gap and the results are given in Fig. 33 b. The distribution of the lines of force was also obtained by the help of the iron filings method. After these two observations diagrams of the isofields (See Fig 34). were drawn from which the variation of the field and therefore the value the precession δ could be determined. A knowledge of the position for the best value of δ determines the region in the inhomogeneous field for which the yield of particles is greatest.

(b)- The magnetic separator was a seamless semicircular tube of copper, 1.5 mm. thick and $12\frac{3}{4}$" mean radius having a cross-section $3\frac{1}{2}$" in diameter (The width of the gap was reduced to 4" in order to have the maximum field gradient within the cross-sectional area). Two flanges, were screwed and sealed on to the two ends. One of the flanges carried

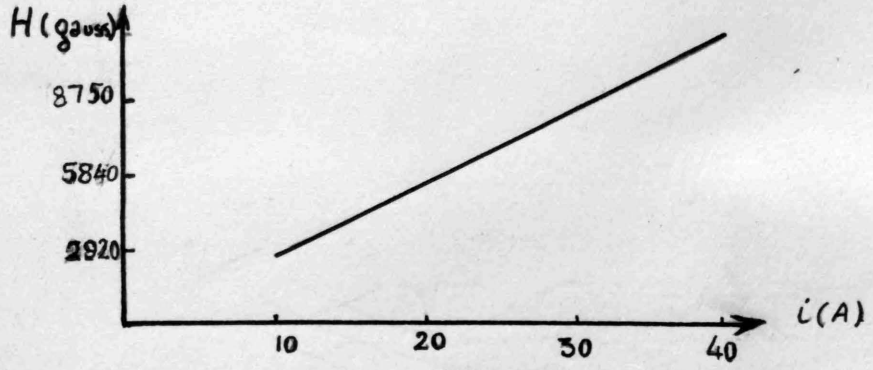

FIG. 33 (a).

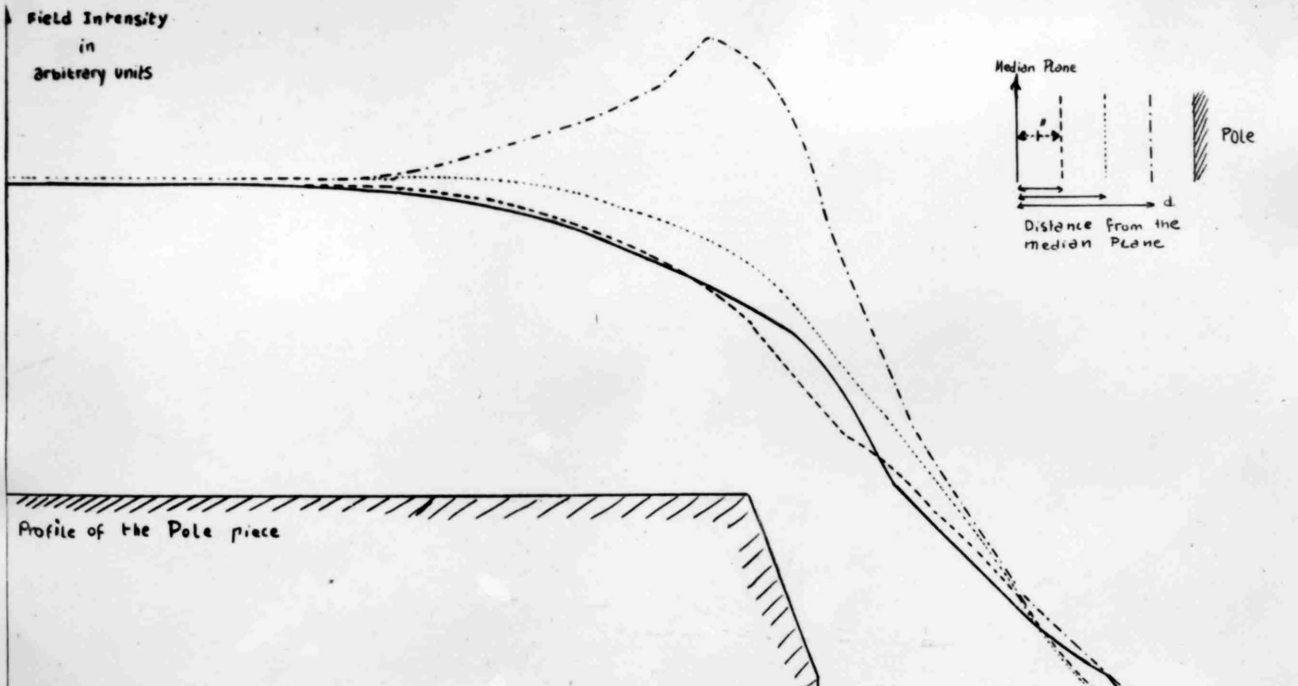

FIG. 33 (b)

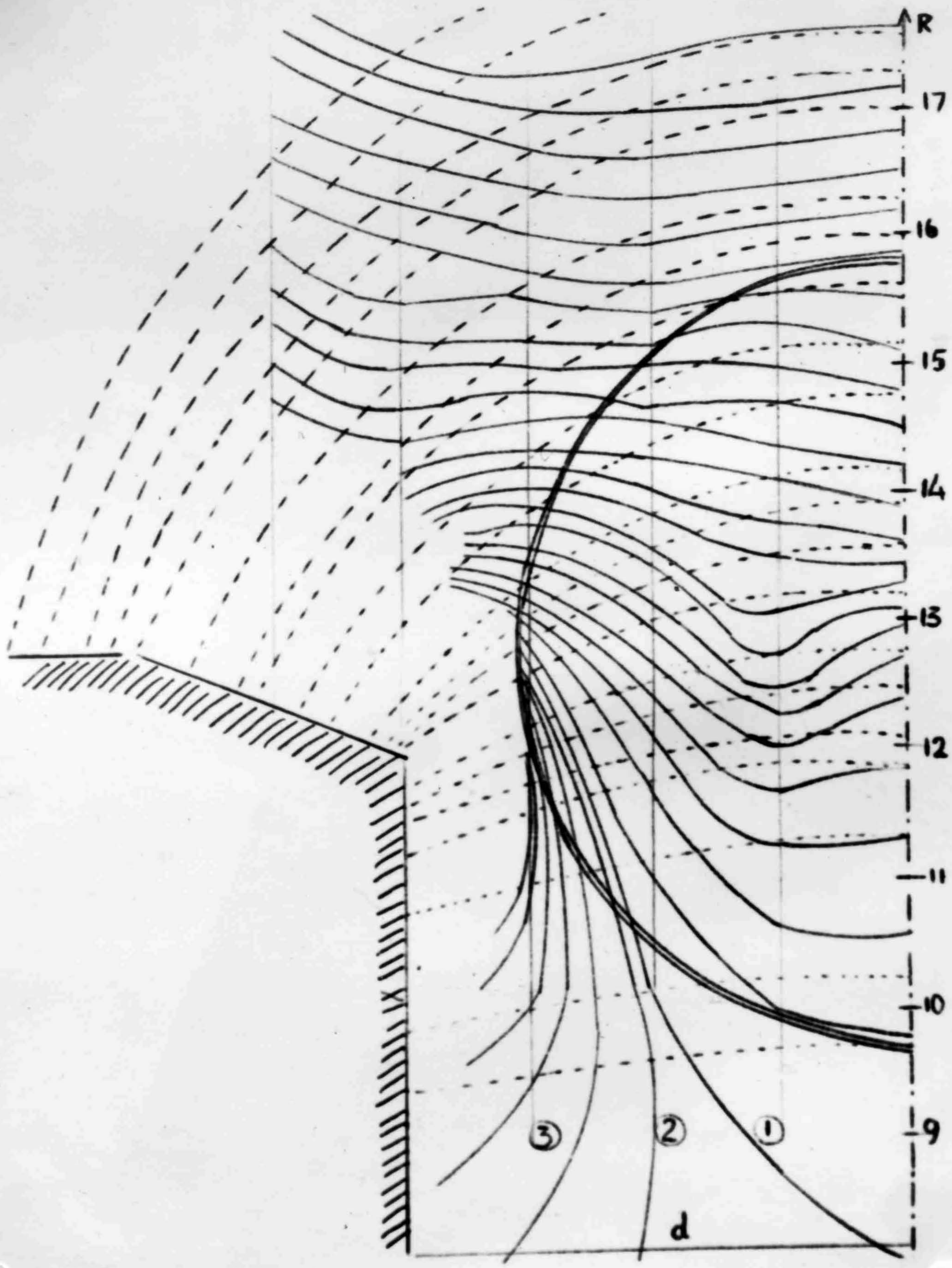

FIG. 34.

the source which could be rotated through 360° by means of a vertical ground joint(A). Near the other end of the tube was another ground joint operating horizontally and having a possible rotation of 180°(B) (This was used to carry the annihilators for the purpose of the main experiment). Fig. 35 . illustrates the construction.

(c)- A β-ray counter was used for the determination of the efficiency of the separator in collecting various β-particles (positive and negative) of different energies from different sources. The cathode was a copper cylinder 1 mm. thick, $2\frac{1}{4}$" in diameter and $2\frac{3}{4}$" long. The anode was a tungsten wire, 2" long, carrying a small glass bead at the end near the window. The window was a very thin sheet of mica (2 mgr/cm^2) sealed on to a thick brass ring which was soldered on to the cathode in order join the counter to the magnetic separator. A rubber ring was inserted between the counter and the tube to reduce the risk of fracture of the thin window. The counter was connected to the separator through a narrow copper tube which permitted simultaneous evacuation. The counter was filled with a mixture of alcohol and argon to a total pressure of 6 cm. in the ratio of 1 to 5 respectively. It gave a very flat and long plateau extending over a range in excess of 300 V. (The threshold voltage was $\sim$ 1200).

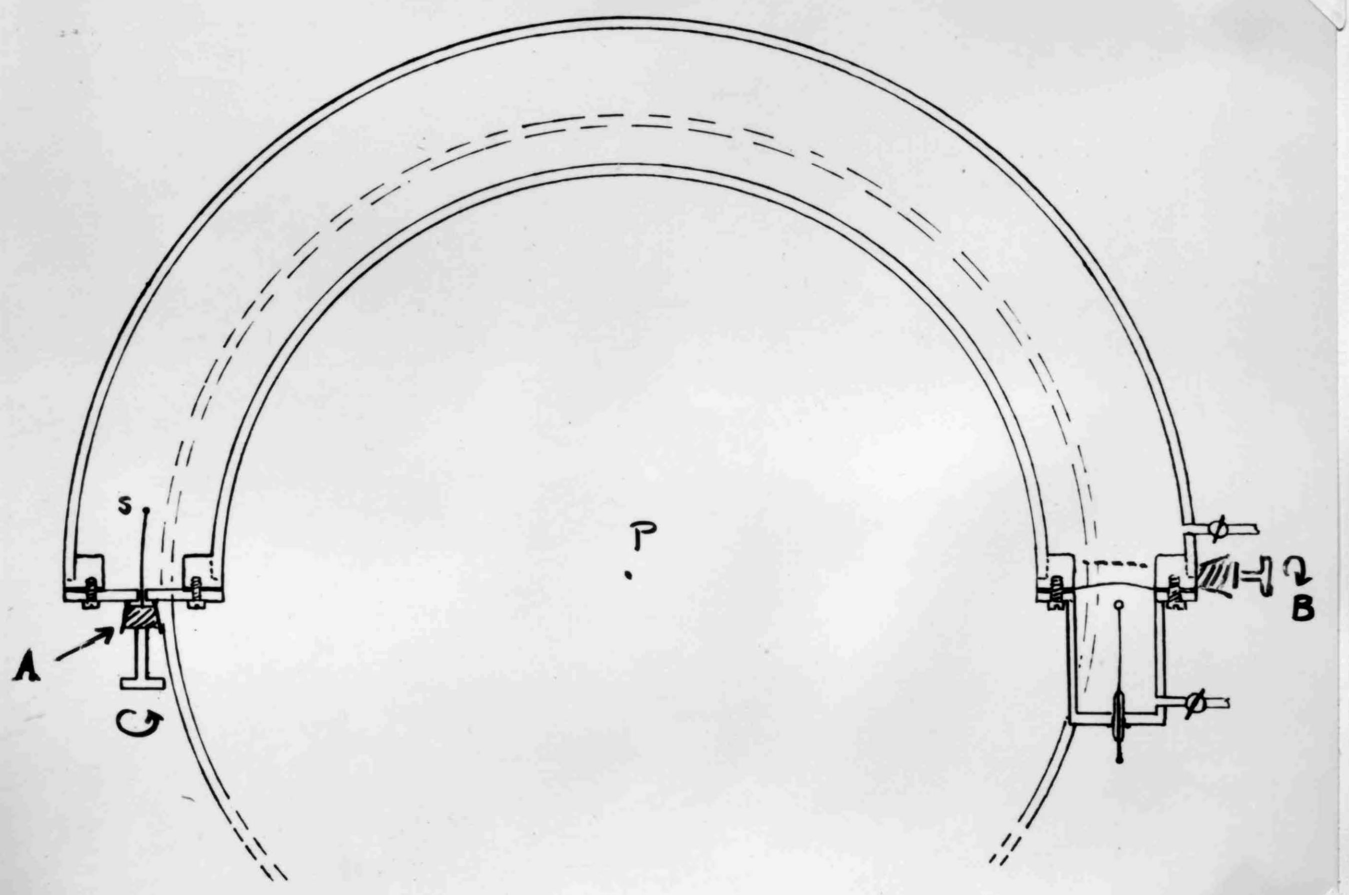

FIG.35.

§3. Test of the efficiency of the separator.

Observations on the fractional yield (the ratio of the number of particles collected to the number of particles emitted) showed that the efficiency of the separator is a funtion of the following factors:

(1)- Source shape and position in the tube.

(2)- The position of the tube in the field.

(3)- Field intensity H.

(4)- Pressure in the tube P.

(5)- The energy of the particles E.

1. Form of the source: Point sources are obviously the ideal type, but for various reasons they are impracticable. In the case of line sources the length must be along the field axis. A rotation of 90^0 reduces the yield by a factor of two. The effect of the decentralisation of the source is shown in FIG 56(a).

2. The separator must be placed so that its centre of curvature is at the mid-point of the gap and should be with its plane perpendicular to the axis of the magnetic field. Small displacements or rotations were found to give rise to very large reductions in the yield factor. Especially the tube must be positioned with great accuracy in the field in the " to and fro " direction.

The variation of the yield with the three dependent variables H, P, and E is investigated in the following way:

Y = f(H); E,P constant. Y = f(P);E,H const. Y = f(E);H,P const.

3. Variation of the yield as a function of the field intensity with E and P constant is shown in Fig. 36 . The source used in this test was RaE β -rays , maximum energy of 1.3 MeV and mean energy 0.3 MeV . For a given value of $P=P_1$, the yield increases rapidly with the increasing H and tends to show a flat maximum at the higher H. For P_2 smaller than P_1 this maximum appears at smaller values of the field and the new maximum yield Y_2 is greater than the previous max. Y_1 The absolute value of the yield was determined by measuring directly the emission from the source with a rectangular counter and with the β -ray counter attached to the separator and found equal to %16 and %30 for the pressures 1 mm. and 0.01 mm. of mercury respectively. All of the figures quoted are subject to a ~~rather~~ small correction due to the difference in the absorption of the window on the counter used with the separator and that on the counter used to measure directly the emission from the source. The latter was 30 mgr/cm^2 in thickness but the correction is not large for RaE.

4. Y = f(P) ; E and H constant.

It is found that the yield rapidly increases with decreasing pressure down to a value of about 0.1 mm of Hg and below that pressure it shows a rather slow increase along a plateau, see Fig. 37 ,a, For this reason the pressure was kept as low as possible during the course the main experiment, since any change in pressure at low pressures does not produce any

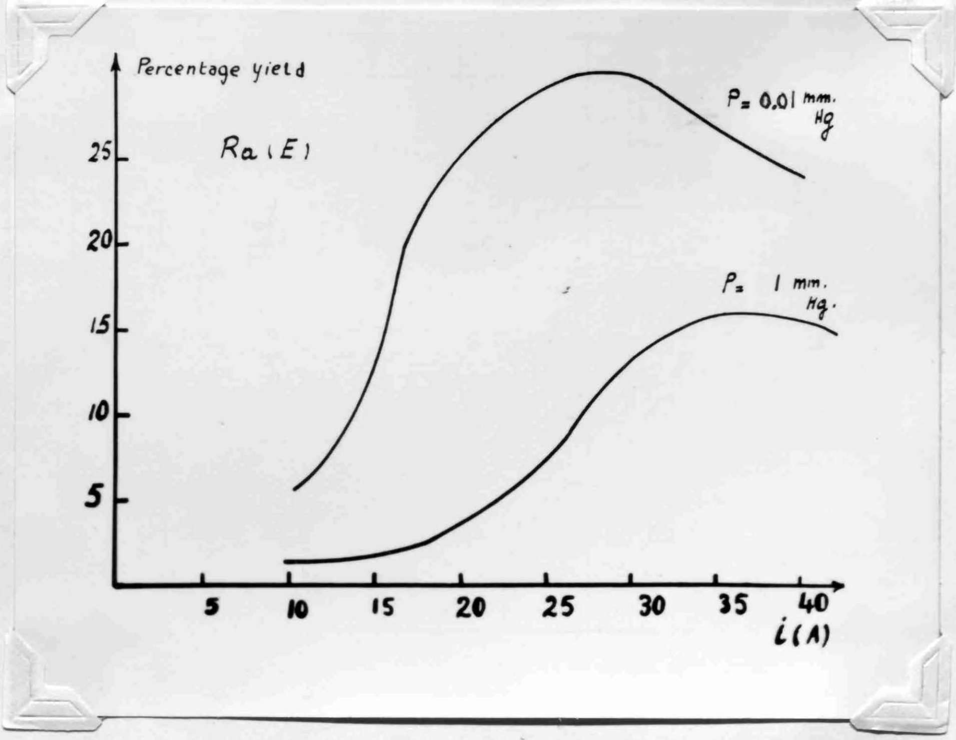

FIG. 36.

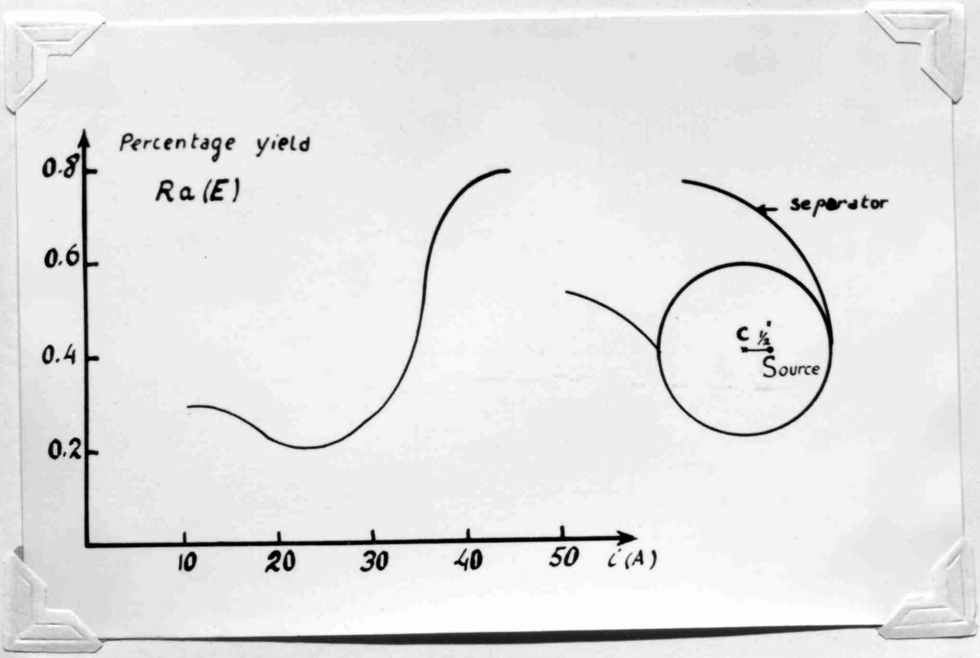

FIG. 36 (a)

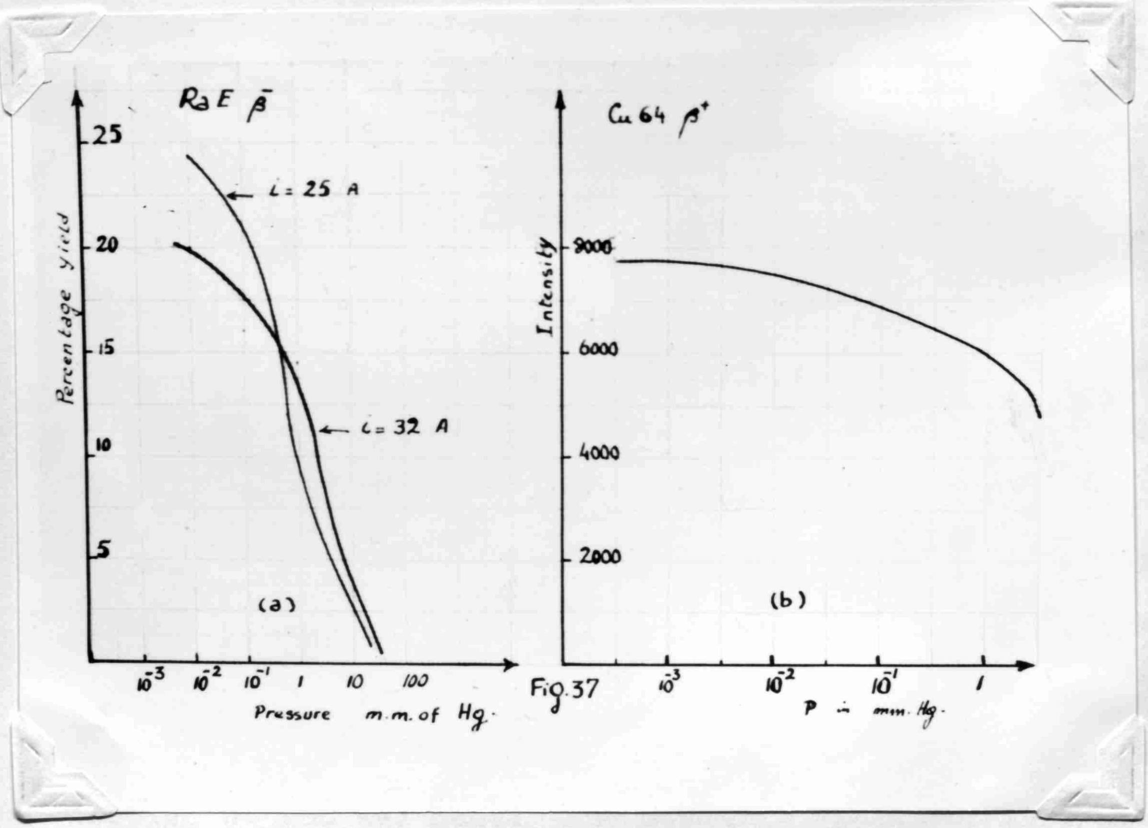
RaE β^-
Percentage yield
25
20
15
10
5
i = 25 A
i = 32 A
(a)
10^{-3} 10^{-2} 10^{-1} 1 10 100
Pressure m.m. of Hg.
Cu 64 β^+
Intensity
8000
6000
4000
2000
(b)
10^{-3} 10^{-2} 10^{-1} 1
P in mm. Hg.

Fig. 37

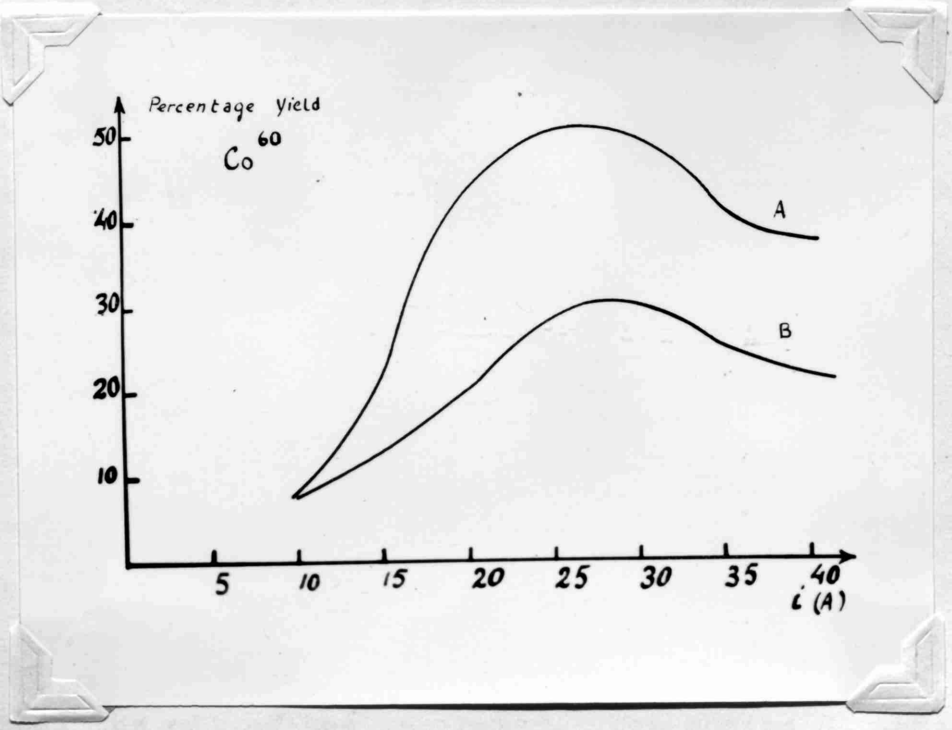
Percentage yield
Co^{60}
50
40
30
20
10
A
B
5 10 15 20 25 30 35 40
i (A)

FIG. 38

appreciable effect on the counting rate. (FIG 37 . b.)

5. $Y = f(E)$; H and P constant.

Three different radioelements Co^{60} , RaE , Cu^{64} were used as sources to determine how the yield might depend on the energy of the radiation.

(a) RaE : The best yield obtained in these experiments with very thin old radon needles was in excess of %30 and it was secured at P= 0.01 mm of Hg and i= 27.5 A.

(b) Co^{60} : An old nickel wire (mainly cobalt) source of about 100 Kev mean energy and 0.4 Mev maximum energy was studied at the same pressure as radium (P= 0.01 mm of Hg). Because of the reduced energy of the β -rays a window correction of %30 was made. The measured yield for this source had a maximum value of %50 at i = 27.5 A. FIG.38.

The measured values of the two maximum yields for RaE and Co^{60} show that it is easier to bring soft β - particles round the separator. This fact indicates that at the pressures obtaining in the apparatus the length of total path travelled by the β -rays is not a determining factor in the yield. (The paths of the rays of Co^{60} are on the average much longer than those of the particles from RaE). We can explain the result by considering particles which do not travel in the median plane. Those particles which are emitted at an angle to that plane will move towards the wall of the separator. The chance of deflecting them towards the median plane is greater for the particles of small energy. Hence presumably the lower yield obtained for RaE is due to the fact that the high energy particles from this source are more frequently lost by striking the wall of the separator.

(c)- Cu^{64} : The above yields could have been more accurately measured by adopting the technique now described for Cu^{64}. In this second method of determining yield the errors due to window thickness and estimation of the solid angle employed were eliminated. The procedure was as follows: The source of Cu^{64} was mounted at one end of the separator and the numbers of particles arriving at the other end were measured with the standard β -ray counter (mica window) The tube pressure was 0.0005 mm of Hg and the field current was set at $i = 8$ A, corresponding to 2160 gauss. (These values of the pressure and the field were chosen during the course of the main experiment because it provided the max. rate of counting. A curve indicating the distribution of of the intensity of the annihilation radiation as a function of the field is given in Fig. 39.). Next the same source was placed at a point in the separator immediately above the counter(counter being still attached to the tube). The separator was evacuated to the same pressure as before . Magnetic field was switched on in order to:

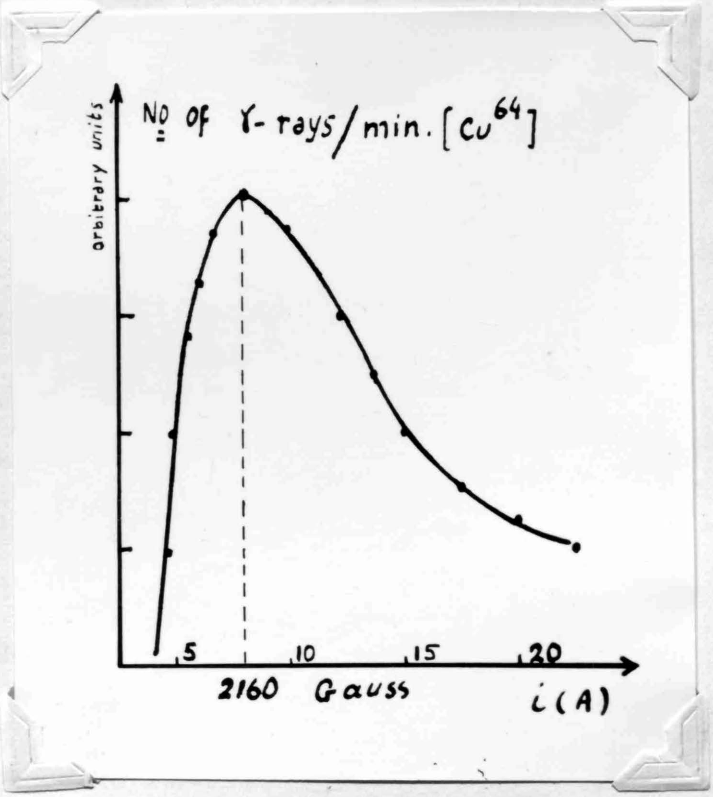

FIG. 39.

(i)- get rid off the electrons from the source,

(ii)- provide the same solid angle, approximately 4π, for the positrons entering the counter. The number of counts obtained in these circumstances was corrected for the decay of the source and the final ratio n/N was found to be %10 . The arrangement is suchnthat the measured value of N may be too high on account of penetration of the counter by negative β - rays before they pass along the separator in the the opposite direction to the positrons. Fig. 40 . The source distance was $\sim$ 1 cm and H was $\sim$ 2000 gauss. Thus ρ , the radius of curvature for the electrons of average average energy 0.3 MeV would be about 1.5 cm which gives them a chance of penetrating the counter. A method of allowing for the electron component of the counting rate(by comparison with the distribution of the γ - rays resulting from the annihilation of positrons as a function of the field intensity) was readily obtained and the corrected value of the yield was %16 . It should be noted that this value of %16 would be raised slightly if

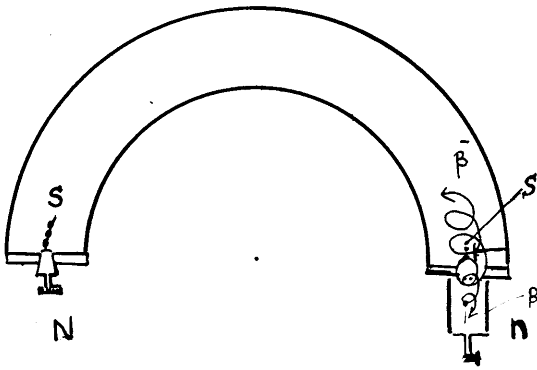

FIG. 40.

correction is made for the counts produced by X-rays (Ni X-rays from K-capture) and γ-rays (γ-radiation caused by the annihilation of positrons in the source and the surroundings of the counter) .

Section B:- Experiment on the Annihilation Radiation.

g.1. Electronic Devices: These consisted of a coincidence circuit, two amplifying probe units (one for each counter) and three scalers (Scaling Unit Type 200 A) to measure the two single counts and coincidences simultaneously. The supply voltages for the amplifiers and the coincidence unit were obtained from the scalers. The mixing circuit(the coincident Unit Type 1035) was designed to give three positive outputs which were separately fed to the three scalers. The coincidence output consisted of pulses of 20 volts in amplititude which were produced when the two counters discharged simultaneously: a negative pulse from the first probe unit (Probe Unit Type 1014), applied to the grid of the first valve, cut this triode off and, the large wide positive pulse produced from the anode passed through a cathode follower, and after being differentiated by a condencer and resistence passed through a diode producing a positive pulse of 5 volts amplitude across a resistence. The process is repeated for the second input and the resulting pulses are applied to the grid of a pentode which only takes anode current when the pulse amplitude exceeds 5 volts . Hence we can record a coincidence only when two single pulses are superimposed i.e only when the input pulses are coincident within the resolving time of the circuit. The latter was determined by measuring the chance coincidences produced by :

a- two independent sources; lead shieding between the two counters.

b- one source; counters set apart widely.

The value of the resolving time was found to be 1.49 μ sec. and 1.50 μ sec. for method (a) and (b) respectively ,and checked from time to time during the course of experiment.

The high voltage for the counters was supplied by a stabilised 2.2 KV power pack provided with the two potantiometer (P.U. Type 1007) which permitted independent adjustment of the voltage on each counting tube. The two rectangular coincidence counters were the same as previously described.

§.2. <u>Experimental arrangement</u>: Magnetic separator was mounted in its best position in the magnetic field; to close the counter end an aluminium sheet and a copper ring of the same total thickness as the β -ray counter flange were screwed on to the tube and sealed carefully in order to keep the whole system vacuumtight. To reach a pressure of about 10^{-4}mm. of Hg and to ensure the stability of the vacum the system was continuously evacuated by the help of a single stage oil diffusion pump backed with a Hivac.

The source consisted of a number of wires of 0.018" diameter and 1" length . Usually 5 or 6 such wires were used in one mounting to provide the required intensity. It was found by experiment that the most efficient arrangement was obtained by mounting these wires 5 mm. apart (parallel to each other and to the axis of the magnetic field) on a very thin tungsten wire support at right angles to it.

In the presence of the magnetic field the positrons travelled round the separator and on striking the annihilator ½" above the flange produced the source of radiation to be investigated. The annihilators were rectangular sheets of lead and aluminium of nearly equal superficial mass stuck together and screwed on to the horizontal ground joint. By rotating the knob either annihilator could be turned to receive the particles without interfering with the vacuum. A large lead block (3" by 15") was put on the way of unwanted γ-rays from the source between the two ends of the tube.

The two coincidence counters, screened to avoid interference, were set 3 mm. apart and screwed on to a metal plate which could slide between the two metal bars fixed on another metal plate . This arrangement allowed rotation of the counter assembly around an axis parallel to the axis of the field. With the help of this arrangement the distance of the counters and their angular position relative to the source could be adjusted as required. As a result of the several tests the maximum ratio of coincidences to single counts was obtained for the geometry in which $\theta = 45^{\circ}$ and d = 1" (Fig. 41.) The reasons for the counters being set as described were :

(a) to keep them out of the strong field,

(b) to subtend as large a solid angle at the source as possible. When they were placed vertically below the annihilator the loss of energy of the secondary electrons in the thin copper walls was excessive since they all made several passages through the counter in the strong fringing field.

Under these conditions, at the beginning of a run the number of single counts in the first and second counters were of the order of 40000 per minute and 10000/min. respectively and approximately 500 coincidences with no absorbers and about 25 at infinite absorber thickness were obtained.

§.3. Three series of experiments were carried out, each involving several differences in the method of taking and analysing the data.

1- The first run was made with a single source of five wires. To cover the full range of the two absorption curves with lead and aluminium annhilators while employing only the one source and to maintain the consistency of the experimental conditions observations were continuously performed for a

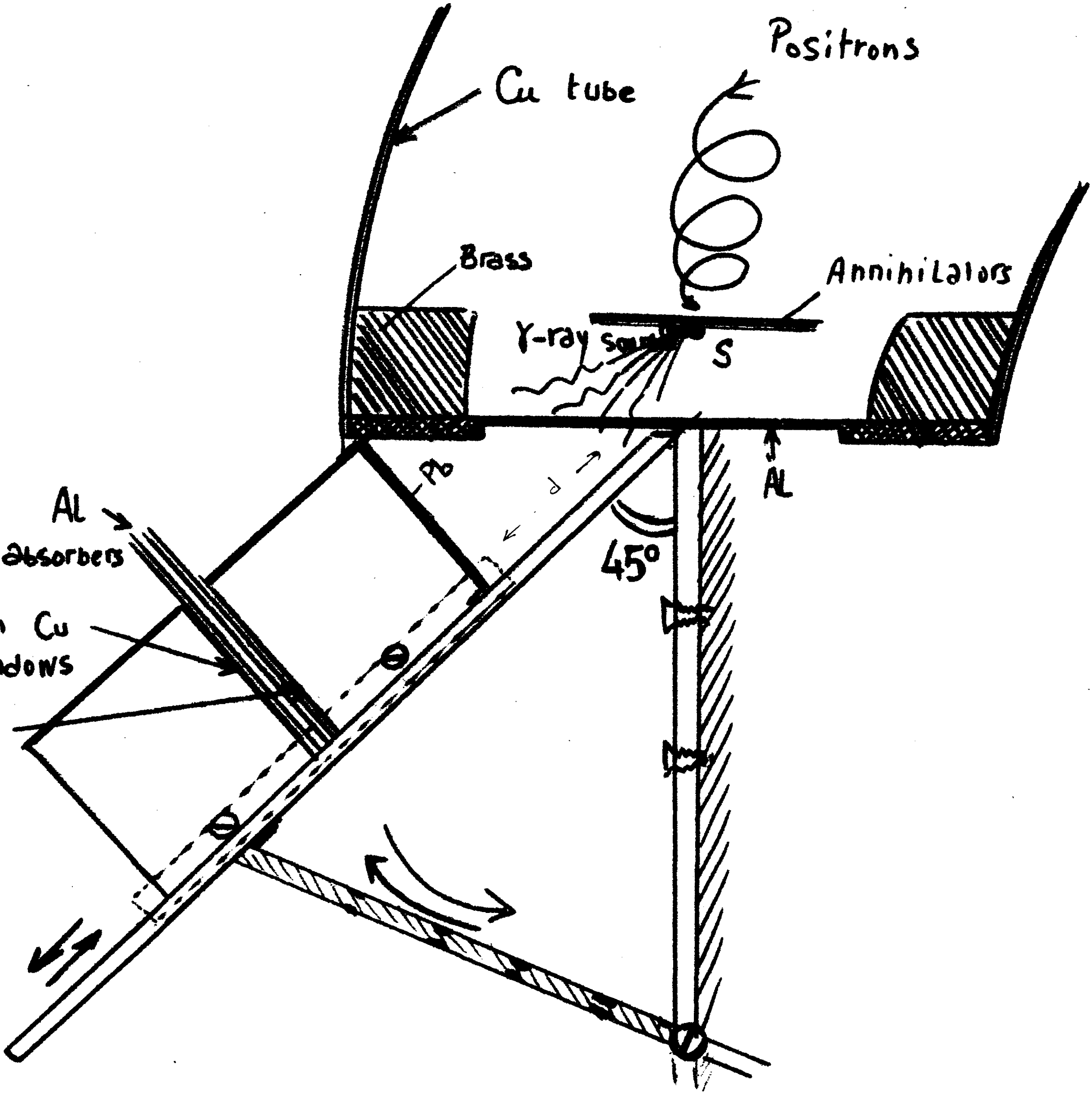
Positrons
Cu tube
Brass
Annihilators
γ-ray
S
AL
Pb
d
45°
AL absorbers
Thin Cu windows

FIG. 41.

period of over 36 hours in each case. Two measurements on each point of each curve were taken in the course of decreasing the thickness of absorber. The curves were studied up to the maximum number of absorbers (12 of 0.01" thickness each, which is the range of 2 MeV electrons) which was well beyond the region of the possible maximum energy of the annihilation radiations.

The real number of coincidences was calculated from the total number of observed coincidences by subtracting the chance coincidences and the cosmic-ray background . The latter was studied in the new system as a function of the absorber thickness taking several hours measurement for each absorber. On the average the number of cosmic ray coincidences varied between 2 and 6 per minute for $x \geqq 12$ and $x = 0$ respectively. (Here x is the absorber thickness)

The readings in the presence of the source were taken alternately for Pb and Al in the following order:

(a)- Ten minute readings for coincidences N_c at $x \neq 0$ The total counts were found to vary between ~ 20 -50 / min. as the number of absorbers varied between 12 and 1 .

(b)- Simultaneously with starting to count coincidences the single counts were measured for a minute or two.

(c)- The number of coincidences N_0 for $x = 0$ was measured at the beginning, middle and at the end of the run, and the decay correction for each point was made referring to a single time origin. Each number of coincidences at an absorber thickness was corrected for cosmic rays and chance coincidences and decay and was normalised dividing by the number of coincidences at zero absorber thickness corrected for chance and cosmic ray coinsidences. The result of this run is shown in Fig.42 . The ordinate indicates the ratio of n_c/N_0 . The abscissa shows the number of aluminium absorbers. The absorption curve obtained with lead annhilator is still above that for an aluminium annihilator each ending more or less in the same point within the probable error . Naturally in this method large statistical errors do not allow us to make further very definite conclusion. What we can say as a first approximation is this that the nuclear γ-rays do not produce an appreciable effect on the process we observed. This makes the previous observation more reliable.(Cf. Chap.IV.).

II- In order to reduce the statistical errors a single pair of points(one point on each curve) was examined carefully with one set of wires as source. Because the maximum rate of delivery of the sources from Harwell was one per week , full curves were obtained only after several months.

The procedure of taking readings for each pair of points was as follows:

(a)- Number of coincidences at zero absorber was measured

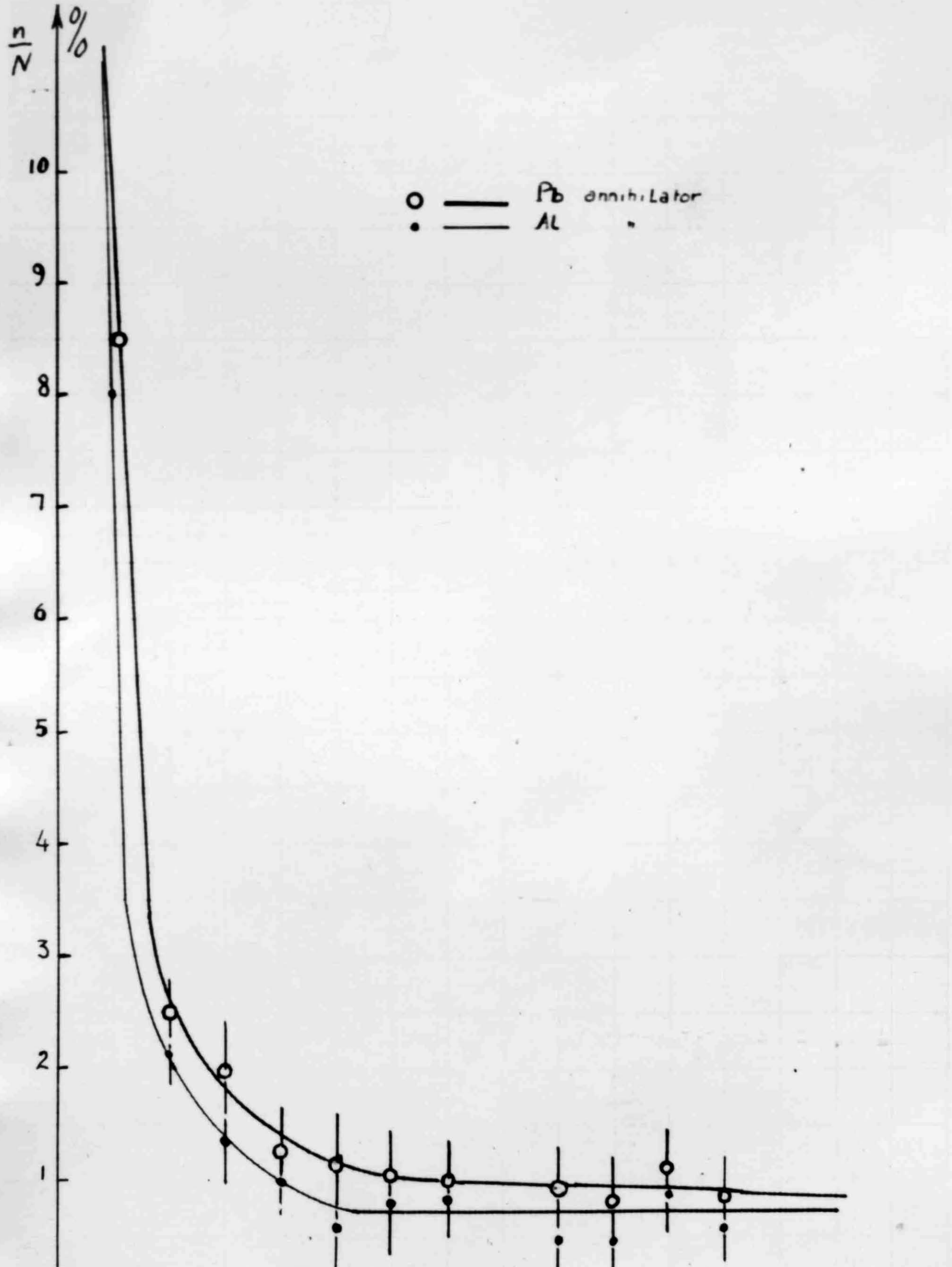

Fig. 42

for 5 or 10 minutes.

(b)- Number of single counts in the first and second counter was simultaneously measured with (a) for the same period. i.e. the three scalers were switched on and off exactly at the same time.

(c)- Number of coincidences at absorber thickness x was measured over a period of 5-6 hours. Over $2\,10^5$ coincidences were made.

(d)- Number of single counts in both counters was measured during the first minute of (c) { because the value of the single counts in the second counter varied with the absorber thicknesses by about ~~$~~ 10 and even the no. of single counts in the first counter was slightly affected by the presence of the absorbers.)

(e)- Both single counts and coincidence counts were checked nearly every half - hour in order to ensure the stability of the experimental arrangement.

(f)- (a) and (b) were repeated at the end of the run to avoid any accidental changes.

These long observations need a very elaborate decay correction because of the short life-time of the source. The proper form of correction made for the decay, chance coincidences and the background is summarised in the following formula:

$$nc = \frac{\lambda(t_2-t_1)\left[\frac{n_t}{t_2-t_1} - B - \frac{n_1 n_2 \tau/60}{\lambda(t_2-t_1)}\left(1-e^{-2\lambda(t_2-t_1)}\right)\right]}{e^{-\lambda t_1} - e^{-\lambda t_2}}$$

where,

n_c = Real number of coincidences per minute at an absorber thickness x .

λ = Decay constant for Cu^{64} positrons which is equal to $9.01 \; 10^{-4}$ per minute .

t_2-t_1 = Time interval during which the integral number of coincidences is observed .

n_t = Integral number of coincidences.

B = Cosmic-ray plus ordinary backgound coincidences/ min.

n_1 = Number of single counts in the first counter at the instant t_1 .

n_2 = Number of single counts in the second counter at t_1 .

τ = Resolving time of the coincidence circuit.

In order to avoid any confusion the necessity of employing such formula is explained below: The square bracket indicates the real number of coincidences. The first term n_t/t_2-t_1 is the rate of average number of total coincidences as a result of an observation of duration $t = t_2-t_1$. Since n_t is the integral number of coincidences measured over a period t , the average number corresponds to a time $t_1+\tau_m$ where τ_m (mean time) is given by

$$e^{-\lambda\tau_m} = \frac{1 - e^{-\lambda t}}{\lambda t} .$$

τ_m is only slightly different from t/2 for an observation of duration 18.5 hours for which $\lambda t = 1$.

$e^{-\lambda t/2} = 1/\sqrt{e} = 0.6065$, and $e^{-\lambda \tau_m} = 1-1/e = 0.6321$, Thus the difference between the two is about 4.5%. Therefore for the short readings of 10-20 minutes this difference is entirely negligible. Hence in such short readings the average number of coincidences is regarded as corresponding to a time given by $(t_2-t_1)/2$, but in every reading exceeding half an hour the corrections are made by referring to τ_m . The second term is the background correction for cosmic rays and etc., it is assumed to be constant per minute for each x at any time. The third term indicates the chance coincidences correction. The latter would occur with the rate of $2n_1n_2\tau/60$ per minute at the time origine and because of the decay the number would be $2n_1n_2\tau/60.e^{-2\lambda t}$ after a time t. During the time interval t_2-t_1, the integral number of the chance coincidences would be

$$2n_1n_2\frac{\tau}{60}\int_0^{t_2-t_1} e^{-2\lambda t}\,dt$$

Hence the rate of chance coincidences at the time $t_1+\tau_m$ will be

$$C = \frac{n_1n_2\tau/60\,(1-e^{-2\lambda(t_2-t_1)})}{\lambda(t_2-t_1)}$$

The decay correction for the real number of coincidences referred to the moment $t_1+\tau_m$ was made relative to an arbitrary time origin t_0 from which t_1, t_2 are measured.

The content of the square bracket has to be multiplied by a factor $e^{\lambda(t_1+\tau_m)}$ which is equivalent to division by

$$\frac{e^{-\lambda t1}\left(1-e^{-\lambda(t2-t1)}\right)}{\lambda(t_2-t_1)}$$

which is equal to

$$\frac{e^{-\lambda t_1}-e^{-\lambda t_2}}{\lambda(t_2-t_1)}\ .$$

The accurate values of $e^{-\lambda t}$ for $0<\lambda t<1$ were obtained from a table using up to five or six decimals.

The numerical values calculated for each observations from the above formula are given in Appendix V. Fig. 43. ilustrates the result of the experiment after n_c and N_c were corrected and the ratio of n_c/N_c plotted against the energy of the recoil electrons. The shape of the absorption curve in general agrees with the previous one, and confirms the results obtained before with a much increased accuracy (free of large statistical errors) (See App. V)

From this graph, the following qualitative conclusions can be deduced at once :

(1)- The difference of intensity between the two curves obtained with Pb and Al annihilators in favor of lead proves the existence of one quantum annihilation. (cf. Chapter IV)

(2)- The different slope of the tails of the two curves

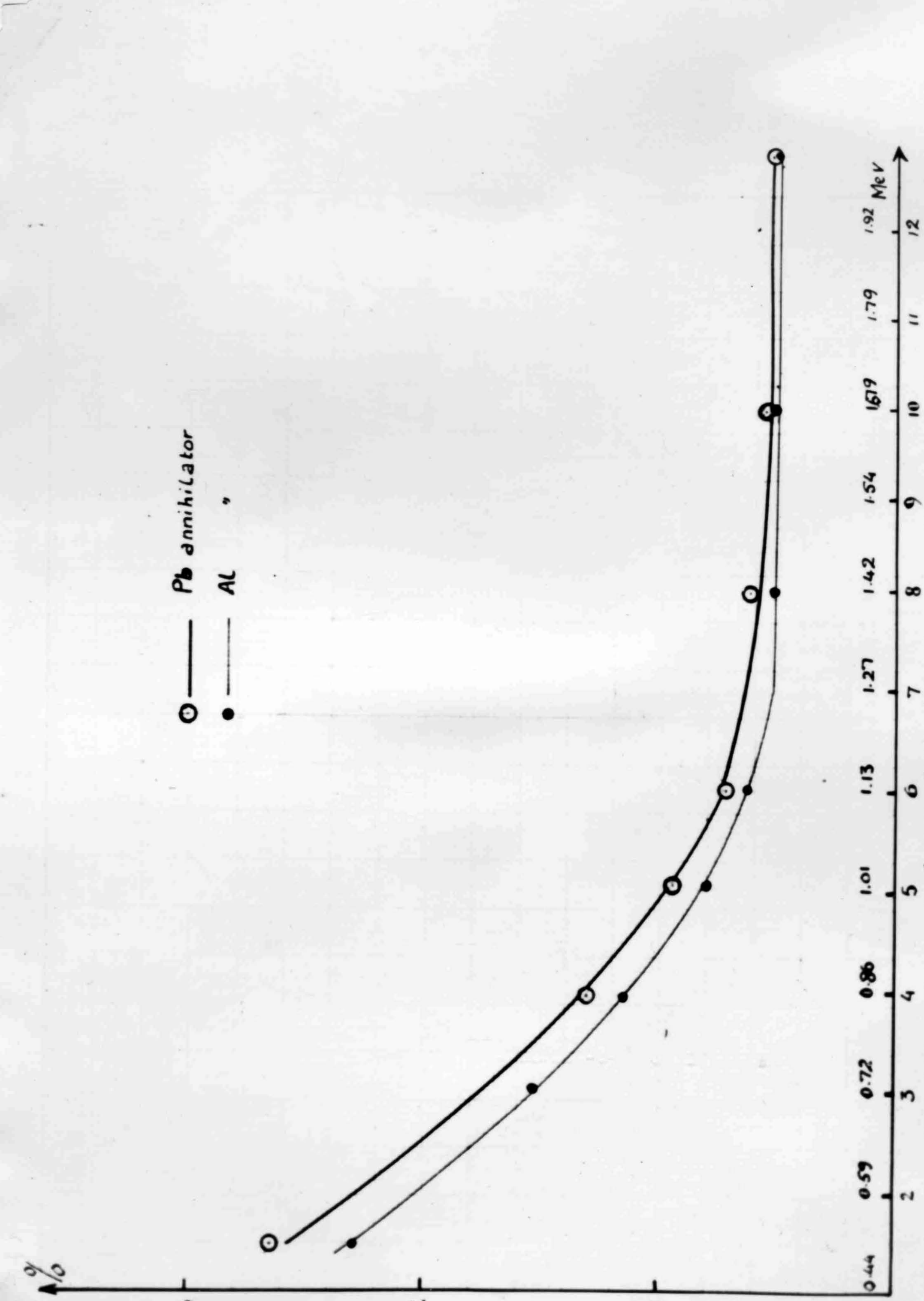

$\frac{n}{N_c}$ %
3
2
1
Pb annihilator
Al "
0.44
0.59
0.72
0.86
1.01
1.13
1.27
1.42
1.54
1.69
1.79
1.92
MeV
2
3
4
5
6
7
8
9
10
11
12
Number of absorbers

FIG 43

near the end point verifies that this radiation is produced only in a heavy annihilating medium in sufficient amount to be observed.

(3)- A pronounced tail beyond the strong component of 0.5 MeV, in both materials, indicates the existence of the two-quanta annihilation radiation in motion.

To be able to make a quantitative analysis of these curves an extrapolation back to the real zero absorber thickness is required. This was done firstly by plotting the logarithmic intensities against the energies, and allowing for the two copper windows of 0.001" thickness (64.72 $\frac{mgr}{cm^2}$)

In the case of aluminium the logarithmic absorption curve could be easily decomposed into two nearly straight lines of different slopes. Neglecting the latter which is obviously very small compared with the main radiation (See Fig. 44 .) a factor of 10 was obtained from the extrapolation of the first line, undoubtedly due to the 0.5 MeV radiation. In the numerical calculation of the areas S_{Pb} and S_{Al} under the two curves for lead and aluminium , this factor of 10 was taken into account.

If we denote the difference of areas $S_{Pb} - S_{Al}$ by s , the ratio of s/S from the measurement of these areas was found approximately equal to 5% . This can be interpreted in the following way :

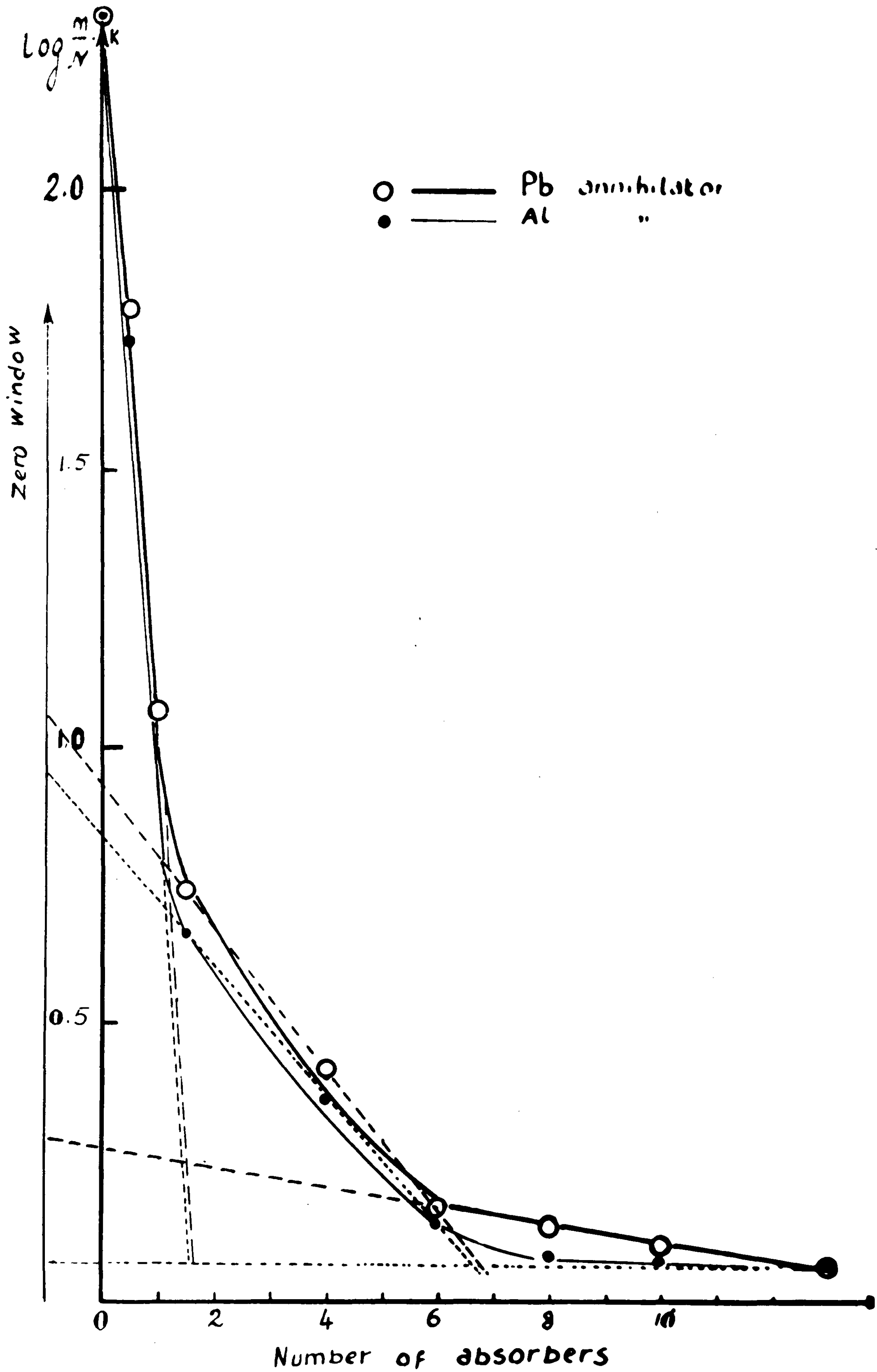
Log $\frac{m}{N}$ K
Pb annihilator
Al "
2.0
1.5
1.0
0.5
Zero window
0
2
4
6
8
10
Number of absorbers

In the case of Pb annihilator we have three types of radiation:

1. Two-quanta annihilation radiation at rest for which the absorption coefficient of the secondary electrons is denoted by μ_1 and the numerical value of μ_1 can be obtained from the slope of the first line in the logarithmic plot of the absorption curve.

2. Two-quanta annihilation radiation in motion for which the absorption coefficient is μ_2.

3. One-quantum annhilation radiation for which the absorption coefficient is μ_3.

In the case of Al annihilator, according to the result of the experiment and the theory, we have in practice the first two components of the radiations only and not the third one (cross-section for low value of Z is very small). Then the area under the absorption curve obtained when using Pb as annihilator is given by

$$S \int_0^x y dx = \int_0^x I_{01}\, e^{-\mu_1 x} dx + \int_0^x I_{02}\, e^{-\mu_2 x} dx + \int_0^x I_{03}\, e^{-\mu_3 x} dx$$

where I_{01}, I_{02}, I_{03} are the intensities of the three types of radiation measured at zero absorber thickness.

Then

$$S_{Pb} = \frac{I_{01} - I_1}{\mu_1} + \frac{I_{02} - I_2}{\mu_2} + \frac{I_{03} - I_3}{\mu_3}$$

I_1, I_2, I_3, are the intensities of the radiations at an absorber thickness x. In considering the total area we are dealing with values of x at which the intensities of the radiations are reduced to zero. Hence we can regard I_1, I_2, I_3 as negligible compared with the intial intensities I_{o1}, I_{o2}, I_{o3}. Therefore

$$S_{Pb} \cong \frac{I_{o1}}{\mu_1} + \frac{I_{o2}}{\mu_2} + \frac{I_{o3}}{\mu_3}$$

and

$$S_{Al} \cong \frac{I_{o1}}{\mu_1} + \frac{I_{o2}}{\mu_2}$$

and

$$S_{Pb} - S_{Al} = \frac{I_{o3}}{\mu_3}$$

Here we are assuming that I_{o2} is the same for Al and Pb, which is true theoretically and is in essential agreement with the results. We deduce therefore that the difference of the areas under the two curves is proportional to the intensity of the hard radiation due to the one-quantum annihilation process; the factor of proportionality being the absorption coefficient for that radiation and it can be measured by the help of the logarithmic plot of the curve. Knowing the values of μ_1 and μ_2 as well, we can express the ratio of s/S as a function of these measurable quantities and I_{o3}. This is given by

$$s/S = \frac{S_{Pb} - S_{Al}}{S_{Al}} \cong \frac{I_{o3}/\mu_3}{\frac{I_{o1}}{\mu_1} + \frac{I_{o2}}{\mu_2}}$$

or, in order to introduce the ratio of the absorption coefficients this relation can be written as:

$$s/S = \frac{I_{o3}}{\mu_3/\mu_1 (I_{o1} - I_{o2}\,\mu_1/\mu_2)}$$

In this last relation μ_3/μ_1 and μ_1/μ_2 are measured from the graph (44) and found equal to ~ 0.015 and ~ 10 respectively. s/S was determined from the ordinary absorption plot. To estimate the I_{o3} in terms of I_{o2} and I_{o1} another relation between the three is required. This can be obtained firstly from the ratio of the logarithmic intensities at zero absorber, extrapolated to the absolute zero absorber thickness which gives us I_{o2}/I_{o1} equal to ½% . As an alternative approach we can introduce the theoretical value of the cross-section σ_2 in order to obtain the equivalent of an extra relation connecting the quantities in the above equation. The justification for this step is found now to lie in the overall agreement which follows between our experimental results and theory: for the Cu^{64} source the annihilation in motion would be mainly due to the positrons of energy (on the average) 0.3 MeV and these have a range of 80 mgr/cm^2 which correspond to 0.0073 cm of range in lead. There are approximately 3.2 10^{22} atoms per cm^3 in lead and hence 2,3 10^{20} atoms in the range of the electrons (n_2) σ_2 per atom in lead* for $E_k = 0.3$ MeV is 2.2 10^{-23} cm^2. $n_2\sigma_2 = 2.2 \times 2.3 \times 10^{-23} \times 10^{20}$

---

*Cf. Chapter II. Fig. 13 .

which is equal to 5.10^{-3}. If we take this value of ½% as the ratio of two-quanta annihilation "in motion" to "at rest" and substitude in the following relation

$$s/S = \frac{I_{03}}{0.015\ (I_{01} - 10\ I_{02})}$$

we will have

$$= \frac{I_{03}}{I_{02}} \left(\frac{0.015}{0.005} - 0.15 \right)^{-1} = 5\%$$

Finally as the ratio of one-quantum annihilation in motion to two-quanta annihilation we obtaine

$$\frac{I_{03}}{I_{02}} = 16\%$$

As we have seen in Chapter II the theoretical value of the ratio of the two cross-sections calculated on the basis of the Born approximation for both processes has a maximum limit of about 15% . The actual value of the average cross-sections σ_1 and σ_2 for the Cu^{64} positrons could be calculated, over the all energies, from

$$\frac{\int_0^{E_{max}} P(E).\ \sigma(E)\ dE}{\int_0^{E_{max}} P(E)\ dE}$$

or, to a first approximation, the ratio of the average cross-sections $(\sigma_1)_A$ / $(\sigma_2)_A$ will be equal to

$$\frac{\sum_{i=1}^{n} N(E)_i \sigma_1(E)_i}{\sum_{i=1}^{n} N(E)_i \sigma_2(E)_i} = \frac{N(E)_1 \sigma_1(E)_1 + N(E)_2 \sigma_1(E)_2 + \dots + N(E)_n \sigma_1(E)_n}{N(E)_1 \sigma_2(E)_1 + N(E)_2 \sigma_2(E)_2 + \dots + N(E)_n \sigma_2(E)_n}$$

where;

$P(E)$ is the energy distribution of Cu^{64} positrons, and $N(E)$ = number of the positrons at a given energy; this was obtained from a curve illustrating the momentum spectrum of the positrons from Cu^{64} (54), and $\sigma_1(E)$, $\sigma_2(E)$ are the cross-sections as a function of energy for one and two quanta annhilation processes and their numerical values were taken from the Fig. 13. The result of the numerical calculations gives a value of 10% as $(\sigma_1/\sigma_2)_A$ which is in fairly good agreement with the ratio of the intensities obtained from the result of our observations. As a further justification of this comparison it would be necessary to show that these two ratios are identical, i.e. $I_{o3}/I_{o2} = \sigma_1/\sigma_2$.

Let us suppose that originally we have N_o positrons and let us assume that all these positrons will annihilate in the medium concerned; then considering that we have an inhomogeneous beam of positrons we can regard them as being absorbed exponentially. Hence for a substance of density ρ the absorption of positrons may be described by the equation

$$N = N_o\, e^{-\mu/\rho\, m}$$

where, μ/ρ is the ~~mass~~ absorption cefficient, m is the superficial mass of the absorber i.e. annhilating material, N is the number of positrons which survives. Thus the number of positrons which is annihilated will be $N_o - N$. This, to a first approximation, is equal to $N_o \mu m/\rho$. Therefore the intensity of the annihilation radiation which is produced will be proportional to this quantity. On the other hand, by definition, the cross-section is the absoption coefficient per atom (or per electron). If we denote the number of atoms per cm^3 of the annihilating material by n, the cross-section per atom σ will be equal μ/n, hence, i, the intensity of γ -rays produced in a given material will be

$$i \cong n \sigma N_0 \; m/\rho$$

In lead the component of annihilation radiation due to one-quantum process will be

$$i_1 = n \sigma_1 N_0 \; m/\rho$$

and of that due to the two-quanta process will be

$$i_2 = n \sigma_2 N_0 m/\rho$$

and the number of detected quanta will be proportional to $i_1 \varepsilon_1$ and $2 i_2 \varepsilon_2$ respectively, where ε_1 and ε_2 are the efficiencies of the counter for both radiations. It is known that $2\varepsilon_2 \cong \varepsilon_1$. Hence the ratio of the intensities* is the same as the ratio of the cross sections.

---

* The absolute intensity of the coincidences which are measured can be expressed in terms of the parameters which are involved in the experimental arrangement. We have $I = k n_0 \frac{L}{A} \sigma \, m \, \chi_0 r$ where k is a complicated proportionality factor which is a function of solid angle and probably energy loss. N_0 is the number of atoms per c.c in material of counter, χ = cross-section for Compton and Photo-electron (an average combined one here), L = Loschmidt constant A = atomic weight and m = superficial mass of the annihilator r = range of secondaries produced in wall of counter.

Apart from the intensity of the radiations the energy value of the γ-rays due to one-quantum annihilation seems to agree quite well with theoretical prediction. The end point obtained from the logarithmic plot, and also ~~well~~ from the ordinary plot of the absorption curve tends to be between six or seven absorbers, which correspond to ~~the~~ ranges equivalents of 1.13 and 1.27 MeV respectively. Since the cross-section for compton electrons is much higher than the cross section for photoelectrons for γ-rays of energy about 1 MeV we can assume to a first approximation that the ranges we measure in Al can be considered as the ranges of compton electrons. If we assume that the collisions are head-on ($\theta = \pi$, $\varphi = 0$), $E = 2h\nu_0\alpha/(1+2\alpha)$, where $\alpha = h\nu_0/mc^2$. From this formula we find that for the measured value of E, $h\nu_0 = 1.34$ MeV. On the other hand, for a positron of energy 0.66 MeV, the maximum energy of annihilation radiation is $h\nu_{0\,max} = \frac{1}{2}mc^2 + mc^2 + E_k = 1.41$ MeV, which is in good agreement with the above value. Photoelectrons corresponding to this energy would give us, if we take into account the binding energy of the K-shell, a minimum of 1.31 MeV recoil energy. If we took the end-point as corresponding to No.7 absorber this would be equivalent to an energy of 1.27 MeV. which is close to the above value.

To make certain the existence of the hard component due to the two-quanta annihilation in motion, since this radiation appears in both curves taken with lead and aluminium annihilator , a comparison between the result for a Cu^{64} source and that of a source of γ-ray ~~emitter~~ of energy near* 0.5 MeV would be desirable. For that purpose a Sn source, known to emit 0.6 MeV γ-rays was tried first and found to exhibit a strong tail up to 1.2 MeV range. This was in disagreement with tabulated data but it may have been due to impurity or deficiency in previous work. Next a very thoroughly studied source Au^{198}, which emits γ-radiation of energy 0.41 was chosen (86-90). A small piece of gold foil, activated in the pile, was mounted on the annihilators after being covered with a thin mica sheet. The absorption measurements were carried out in exactly identical circumstances as that ~~of~~ for Cu^{64} source . The number of coincidences were measured even for the high values of the absorber thickness. The results are shown in Fig. 45 . As seen from the graph a very flat background was obtained up to the second absorber in coming down to the zero absorber. This finding is entirely different from the case of Cu^{64}.

---

* The ideal thing to have would be a non-positron emitter source of 0.51 MeV γ-ray, but no such source of accurately known energy is available.

FIG. 45

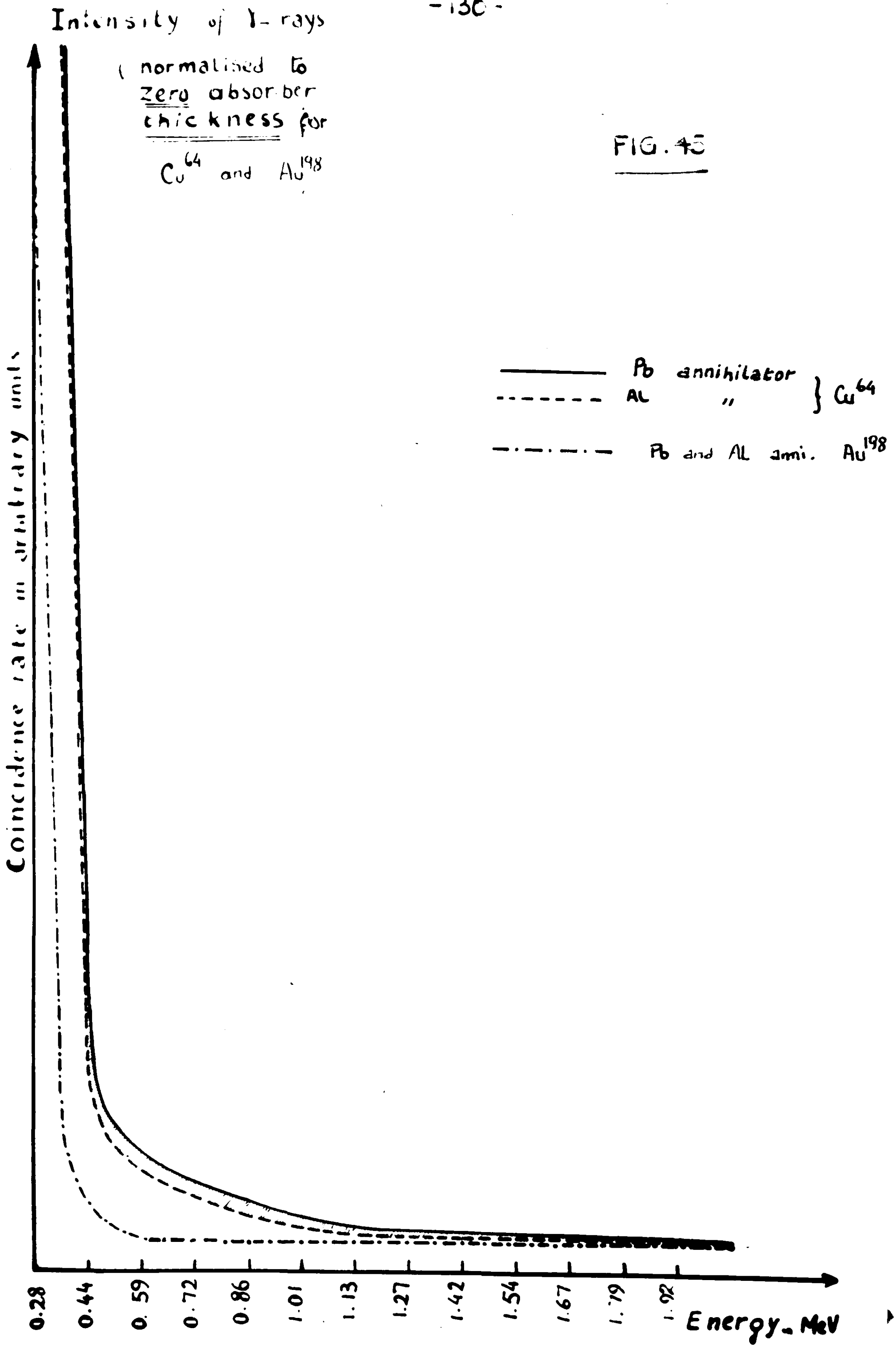

Ordinates normalised to zero absorber after removal of individual backgrounds.

Another difference was the intensity of the background. It was by a factor of 5 higher than the background which was obtained with Cu^{64} . This was true when the number of coincidences from both radiations (Cu^{64} and Au^{198}) were normalised to the number of coincidences at zero absorber. However the effect of the counters windows for both radiations had still to be taken into account. To be sure about this relatively high background one more absorption curve with gold was taken by mounting the source on the lead annhilator. The result was nearly the same as for Al, (Pb curve being slightly below the Al curve) .

From the logarithmic plot of the absorption curves for gold, extrapolated to zero window thickness, it was found that an additional factor of about 2 seemed necessary for the normalisation of the number of coincidences from gold source with that of copper source in order that the background intensities should be the same. To obtain the precise value for the window correction the following experiment was planned and carried out with both sources Cu^{64} and Au^{198}. The two square counters, as used for the previous experiment, were mounted in a flask with the same geometry as in the previous setting, and the two windows facing each other were removed. The whole assembly was evacuated and filled with the same mixture at the same pressure. The sources were mounted alternately on the flask (See Fig. 46 .) being wrapped with a sheet of lead and both being at the same distance from the first counter. The number of coincidences was measured and also the single counts readings were taken in both counters and the relative coincidence intensities were calculated in terms of the single counts for both sources. The same process was repeated after inserting two copper foils of 0.001" thick each(which is the equivalent of the two window thickness) into the space between the two counters. This simulated the windows used in normal practice. The whole system was again evacuated and refilled as usual. In the latter case the relative number of coincidences was reduced from 36.6% to 1.81 % for gold, and from 39.8 % to 4.29 % for copper. This implies a correction by a factor of 2.37 for gold. Incidentally it should be noted that the ratio of 39.8/4.29 gives a factor of 9.25 for the extrapolation of the annhilation radiation to the zero window thickness. This is in good agreement with the factor of 10 which we accepted earlier in the analysis of our curves.

To make sure that the two counters with no window present do not cause any additional coincidences due to the sympathetic discharge (induced say by photo-emission) the same test was repeated with a very thin aluminium foil between the two. The ratio of the number of coincidences

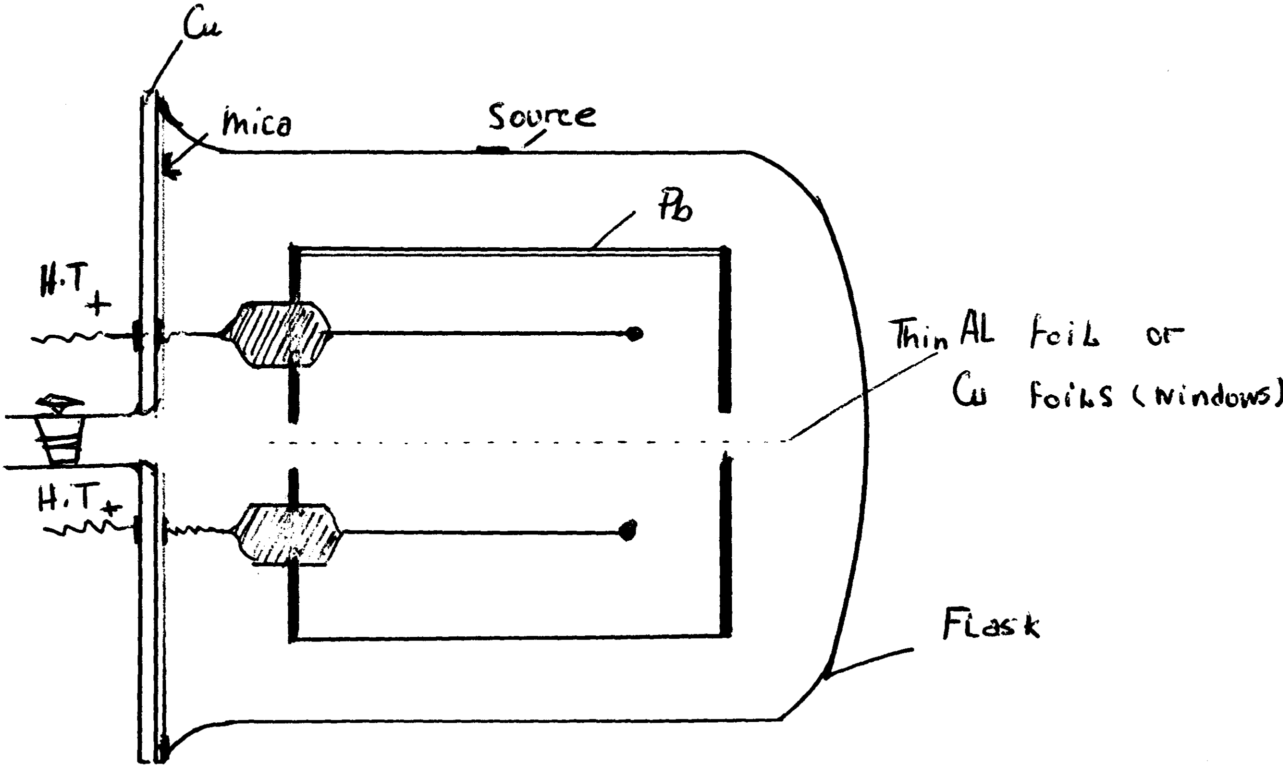

FIG. 46 .

to the number of single counts per minute for Au and for Cu was 23.2 % and 24.7 % respectively. The agreement of the two ratios among themselves verifies that the two ratios obtained with no window are free of errors. (The reduction in the value of the ratios when Al foil is used is mainly due to the scattering effect). Having traced 2.37 parts of the factor of 5 in background intensity ratio we can proceed further to explain the high background in the case of the gold source. Thus it can be definitely assumed that the remaining background in each case (Cu^{64} and Au^{198}) is due to the :

(a)- Double Compton process.

(b)- Double Photo process.

By (a) we understand that a compton process at one counter yields a secondary electron which triggers it and a softer quantum which succeeds in triggering the other counter.

By (b) we mean that an act of photo-electric absorption gives a triggering photo-electron and an X-ray quantum (normally K-level) which triggers the second counter. The first of these processes will obviously not vary rapidly with quantum energy , but it is known that the cross section for the photo-electric effect varies with the -7/2 power of the energy of the incident γ-rays

$$\phi_K = \phi_0 \frac{Z^5}{(137)^4} \, 4\sqrt{2} \, (\mu / k)^{7/2}$$

Hence for the ratio of the cross-sections, ϕ_{Au}/ϕ_{Cu} we obtain a factor of

$$f = \left(\frac{k_{Cu}}{k_{Au}}\right)^{7/2} = 2.1$$

where $k_{Cu} = 0.51$ MeV and $k_{Au} = 0.41$ MeV . We have therefore a definite explanation of the relatively high background on the absorption curve for gold since $f = 2.1$ is very close to the ratio of 5 to 2.37 , the required factor of normalisation for zero window thickness for both radiations (gold and copper γ-rays).

Furthermore the very close agreement means that the remaining background in both cases is due to the photo-electron- Xray coincidences and not to the compton electron- γ -ray coincidences. In other words the double compton effect is negligible beside the double photo effect. Sufficiently careful study of the rate of diminution of the background intensity with aluminium absorbers should give a coefficient of absorption corresponding to the K X-rays of lead.

III - As an additional check on the main experiment and in order to avoid any systematic error in the " long run " technique , the relative intensities of the γ -radiations produced in lead and aluminium as annhilators, were alternately measured every minute and the sums of the total number of coincidences per minute plotted against the absorber thicknesses;Fig. 47 . shows the consistency of the nature of the

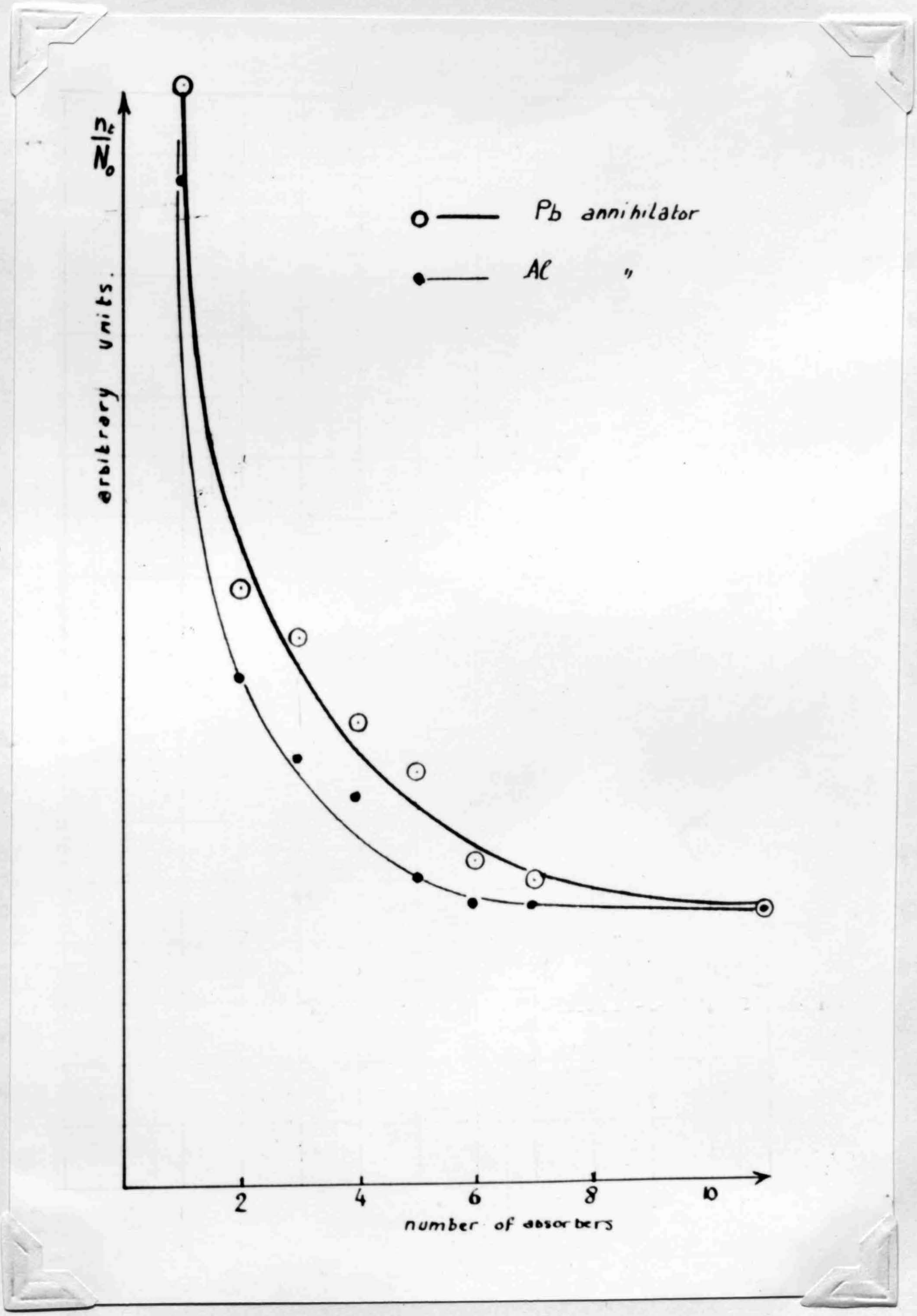
n_t / N_0
arbitrary units.
Pb annihilator
Al "
2
4
6
8
10
number of absorbers

FIG. 47.

Section C:- General Remarks and Conclusions .

The experimental results seem to exhibit an adequate proof of the existence of hard radiation from the annihilation of positrons at a nucleus. This " one-quantum annihilation" radiation is observable only when a heavy substance is used as an annihilator. The experiments establish also very definitely the existence of radiation produced in the process of two-quanta annihilation in motion . The ratio of the intensity of single quantum radiation to that of the two-quanta radiation in motion agrees with the theoretical value within a factor of two.

Moreover, the comparison of the results obtained in studying the absorption of the radiations produced by :

(a) A total source of Cu^{64} (cf. Chapter IV) , and,

(b) The positrons only from source Cu^{64} (cf.Chapter VI),

shows that the effect of any nuclear γ-radiation ascribed to the source is quite negligible. This close agreement in the two studies throws considerable doubt on the results of Deutsch for Cu^{64} radiations. This remark is supported to some extent by the separate work discussed in Chapter V.

---o-0-o---

CHAPTER VII

PROPOSALS FOR FUTURE INVESTIGATIONS.

In this chapter a list of suggestions will be given for further experiments on the annihilation of positrons. First of all we shall mention those which arise as a result of our own work. For the most part they will show that it is desirable to prosecute experiments of a type similar to those described here but with improved experimental conditions or with rather different methods, not possible to put into practice or adopt during the course of the present work. Afterwards we shall pass on to suggestions for experiments on points which have been neglected or not clearly established so far in connection with ~~the~~ positron annihilation in general.

(A): 1- An investigation of the angular distribution of the two-quanta annihilation radiation as a function of the energy of the positrons is of importance. This introduces the necessity of obtaining positron sources* of different

---

* A list of the positron emitters with histograms showing the life-time and the energy distribution among these substances is given in Appendix. II

energies and suitable life-times, or obtaining sufficiently intense sources to permit magnetic resolution of the positrons. This second possibility is preferred because it allows us to define the direction of incidence of the positrons ; the experiment also requires very high efficiency counters (for γ- radiation) of small solid angle such as crystal plus photomultiplier counters. The study of the various angular distribution curves normalised at the peak might produce interesting results, such as the variations of the probability of annihilation in motion with energy or the cross-section for the two-quanta annihilation process.

2- Study of one-quantum annihilation by (a)- the routine coincidence absorption method using a very slow positron source for which the two-quanta annihilation in motion is negligible. It was hoped that Ni^{59} tabulated as a source of upper energy 50 Kev, would be used. No such material was obtained in long-term irradiation of nickel in the Harwell pile. (b)- detecting the coincidences between the one-quantum annihilation radiation and the X-ray produced in the annihilating material (because a K-electron will be missing after annihilation takes place). High efficiency proportional counters filled with krypton or xenon to make them sensitive to X-rays, are preferable as detectors. Determination of the energy of the X-ray characteristic of the annihilating material could be made directly by using the proportional tube calibrated with known radiations. One of the complicating features is the presence of strong γ- radiation (0.51 Mev) and we need to separate the pulses due to the X-rays from the γ-ray pulses. Therefore the cylinder should be of a light material such as carbon to reduce photoelectric effect from it relative to the gas effect. Since the X-ray pulses will be of nearly uniform amplitude the use of a pulse amplitude selector will automatically rid us of much of the γ-ray effect. Again it is possible to use a special system of counters within a container; the inner one (Fig. 48) is made of wires parallel to the axis of revolution and it is surrounded by a set of counters. Possible improvements achieved with this system are: (i) reduced γ-effect since this occurs at outer wall and outer tubes are in anti-coincidence; (ii) reduced wall effect for X-rays. Here most of the counts of the counter, corrected by anti-coincidence, are due to absorption of X-rays in the gas. Again the pulse amplitude measures the X-ray energy when used proportionally.

3- (β , γ) correlation from Cu^{64} could be checked very thoroughly with the help of the trochoidal method. A seperator preferably semi-circular as used in the present work, can be placed in the fringing field of the magnet with a pair

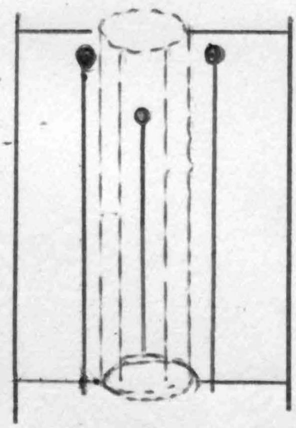

FIG .48.

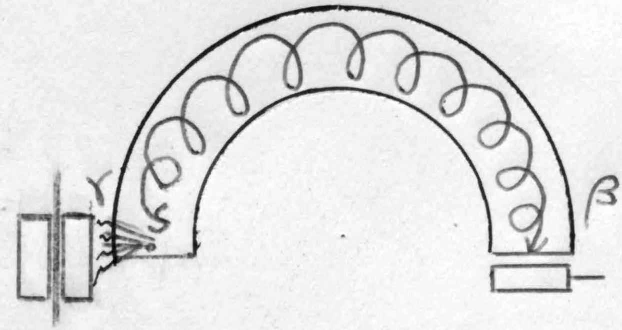

FIG. 49.

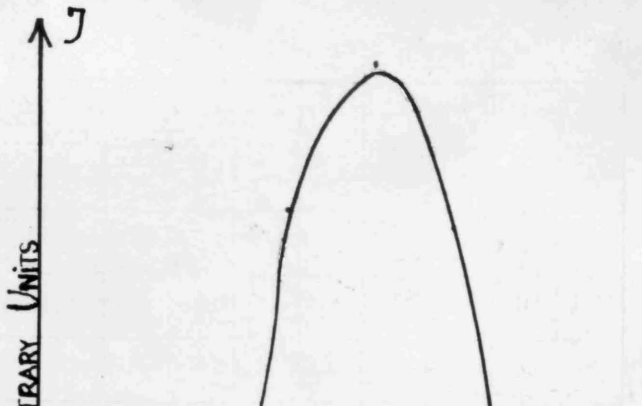

FIG. 50.

of coincidence counters to measure the energy of the γ-rays and a thin window β - tube which is used to detect the positrons or the electrons. Fig 49. The single counter is connected to the first two in coincidence to give (β, γ) and (γ, γ) coincidence rates. This arrangement is satisfactory in the sence that it operates with nearly whole emission of β^- or β^+ particles but it separates from other interfering effects.

4- Study of γ-radiations from Cu^{64} by means of an upto-date β-ray spectrometer and by changing the annihilating material around the source. Although the mean energy of the annihilation radiation(one-quantum process) and the nuclear radiation coincide at 1.35 mev the shape of the secondary electron spectrum will determine whether the radiation is really homogeneous (nuclear) or inhomogeneous (one-quantum annihilation radiation). The expected energy distribution of one-quantum annihilation radiation from Cu^{64} is shown in Fig. 50 . The changing of the annihilating material from, for instance, aluminium to lead will indicate whether or not the nuclear γ-ray alone is responsible for 1.35 mev γ - radiation.

(B): 1- With the help of Wilson chamber photography method from the investigation of positron tracks coming to an abrupt termination and the determination of the range distribution, or probably better, energy distribution of the positrons at the instant of annihilation it should be possible to study statistically, if somewhat laboriously, the process of annihilation at rest and in motion.(use of a magnetic field and track curvature measurements are necessary). The experimental efficiency may be increased by using counters in anti-coincidence in order to detect the positrons which are definitely stopped in the cloud chamber.

2- Wilson chamber investigation of the energy spectrum of the annihilation radiation by photography of Compton electrons from radiators illuminated with annihilation radiation could be carried a stage further than past experiments. Possibily, if intensity considerations permitted (somewhat better sources are now available) magnetic resolution of the positrons prior to the annihilation would yield more definite information.

3- Temperature effect of annihilation medium upon intensity of annihilation could be investigated in order to obtain the annihilation probability as a funtion of energy for very slow positrons .

4- The advance of the technique of using photo-multiplier detectors for radiations makes attempts to determine, by accurate delay counter coincidence experiments, the life times of positrons (e.g. by delayed coincidences between positrons entering an absorber and the detection of the quanta emission) a nearly practicable method of studying in some detail the time-sequence of ionisation and annihilation events.

--oOo--

Acknowledgements

My thanks are due to Prof. P.I. Dee and Dr.S.C. Curran who supervised this work and helped to make it successful with their suggestions and stimulating discussions. I would also like to express my gratitude to Dr. W. Mc Farlane for his deep interest in my work and for his continuous help in many directions, and to his wife who kindly provided every facility during my stay in their house to enable me to complete my studies. I am also indepted to Mr. J.T. Lloyd, the chief technician of the department, whose assistance was very valuable during this research.

Finally I would like to thank the University of Istanbul for the grant they provided from September 1946 to June 1949 .

——:o:——

REFERENCES.

1. C.D.Anderson, Science, 76, 238, (1932). Phys.Rev., 41, 405, (1932).

2. P.A.M.Dirac, Proc.Roy.Soc.A., 126, 360, (1930).

2a. P.A.M.Dirac, Proc.Camb.Phil.Soc., 26, 361, (1930).

3. G.T.P.Tarrant, Proc.Roy.Soc.A., 128, 345, (1930).

4. C.Y.Chao, Proc.Nat.Acad.Sci., 16, 431, (1930).

5. C.D.Anderson, Phys.Rev., 43, 491, (1933), 44, 406, (1933)

6. J.Chadwick, P.M.S.Blackett, & G.Occhialini. Nature, 131, 286 & 473, (1933).

7. I.Curie and F.Joliot, C.R., 196, 1105, (1933).

8. J.R.Oppenheimer & M.Plesset, Phys. Rev., 44, 53, (1933).

9. W.Heitler & F.Sauter Nature, 132, 842, (1933).

10. H.Bethe & W.Heitler, Proc. Roy. Soc., 146, 83, (1934).

11. Grosew & Frank, C.R.(Doklady), 19, 49, (1938).

12. H.R.Hulme & J.C.Jaeger, Proc.Roy.Soc., 153, 443, (1936)

13. F.Simon & K.Zuber, Proc.Roy.Soc., 159, 383, (1937).

14. Ogle & Kruger, Phys.Rev., 67, 273 & 282, (1945).

15. F.Perrin, C.R., 197, 1100, (1933).

16. Marques da Silva Ann.de Phys., 11, 504, (1939).

17. Chizzeti & Borsellino Ric.Sci., 16, 625, (1946).

18. Watson, Phys. Rev., 72, 1060, (1947).

19. Borsellino Helv.Phys.Acta, 20, 136, (1947).

20. Memirowsky, J.Phys.U.S.S.R., 11, 94, (1947).
20.a V. Votruba Phys. Rev. 73, 1468 (1948)
21. Furry & Carlson, Phys. Rev., 44, 237, (1933).

22. Heitler & Nordheim, J.de Phys. 5, 449, (1934).

22a. L.Nordheim, J.de Phys., 6, 135, (1935).

22b. J.R.Oppenheimer, Phys.Rev., 47, 146, (1935).

22c. J.William, Nature, 135, 66, (1935).

22d. H.J.Bhabha, Proc.Roy.Soc.A., 152, 559, (1935).

23. D.Sobobeltzyn, Nature, 133, 128, (1934).

24. Skobeltgyn & Stepanawa, J.de Phys. 6, 1, (1935), Nature, 137, 272, (1936).

25. M.da Silva, C.R., 202, 2070, (1936).

26. Champion & Barber, Nature, 140, 105, (1937).

27. Feather & Dunworth, Proc.Camb.Phil.Soc., 34, 435, (1938).

28. S.de Benedetti, J.de Phys., 7, 205, (1936).

29. F.C.Champion, Proc.Roy.Soc.A., 153, 353, (1935).

30. Staub, Helv.Phys.Acta, 9, 306, (1936).

31. Crane & Halpern Phys. Rev., 55, 838, (1934).

32. Alichanow, Alichaniew, & Kosodaew, J.De Phys., 7, 163, (1936).

33. F.Perrin, C.R., 197, 1302, (1933).

34. F.W.A.Fowler & C.Lauritsen, Phys.Rev., 56, 840, (1939).

35. Halpern & Crane, Phys. Rev., 55, 260, (1939).

36. Oppenheimer & Nedelski, Phys.Rev., 44, 948, (1933).

37. Rose & Uhlenbeck, Phys.Rev., 48, 211, (1935).

38. Jaeger & Hulme, Proc.Roy.Soc.A.,148, 708, (1935).

39. Spees & Zahn, Phys.Rev.,57,72,(1940);58,861,(1941)

40. C.Y.Chao, Phys.Rev., 36, 1519, (1930).

41. C.Y.Chao, Proc.Roy.Soc.A., 135, 206, (1932).

42. L.H.Gray & G.T.P.Tarrant, Proc.Roy.Soc.A., 136, 662, (1932).

43. L.H.Gray & G.T.P.Tarrant, Proc.Roy.Soc.A., 143,681 & 706, (1934).

44. P.M.S.Blackett & G.P.Occhialini, Proc.Roy.Soc.A., 139, 669,(1933).

45. F.Joliot, J.de Phys.,5, 229, (1934).

46. J.Thibaud, C.R.,197, 1629, (1933).

47. O.Klemperer, Proc.Camb.Phil.Soc.,30, 347, (1934)

48. Crane & Lauritsen, Phys.Rev.,45, 430, (1934).

49. E.McMillan, Phys.Rev., 46, 868, (1934).

50. Richardson & Kurie, Phys.Rev., 50, 999, (1936).

51. J.R.Richardson, Phys.Rev., 53, 124, (1938).

52. J.R.Richardson, Phys.Rev., 53, 610, (1938).

53. M.Deutch, Phys.Rev., 72, 729, (1947).

54. C.S.Cook & L.M.Langer, Phys. Rev.,73, 601, (1948).

55. J.W.M DuMond, D.A. Lind & B.B Watson Phys. Rev.,75, 1226, (1949).

56. S. van Woorhis, Phys. Rev.,50, 895, (1936).

57. A. Tyler, Phys. Rev.,56, 125, (1939).

58. A.A.Townsend, Proc.Roy.Soc.A.,175, 48,(1940).

59. J.Bacchus, Phys.Rev.,68, 59, (1945).

60. G.L. Lawson Phys.Rev., 56, 131 (1939).

61. Alichanon, Alichanian, & Arzimonicz, Nature, 137, 703, (1936).
C.R.(Doklady),1, 287, (1936).

62. R.Beringer and C.G.Montgomery, Phys.Rev., 61, 222, (1942).

63. J.A.Wheeler, Ann. N.Y.Acad.Sci., 48, 219, (1946).

64. H.S.Synder & S. Pasternack, Phys. Rev.,73, 440, (1948).

65. Bleuler & Bradt, Phys. Rev., 73, , (1948).

66. Pryce and Ward, Nature, 160, 435, (1947).

67. E.Bleuler & der Haar, Science, 108, 10, (1948).

68. Fermi and Uhlenbeck Phys. Rev. 44, 510, 1933

69. P.M.S.Blackett & G.P.Occhialini, Proc.Roy.Soc.A., 144, 235, (1934).

70. H.Bethe, Proc.Roy.Soc.A.,150,129, (1935).

72. J.Solomon, J.de Phys.,6, 114, (1935).

71. J.C. Jaeger and H.R. Hulme Proc. Camb. Phil. Soc. 32 (1936) 158.

73. H.R.Hulme & H.J.Bhabha, Proc.Roy.Soc, A.,146, 723, (1934).

74. S.C.Curran & J.M.Reid, Rev.Sci.Instr., 19, 67, (1948).

75. R.W.Pringle, J.Sci.Instr.,25, 423, (1948).

76. Bradt et al. Helv.Phys.Acta.,19, 219, (1946).

77. Bradt et al. Helv.Phys.Acta.,19, 77, (1946).

78. (a) Deutsch, Elliott, Robert Phys. Rev. 68. 193, 1945
(b) E.N. Jensen, L.J. Laslett and W.W. Pratt " " 73, 529 1948
(c) " " " " " 75, 458 1949.

78 (d) Jensen et al... Phys. Rev. 76, 430 1949
(e) Alburger " " " 435 "
(f) Lind Dumond & Brawn Bul. A. Phys. Soc. 24, 6, 12, 1949

79. Langer, Cook & Sampson. Phys.Rev.,71,906, (1947).

80. Heyn, Physica, 4,16, (1937).

81. Huber, Helv. Phys. Acta, 16, 226, (1943).

82. Seaborg, Rev.Mod.Phys.,(1944).

83. M.Good, S.Peaslee, & M.Deutch, Phys. Rev.,69, 313, (1946).

84. C.S.Wu & R.D.Albert, Phys. Rev., 75, 315, (1949).

85. J.Thibaud, L.Cartan & P.Comparet, "Quelques techniques actuelles en physique nucleaire" (Paris, 1939).

86. J.L. Lawson, J.M. Cork Phys. Rev. 58, 580, (1940)

87. E.H. Plesset Phys. Rev. 62, 181 (1942)

88. K. Siegbahn Proc. Roy. Soc. 189, 527, 1947

89. DuMond, Lind, Watson Phys. Rev. 73, 1392, (1948)

90. Siegbahn Phys Rev. 75, 3, (1949)

APPENDIX.

I. Comparison of creation and annihilation processes.

Creation of pair.

A pair can be produced by the interaction of:-

1. Photon with nucleus ($E_N = 0$) if $k_p = h\nu \geqslant 2mc^2$.

2. Photon with electron ($E_- = 0$) if $k_p \geqslant 4mc^2$

3. Electron with electron if $E' = 0$ and $E_i = 6\text{-}7mc^2$. (6-Perrin, 7-Heitler).

4. Photon with photon. if $E' + k_p \geqslant 2mc^2$.

5. Electron with nucleus ($E = 0$) if $E'_- \geqslant 2mc^2$.

6. Heavy particle with nucleus ($E = 0$) if $E_- \geqslant 2mc^2$

Annihilation of pair.

A pair can be annihilated by the combination of a positron with an electron which is:-

1. Strongly bound to a nucleus giving a single photon ($k_s > 2mc^2$).

2. In the neighbourhood of another electron giving electron ($E_- = \frac{2mc^2}{3}$) and photon ($k_s = 4mc^2/3$).

3. In the immediate neighbourhood of another electron giving a single electron ($E_- = 2mc^2$).

4. Loosely bound or free (in matter) giving photon ($k_1 = mc^2$) and photon ($k_2 = mc^2$)

5. In the neighbourhood of a bound electron giving a single electron

6. In the neighbourhood of two other electrons giving electron ($E_- = mc^2$) and electron ($E'_- = mc^2$)

7. γ-ray emitted by a nucleus in the field of the same nucleus ($k \sim 5mc^2$)	7. A K-electron.

II. List of Positron Emitters.

Element	Half-life	Energy in MeV.	Produced by
C_6^{10}	8.8 sec.	3.4 clch.	B-p-n
C_6^{11}	20.5min.	0.95 clch.	B-d-n; B-p-γ; N-p-n; C-n-2n;
N_7^{13}	9.93min.	0.92, 1.20 (spect.)	C-d-n; C-p-γ; B-α-n; N-n-2n; N-d-H_3
O_8^{15}	126 secs.	1.7 clch.	N-d-n; O-γ-n; N-p-γ; C-α-n.
F_9^{17}	70 secs.	2.1 clch.	O-d-n; N-α-n; O-p-γ.
F_9^{18}	112 min	0.7 clch.	Ne-d-α; O-p-n; F-n-2n; O-d-n; F-d-H_3; F-γ-n.
Ne_{10}^{19}	20.3 secs.	2.20 clch.	F-p-n.

Element	Half-life	Energy in MeV.	Produced by
Na^{22}_{11} (γ)	3 years	0.58 clch.	Mg-d-α ;F-α -n;Ne-d-n.
Mg^{23}_{12}	11.6secs.	2.82 clch.	Na-p-n; Mag-γ-n.
Al^{26}_{13}	7.0 scs.	2.99 clch.	Na-α-n;Mg-p-n;Mg-p-γ;Al-p-n.
Si^{27}_{14}	4.9 scs.	3.74 clch. 3.54	Al-p-n; Mg-α-n.
P^{29}_{15}	4.6 sec.	3.63 clch.	Si-p-n.
P^{30}_{15}	2.55min.	3.0 clch. 3.5 spect.	Al-α-n; S-d-α; P-n-2n; P-γ-n.
S^{31}_{16}	3.2 secs.	3.85 clch.	P-p-n; Si-α-n; S-γ-n.
Cl^{33}_{17}	2.4 scs.	4.13 clch.	S-d-n
Cl^{34}_{17}	33min.	2.5 abs.	P-α-n; S-d-n; Cl-n-2n; Cl-γ-n; S-α-p.
Cl^{36}_{17} (K, β̄)	10^3 yr.		Cl-n-γ; Cl-d-p.
A^{35}_{18}	1.88sec.	4.4 clch.	Cl-p-n;S-α-n.
K^{38}_{19}	7.7min.	2.3 abs.	Cl-α-n; Ca-α-α; K-n-2n; K-γ-n.
Ca^{39}_{20}	4.5 min.		Ca-n-2n ?
Sc^{42}_{21}	0.87 sec.	4.94 clch.	Ca-d-n.

Element	Half-life	Energy in MeV.	Produced by
S^{42}_{21}	13.5 days.	1.4 abs.	K-α-n.
$Sc^{43}_{21}(\gamma)$	4 hrs.	0.4, 1.4 1.13 abs.	Ca-d-n; Ca-p-n.
$Sc^{44}_{21}(\gamma)$	4.1 hrs.	1.5 abs. 1.33 spect.	Sc-n-2n; K-α-n; Ca-d-n; Ti-d-α; Ca-p-n; Sc-d-2n; Sc^{44} (52h) I.T.
Ti^{55}_{22}	3.08 hrs.	1.2 clch.	Ca-α-n; Sc-p-n; Sc-d-2n; Ti-n-2n; Ti-γ-n.
V^{47}_{23}	33 min.	1.9 abs.	Ti-d-n; Ti-p-n.
$V^{48}_{23}(k,\gamma)$	16 days.	1.0 clch. 0.58.	Ti-d-n; Sc-α-n; Cr-d-α; Ti-p-n.
V^{50}_{23}	3.7 hr.		V-n-2n; Ti-d-n; Ti-α-p.
Cr^{49}_{24}	41.9 min.	1.45 abs.	Ti-α-n; Cr-n-2n.
Mn^{51}_{25}	46 min.	2.0 abs.	Cr-d-n; Cr-p-γ.
$Mn^{52}_{25}(\gamma)$	21 min.	2.2 clch.	Fe-d-α; Cr-d-n.
$Mn^{52}_{25}(k,\gamma)$	6.5 days.	0.77 clch.	Fe-d-α; Cr-p-n.
Fe^{53}_{26}	8.9 min.		Cr-α-n; Fe-n-2n; Fe-γ-n.
$Co^{55}_{27}(\gamma)$	18.2 hrs.	1.50 spect.	Fe-d-n; Fe-p-γ.

Element	Half-life	Energy in MeV.	produced by
Co^{56}_{27} (γ, k)	72 days.	1.2 abs.c.c.; coinc. 1.5 spect. coin.	Fe-d-2n;Ni-d-α ; Fe-α-n,p.
Co^{57}_{27} (k, $\bar{e}$, γ)		0.26	Fe-p-γ; Fe-d-n.
Co^{58}_{27} (γ)	72 days.	0.4 abs;0.47 spect.coinc.	Fe-d-n;Mn-α-n;Ni-d-α; Fe-α-n;Ni-n-2p; Fe-α-n; Fe-p-γ.
Ni^{57}_{28}	36hrs.	0.67 abs.	Fe-α-n; Ni-n-2n;Ni-γ-n.
Cu^{58-60}_{29}	81 sec.		Ni-p-n.
Cu^{58-60}_{29}	7.9 min.		Ni-p-n.
Cu^{61}_{29} (k)	3.4 hr.	0.9 abs.	Ni-d-n; Ni-p-n;Ni-p-γ; Ni-α-p;
Cu^{62}_{29}	10.5 min.	2.6 clch.	Cu-n-2n;Cu-γ-n;Co-α-n; Ni-p-n;Ni-p-γ;Cu-d-H_3.
Cu^{64}_{29} ($\bar{\beta}$, k)	12.8 hrs.	0.66 spect.	Cu-d-p;Cu-n-γ;Ni-p-n; Zn-n-p;Cu-n-2n;Cu-γ-n.
Zn^{63}_{30}	38min.	2.3 abs.spect.	Zn-n-2n; Zn-γ-n;Cu-p-n; Ni-α-n;Cu-d-2n;
Zn^{65}_{30}	250 days.	0.4 clch.	Zn-d-p;Cu-d-2n;Cu-p-n; Zn-n-γ; Ga^{65}-K decay.

Element	Half-life	Energy in Mev.	Produced by
Ga^{64}_{31}	48 min.		Zn-p-n.
Ga^{66}_{31}	9.4 hrs.	3.1 abs.	Cu-α-n; Zn-p-n.
Ga^{68}_{31}	68min.	1.9 abs.	Cu-α-n;Ga-n-2n;Ga-γ-n; Zn-p-γ;Zn-d-n;Ge-d-α;
Ge^{71}_{32}	40 hrs.	1.2 abs.	Zn-α-n;Ge-n-γ;Ge-d-p;Ga-d-2n;Se-n-α.
As^{72}_{33}	26 hrs.		Ge-p-n.
As^{73}_{33}	50 hrs.	0.6	Ge-d-n
As^{74}_{33} ($\bar{\beta}$, K)	16 days.	0.9 clch.	As-n-2n; Se-d-α;Ge-p-n.
As^{76}_{33} ($\bar{\beta}$, γ)	26.8 hrs.	0.7,2.6 clch. coin.	As-n-γ;Br-n-α;Ge-p-n; Se-d-n;Se-d-α;
Br^{78}_{35} ($\bar{e}$, γ)	6.4 min.	2.3 abs.	Se-d-n;As-α-n;Br-γ-n;Br-n-2n; Se-p-n.
$Kr^{79,81}_{36}$	34 hrs.	0.4 clch.	Kr-d-p;Br-p-n;Se-α-n.
Y^{88}_{39}	2.0 hrs.	1.2 clch.	Sr-d-n;Y-n-2n;Sr-p-n.
Zr^{89}_{40}	78 hrs.	1.0clch.abs.	Zr-n-2n;Y-p-n;Mo-n-α.
$Mo^{91,93}_{42}$	17 min.	2.65 clch.	Mo-n-2n; Mo-γ-n.
Tc^{96}_{43}	2.7 hrs.		Cb-α-n;Mo-p-n;Mo-d-n.

Element	Half-life	Energy in MeV.	Produced by
Rh^{102}_{45} (β, γ)	210 days.		Rh-n-2n.
Ag^{106}_{47}	24 min.	2.04 abs.	Ag-n-2n;Pd-d-n;Cd-n-p; Rh-α-n; Ag-γ-n; Pd-p-γ; Pd-p-n;Ag-d-p,2n.
Cd^{105}_{48}	33 min.		Cd-n-2n
In^{110}_{49}	65 min.	1.6 spect.	Cd-p-n;Ag-α-n;Cd-d-2n.
In^{111}_{49} (γ, e^-)	20 min.	1.7 clch.	Cd-d-n; Cd-p-n.
In^{112}_{49} (β, γ, e^-)	17.5 min.	1.3 abs.	Ag-α-n;In-n-2n;In^{112}(16.5 min.) I.T.
$Sb^{116,118}_{51}$	3.6 min.		In-α-n.
Sb^{120}_{51}	17 min.	1.53 abs.	Sb-γ-n;Sn-d-n;Sn-p-n; Sb-d-H^3.
I^{124}_{53}	4.0 days		Sb-α-n; Te-p-n.
Ce^{139}_{58}	2.1 min.		Ce-n-2n ?
Pr^{140}_{59}	3.5 min.	2.40clch.	Pr-n-2n.
Nd^{141}_{60}	2.5 hrs.	0.78	Nd-d-H^3;Nd-n-2n;Pr-p-n;Nd-γ-n
Eu^{150}_{63}	27 hrs.		Eu-n-2n ?

Element	Half-life	Energy in MeV.	Produced by
$Dy_{66}^{?}$	2.2 min.		Dy-n- ?
Er_{68}^{165}	1.1 min.		Er-n-2n.
Re_{75}	30-55 min.		W-p-n.
Pb_{82}^{203}	10.25 min.	1.66 abs.	Tl-d-2n.

III. Statistical Distribution of Positron Sources.

a- as a function of the atomic number of the emitters. (FIG. 51.)

b- as a function of the kinetic energy of the emitted positrons. FIG.52

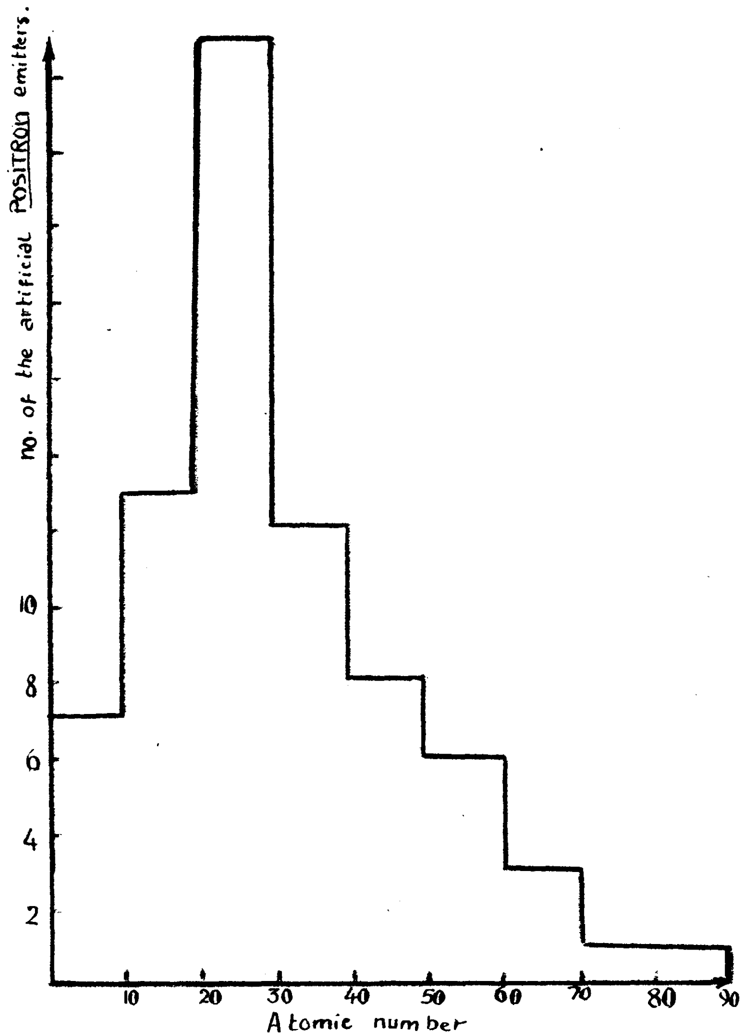

FIG. 51

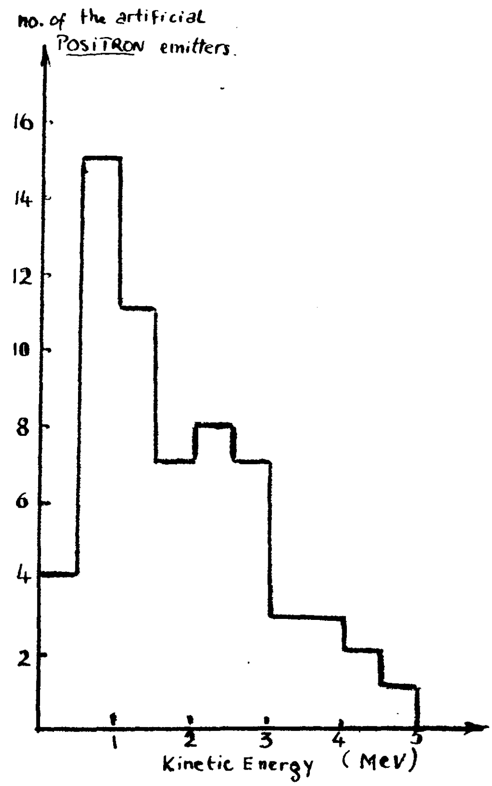

FIG. 52.

IV(8) (β,γ) coincidences from ThC.

i(A)	no of β. per.min.	Total no. (β-γ) coincid./min.	(γ-γ) coincid./min.	Chance /min	Real (β-γ) coin. per minute	$\frac{(\beta-\gamma)}{\beta}$ (10^4)
0.02	1459	72.2±2.7	57.2±3.4	1.20	13.8	96.79
0.04	1833	46.6±1.5	40.6±1.4	0.60	5.4	29.50
0.1	3267	14.5±1.2	8.3±0.8	0.70	5.5	16.83
0.2	10701	25.9±1.6	6.8±0.8	2.30	16.8	15.70
0.3	23158	51.0±2.3	6.2±0.7	4.92	39.9	17.23
0.4	12736	25.8±1.6	1.8±0.4	0.89	23.10	18.15
0.5	15484	29.0±1.7	2.4±0.5	0.82	25.80	16.66
0.6	15867	27.6±1.65	2.0±0.45	1.17	24.43	15.40
0.7	15228	24.8±1.65	1.9±0.46	0.98	21.92	14.41
0.8	12712	21.4±1.5	2.5±0.5	0.78	18.12	14.25
0.9	11336	13.3±1.15	2.8±0.53	0.68	10.82	9.54
1.0	8723	10.9±1.05	3.1±0.55	0.53	7.3	8.37

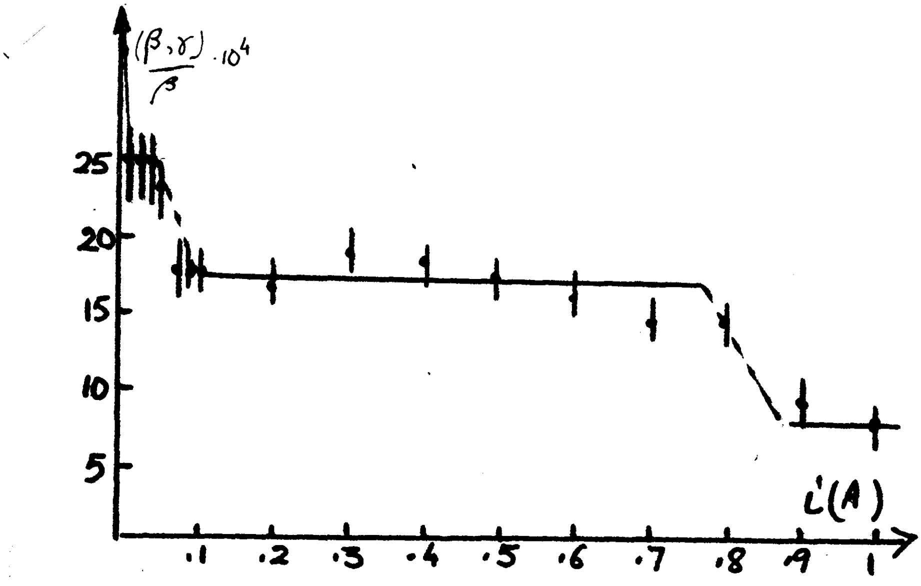

FIG 53

IV.6. (β-γ) coincidences from Th C [with $\frac{1}{2}$"×$\frac{1}{2}$" window present cf Ch. V]

i(A)	Th(β-γ) coinci. plus other coin. per min	(Th-Ra)(β-γ)+ other coincidences per min	Real (β-γ) coinci. per min	No β mm	$\frac{(\beta-\gamma)\text{ coinci}}{\beta}$ 10^4
0.2	23.6±1.5	21.0±1.45	2.6	1302	20.00
0.3	28.6±1.7	22.3±1.5	6.3	8734	7.21
0.4	33.9±1.84	24.3±1.55	9.6	15874	6.05
0.5	17.4±1.3	8.4±0.9	9.0	13991	6.43
0.6	18.4±1.35	11.0±1.05	7.4	16880	4.38
0.7	14.7±1.2	7.6±0.9	7.1	17057	4.17
0.8	12.4±1.1	6.4±0.8	6.0	14241	4.21
0.9	8.8±1.4	4.0±1.0	4.8	11269	4.25

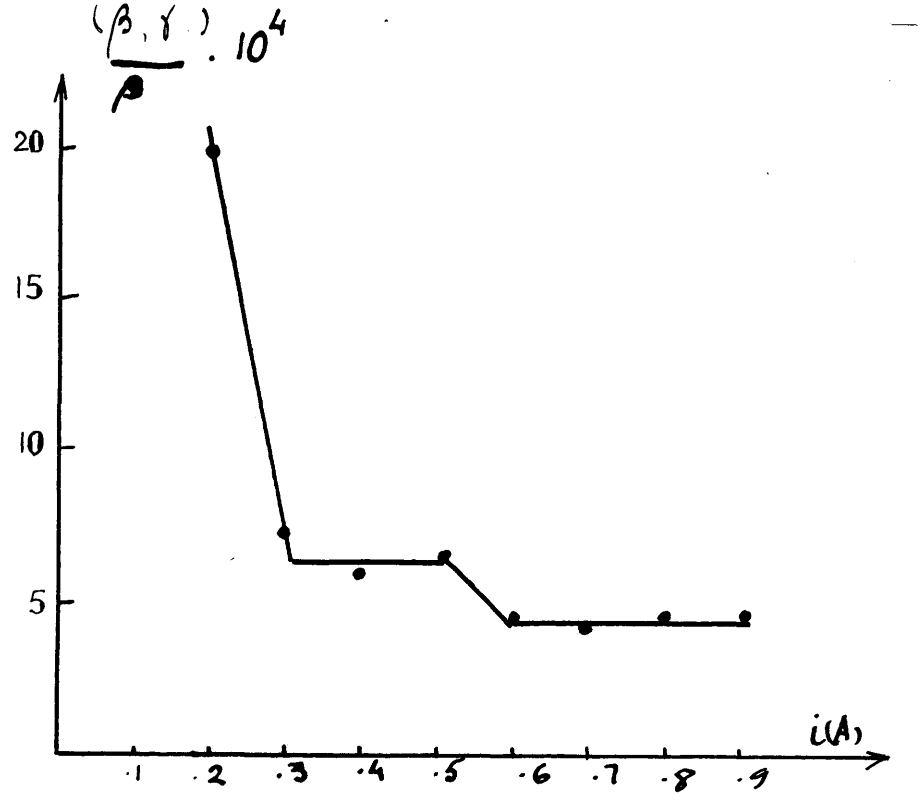

FIG. 54.

The discontinuous nature of the curve illustrates the complexity of the β-γ transition of the source.

APPENDIX V

COMPLETE ABSORPTION CURVE
From 0 to 4 absorbers
TAIL OF THE ABSORPTION CURVE
ON ENLARGE SCALE
From 4 to 12 absorbers
1.3345 (Pb)
1.1779 Al
0.958 (Pb)
0.792 Al
0.715 (Pb)
0.651 (Pb)
0.625 (Al)
0.527 (Al)
(Pb) 0.552
(Al) 0.525
29.786 (Pb)
(Al) 26.607
5.608 (Pb)
2.678 (Pb)
S
0.44 MeV
0.59 MeV
1.01 MeV
1.13 MeV
1.27 MeV
1.42 MeV
1.54 MeV
1.67 MeV
1.79 MeV
1.92 MeV
Two Cu window